Aus der

Neurologischen Universitätsklinik Tübingen

Abteilung für Neurologie mit Schwerpunkt

Neurodegenerative Erkrankungen

Neurophysiological alterations in Freezing of Gait in Parkinson's disease

Inaugural-Dissertation
zur Erlangung des Doktorgrades
der Medizin

der Medizinischen Fakultät
der Eberhard Karls Universität
zu Tübingen

vorgelegt von
Müßler, Hannah Barbara

2026

Dekan: Professor Dr. Bernd Pichler

1. Berichterstatter: Professor Dr. D. Weiß
2. Berichterstatter: Professor Dr. F. Ebner

Tag der Disputation: 08.12.2025

Table of Contents

Figures

Tables

List of abbreviations

aDBS	Adapted deep brain stimulation
BBS	Berg Balance Scale
BDI	Beck's Depression Inventory
BG	Basal Ganglia
cDBS	Conventional deep brain stimulation
CT	Computerized tomography
CWT	Continuous wavelet transformation
DBS	Deep brain stimulation
ECG	Electrocardiography
EEG	Electroencephalography
EMG	Electromyography
ERSP	Event-related spectral perturbation
FoG	Freezing of Gait
FOG-AC	Freezing of Gait – Assessment Course
GPe	Globus pallidus externus
GPi	Globus pallidus internus
HRQoL	Health-related quality of life
HS	Heel strike
IMU	Inertial Measurement Unit
IPG	Implantable pulse generator
IQR	Interquartile range

LCIG	Levodopa Carbidopa Intestinal Gel
LFP	Local field potential
MC	Midcomissural point
MDS-UPDRS	Movement Disorder Society Unified Parkinson Disease Rating Scale
MedOFF	Medication OFF
MedON	Medication ON
MoCA	Montreal Cognitive Assessment
MRI	Magnet resonance imaging
MS	Mid-Swing
NFOG-Q	New Freezing of Gait - Questionnaire
PD	Parkinson's Disease
PIGD	Postural instability gait disorder
PPN	Pedunculopontine nucleus
SD	Standard deviation
StimOFF	Stimulation OFF
StimON	Stimulation ON
SNc	Substantia nigra pars compacta
SNr	Substantia nigra pars reticulata
STFT	Short-term Fourier transform
STN	Subthalamic nucleus
TO	Toe-off
ULF	Upper limb freezing
WT	Wavelet transform

Introduction

Imagine ‘asking’ your feet to move forward, but they ‘refuse’. -Jeff Hausdorff

This quote aptly describes Freezing of gait (FoG), a debilitating motor symptom of Parkinson's disease. Patients experience sudden impaired forward progression of gait and although the will to move forward is present, the feet ‘remain glued to the ground’. It leads to massive restriction of mobility and quality of life, and often results in falls and hospitalization. The missing understanding of the underlying pathophysiology goes along with unexploited therapeutic options. This doctoral thesis aims to analyse the neurophysiological mechanisms underlying FoG in order to contribute to a deeper understanding of its pathophysiology. The insights gained could support the development of new and more effective therapeutic approaches.

1.1 Epidemiology and Clinical Characteristics of Parkinson’s Disease

Parkinson’s disease (PD), described in detail for the first time by James Parkin in 1817, is the second most common neurodegenerative disease after Alzheimer’s disease (Lee & Gilbert, 2016; Savitt et al., 2006). In industrialized countries the estimated prevalence of PD amounts to 0.3% in the general population, 1.0% in people older than 60 years and 3.0% in people older than 80 years, which illustrates advanced age being the best-known risk factor for PD. The medium age of onset is estimated at 60 years (Lee & Gilbert, 2016). It is observed more often in men than in women with a median rate ratio of 1.8 (Hirtz et al., 2007). Overall, PD incidence is significantly greater in people exposed to certain environmental factors, including but not being limited to pesticides, consumption of dairy products and traumatic brain injury, but slightly lower in smokers or caffeine users and a shared genetic susceptibility for melanoma and PD has been observed (Ascherio & Schwarzschild, 2016).

Diagnosing patients with PD can be a lengthy process as early prodromal symptoms such as constipation, rapid-eye-movement sleep behaviour, hyposmia or depression are easily overlooked which oftentimes delays the proper diagnosis in affected patients (Armstrong & Okun, 2020).

The clinical syndrome of idiopathic PD unfolds in two major domains: motor and non-motor symptoms. The cardinal motor symptoms of PD include bradykinesia, tremor, postural instability, and rigidity which is usually asymmetric once symptoms start to manifest clinically. Other features range from gait disturbances to micrography, disturbances of speech and hypomimia (Balestrino & Schapira, 2020). Non-motor symptoms of PD can be found in dysphagia, hypersalivation and autonomic-, gastrointestinal-, sleep-, sensory-, cognitive- and neuropsychiatric disturbances which taken together have a major impact on a patient's quality of life (Balestrino & Martinez-Martin, 2017; Duncan et al., 2014; Schapira et al., 2017).

The clinical manifestation of PD differs and can be very heterogeneous between patients, which renders further subtyping useful, though not entirely straightforward. There are several approaches based on age at onset (early-onset versus late-onset), predominant motor symptom (tremor-dominant versus akinetic-rigid versus postural instability and gait disturbance 'PIGD') or disease progression (mild motor-predominant versus intermediate versus diffuse malignant) (Fereshtehnejad et al., 2015; Jankovic et al., 1990; Kulcsarova et al., 2024; Tolosa et al., 2021). With growing knowledge of PD pathophysiology, new diagnostic methods and the need for early disease detection, biological classification systems are increasingly coming into focus. In the coming years, in vivo detection of neuronal α-synuclein aggregation, neurodegeneration, and genetic factors could contribute to classification and may potentially enable more precise subtyping (Kulcsarova et al., 2024).

1.2 The underlying pathophysiology

The two main pathological features of PD are the loss of pigmented dopaminergic neurons and the presence of Lewy bodies (Balestrino & Schapira, 2020). Neuronal death primarily affects dopaminergic neurons in the substantia nigra pars compacta (SNc), which modulate the activity of the basal ganglia through the innervation of the striatum (Stein & Bar-Gad, 2013).

With neurodegeneration in PD being a slow and gradual process, it is currently graded into three phases: i) the preclinical phase, where neurodegeneration has already started, but without any detectable symptoms ii) the prodromal phase dominated by non-motor symptoms and finally iii) the clinical phase after onset of the characteristic motor symptoms (Kulcsarova et al., 2024). It has been estimated that motor signs first appear, when there is already about a 50% neuronal loss in the substantia nigra (Marsden, 1990).

Defective communication in the nigrostriatal pathway impairs the processing of the striatal inputs from the cortex and thalamus which in turn leads to changes in neuronal activity of downstream basal ganglia nuclei including the globus pallidus externus and internus (GPe and GPi, respectively), the subthalamic nucleus (STN) and the substantia nigra pars reticulata (SNr) (Stein & Bar-Gad, 2013). Subsequently, typical cardinal motor symptoms of PD arise given the altered activity of the basal ganglia (BG) output targets due to abnormal signal processing in the basal ganglia thalamo-cortical network as illustrated in **Figure 1** (Plamen Gatev et al., 2006; Poewe et al., 2017).

Another hallmark of PD is the presence of Lewy bodies which arise during a pathological process when soluble α-synuclein monomers aggregate to insoluble amyloid fibrils and are being deposited as intraneuronal proteinaceous cytoplasmic inclusions in several different brain regions (Kim & Lee, 2008; Melki, 2015). The reasons for aggregation and accumulation of α-synuclein are various, e.g. due to overproduction of the protein or mutations in the pathways of folding or degrading the misfolded protein (Poewe et al., 2017).

Pharmacological treatment of PD aims at replenishing depleted dopamine levels with L-Dopa still being considered as the gold standard for treating motor symptoms (Connolly & Lang, 2014). Non-pharmacological approaches include but are not limited to physical exercise, occupational and speech therapies or more advanced therapies like deep brain stimulation (DBS) (Armstrong & Okun, 2020). Those advanced options are considered when patients can no longer sustain stable plasma dopamine levels as normal physiological uptake and release of dopamine is gradually being diminished over the course of the disease. This reduced buffering capacity sooner or later translates into an increasing

occurrence of motor and non-fluctuations such as the reemergence of motor symptoms ("wearing-off"), sudden off-phenomena, troublesome hyper- and dyskinesias (Goetz et al., 2005; Kim et al., 2020), or the neuropsychiatric sequalae stemming from dopaminergic sensitization (Calabresi et al., 2010; Weintraub & Mamikonyan, 2019; Weiss et al., 2021).

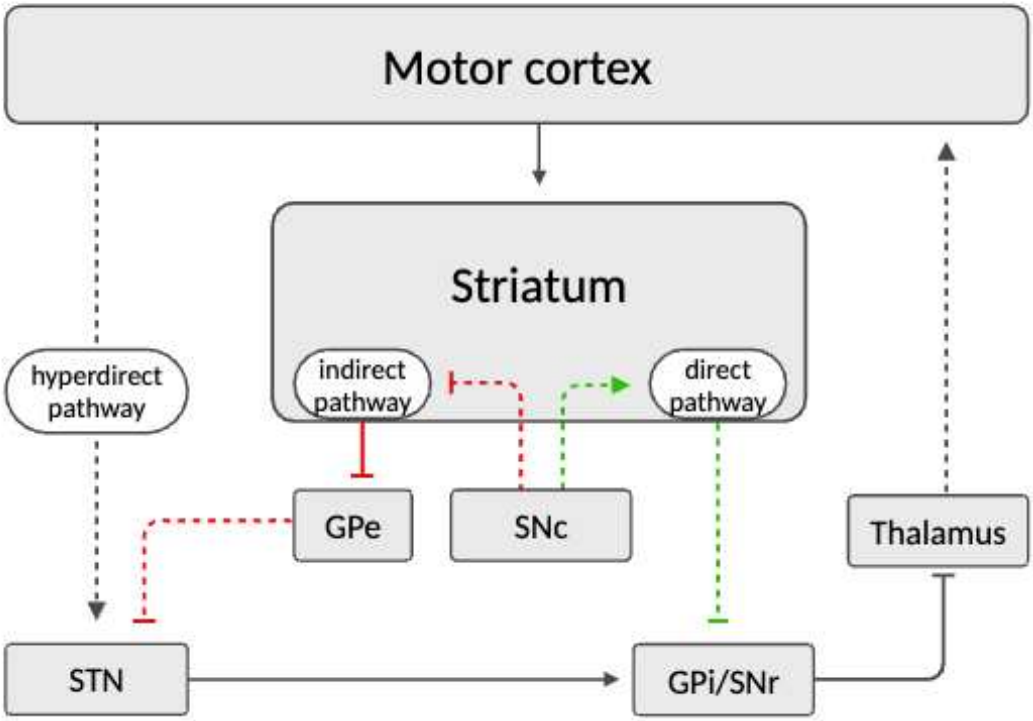

Figure 1. Parkinson's disease related changes in basal ganglia thalamo-cortical network.
Lined arrow/inhibitor = Increased excitatory/inhibitory activity, dotted arrow/inhibitor = Reduced excitatory/inhibitory activity. GPe = Globus pallidus externus, GPi = Globus pallidus internus, SNc = Substantia nigra pars compacta, SNr = Substantia nigra pars reticulata, STN = Subthalamic nucleus. Due to the lack of dopamine and the resulting degeneration of the nigrostriatal pathways, the GPi is less inhibited (direct pathway in green). Conversely, the excitatory input from the STN remains strong (indirect pathway in red and hyperdirect pathway). This results in the overactive inhibitory neurons of the GPi strongly inhibiting the thalamus. As a result, the thalamus's ability to activate the cortex is diminished, leading to inhibited movement in Parkinson's disease. Figure created with Biorender.com adapted from Poewe et al. (Poewe et al., 2017).

1.3 Deep brain stimulation as advanced treatment in Parkinson's disease

DBS has become a relevant treatment option for patients with PD for whom standard dopamine replacement therapy is no longer sufficient, for patients with levodopa induced dyskinesias and for tremor refractory to medication (Mahlknecht et al., 2022). Moreover, DBS has shown to be more effective than medical treatment alone with significant increase in quality of life (Weaver et al., 2009; Williams et al., 2010). It reduces off-time and dyskinesias and instead leads to improvement of motor function (Deuschl et al., 2006; Schuepbach et al., 2013; Vitek et al., 2020; Weaver et al., 2009).

An electrode is implanted stereotactically and bilaterally into the STN, the most common target of DBS in PD or in the GPi, connected with a subcutaneous wire to an implantable pulse generator (IPG) which is placed subcutaneously on the chest (Herrington et al., 2016). However, the underlying mechanisms leading to the therapeutic efficacy remain still not fully understood, although it is increasingly believed that DBS acts via multimodal mechanisms (Ashkan et al., 2017). Initial hypotheses how DBS works were based on the observations that DBS acts like an anatomical lesion. This was interpreted in the context of the rate model which assumes that dopamine depletion leads to increased firing rates in the STN and GPi resulting in decreased thalamic firing and akinesia. DBS, like a lesion, would inactivate the STN (Ashkan et al., 2017). More recent approaches base the effectiveness of DBS more on an interplay of multiple mechanisms: stimulation of axons around the electrode, modulation rather than an inactivation of pathological network activity, disruption of abnormal basal ganglia synchronization, synaptic plasticity and long-term neuronal reorganization (Ashkan et al., 2017; Herrington et al., 2016; Kühn & Volkmann, 2017). Nevertheless, further investigations and understanding are needed to be able to fully exploit the possibilities of DBS.

The short-term efficacy of STN- or GPi-DBS in patients with PD has been reported frequently, enabling the reduction of the L-Dopa equivalent dosage, significant reduction of motor symptom severity and improvement in quality of life (Deuschl et al., 2013; Okun et al., 2012; Schuepbach et al., 2013). It can be

assumed that DBS improves motor function and controls levodopa-related motor complications in PD for over 10 years and longer (Limousin & Foltynie, 2019; Mahlknecht et al., 2022). But there are also limitations using DBS: Stimulation-induced side effects like dysarthria (Tripoliti et al., 2011) as well as incomplete understanding on how to optimize stimulation programming for gait improvement in current DBS therapy make further development inevitable (Habets et al., 2018; Limousin & Foltynie, 2019). Usually, with conventional DBS, fixed parameters delivering continuous stimulation are set by a clinician during outpatient visits regardless of the patients' real-time needs ('open-loop' DBS) (Lozano et al., 2019). In order to tackle these issues, closed-loop, responsive, or adaptive DBS (aDBS) is presently moved forward (Habets et al., 2018; Simon Little et al., 2016). As a classic closed-loop model, the goal of aDBS is to use oscillatory control signals indicative of the patient's real-time clinical state which will be used to adjust the stimulation to reduce side-effects and save energy (Bronte-Stewart et al., 2020; Habets et al., 2018; Little & Brown, 2020). A multicenter clinical trial is currently evaluating the efficacy and safety of aDBS in both clinical and home settings, following pilot studies that have already demonstrated aDBS to be superior to cDBS in terms of improved motor function, better side effect control and lower stimulation energy requirements (Bronte-Stewart et al., 2023). As of now, the main challenge is to identify the input/control variable and define a closed loop strategy.

Different input signals such as surface electromyography (EMG), tremor using accelerometers and cortical signals such as electrocorticography have been considered. Currently, subcortical signals recorded in the basal ganglia, known as local field potentials (LFPs), appear to be the most promising input signal, as they correlate with the patient's clinical state and cardinal motor symptoms (Arlotti et al., 2016; Kühn et al., 2009). The fact that STN-LFP activity patterns and STN-LFP responses to DBS remain stable for years after DBS electrode implantation allows the use of LFP as a long-term feedback signal for adaptive DBS (Anderson et al., 2021; Fasano et al., 2024).

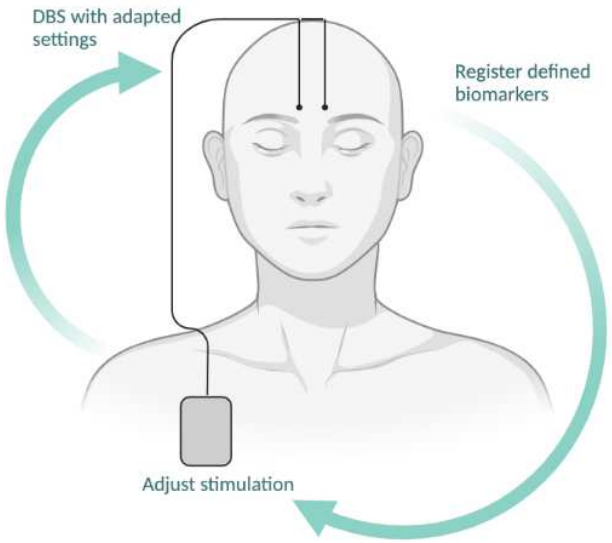

Figure 2. Closed-loop DBS model illustrating real-time feedback integration for adaptive stimulation.
Figure created with Biorender.com

1.4 Neuronal activity in Parkinson's disease

In recent years, more and more attention has been drawn to the pathological neuronal activity in PD (Halje et al., 2019). Brain activity, measurable by EEG or LFP, is usually divided into different frequency sub-bands: delta (0–3 Hz), theta (4–7 Hz), alpha (8–12 Hz), beta (13–30 Hz) and gamma (31–80 Hz) (Berger, 1929; Jasper & Andrews, 1936). The relaxed waking state is typically characterised by alpha waves, the dominant oscillations in the brain (Klimesch, 2012). Beta activity is especially important in the context of motor control, decreasing during the preparation and the execution of voluntary movements (Jasper & Penfield, 1949).

Exaggerated oscillatory activity of neurons in the basal ganglia seems to be a hallmark of PD (Brown et al., 2001; Halje et al., 2019; Kühn et al., 2008; Poewe et al., 2017). LFPs are recordings that reflect summed potentials of a neuronal population, typically centred around an electrode in the case of DBS. Traditionally, LFPs are interpreted within a framework that focuses on their frequency characteristics centred around the frequency bands just described (Brown et al., 2001; Einevoll et al., 2013; Herreras, 2016).

Several studies have already investigated LFPs in Parkinson's patients finding that PD is characterized by widespread synchronized oscillatory activity, mostly in the beta band (10 to 35 Hz) within the circuits connecting the basal ganglia, thalamus, and cortex (P. Gatev et al., 2006). Oscillations that affect large parts of these neuronal networks - particularly visible in exaggerated beta synchronisation at rest - appear to be associated with the typical motor Parkinson's symptoms, their development and severity (P. Gatev et al., 2006; Hammond et al., 2007; Khawaldeh et al., 2022).

There are multiple studies linking dopaminergic medication and DBS to suppressed beta activity and vice versa (Brown et al., 2001; Priori et al., 2004; Quinn et al., 2015). Clinically, reduction of beta activity by dopaminergic therapy or DBS presents with improvement of bradykinesia and rigidity (Feldmann et al., 2021; Kühn et al., 2008; Kühn et al., 2006; Quinn et al., 2015). Furthermore, beta activity correlates with motor impairment over the long term, hence it is being considered as potential biomarker for aDBS (Neumann et al., 2017). When talking about beta activity, it should be mentioned that the beta band can be further subdivided into high and low beta with some different clinical implications. Low beta activity (13-20 Hz) is more sensitive to antiparkinsonian medication, therefore higher in patients off medication and decreases with the administration of levodopa (Mathiopoulou et al., 2024; Priori et al., 2004). A correlation was found between oscillatory activity in the STN and symptom severity in PD, with mean activity in the low beta band (13-20 Hz) correlating significantly with bradykinesia (Feldmann et al., 2021; Neumann et al., 2016). An improvement in motor function was achieved by increasing stimulation amplitude of DBS and thus decreasing activity in the low beta band (Feldmann et al., 2021). Whereas low beta plays a more local (intraregional) role, high beta (21-35 Hz) seems to be more related to communication of more distant brain areas (Yin et al., 2021) and interpreted more as physiological and prokinetic rather than pathological (Ozturk et al., 2020). High beta has been hypothesized as an electrophysiological manifestation of the hyperdirect pathway, which connects the cortex to the basal ganglia via the subthalamic nucleus (STN). Exaggeration of this pathway's

activity may contribute to subcortical synchrony in the lower beta band, potentially implicating it in the oscillatory network dysfunction observed in Parkinson's disease (Oswal et al., 2020).

In general, human movements entail alterations in oscillatory neural activity throughout the basal ganglia thalamo-cortical network , where movement-related suppression of alpha and beta oscillations occurs alongside heightened gamma power indicative of active information processing in the sensorimotor cortex, STN, and GPi (Brittain & Brown, 2014; Pfurtscheller & Lopes da Silva, 1999; Pfurtscheller et al., 1993). Alpha and beta oscillations within the basal ganglia thalamo-cortical network are commonly labeled as "anti-kinetic" signals due to their prominence during periods of motor inactivity (Engel & Fries, 2010; Stolk et al., 2019). Nevertheless, the precise functional significance of these oscillatory activity alterations, particularly which signals are indispensable for actual movement execution, remains inadequately understood (Cross et al., 2021), a crucial aspect for understanding movement disorders like Parkinson's disease and specific motor symptoms such as Freezing of Gait.

1.5 Freezing of gait as an unmet symptom of Parkinsons's disease

Freezing of Gait (FoG) is a prevalent and burdensome symptom, impacting approximately 40% of individuals in early and up to 80% in the advanced stages of PD (Tan et al., 2011). A universally accepted definition entails the "*brief, episodic absence or marked reduction of forward progression of the feet despite the intention to walk*" (Nutt et al., 2011), with patients frequently experiencing the feeling as if "*their feet get glued to the ground*" (Bloem et al., 2004; Gao et al., 2020; Giladi & Nieuwboer, 2008). Most FoG episodes last less then 10 seconds and only very few longer than 30 seconds (Schaafsma et al., 2003). The presentation of FoG can be differentiated according to its clinical manifestation – more precisely based on the type of leg movement - into three different types: shuffling forward with small steps, trembling in place or total akinesia (Bloem et al., 2004; Salomon et al., 2024), of which the first two are the most common manifestations (Schaafsma et al., 2003). Another categorisation considers the

circumstances under which freezing occurs. By far the most FoG events are triggered by turning movements, followed by freezing episodes during forward walking and rarely during initiation of gait (Salomon et al., 2024). Other provoking factors include walking through narrow spaces, as well as cognitive stressors like performing a secondary task while walking. It is more common in the medical off-state and occurs more frequently with disease progression (Bloem et al., 2004; Schaafsma et al., 2003).

FoG is identified as one of the most important contributors to falls in PD patients (Canning et al., 2014; Okuma et al., 2018) and significantly reduces health-related quality of life (HRQoL) (Moore et al., 2007). Risk factors for FoG are gait disorders, PIGD phenotype and lower striatal dopamine active transporter uptake (Gao et al., 2020).
Regarding its treatment, levodopa replacement therapy remains the cornerstone of its remedy. In patients whose FoG worsens due to fluctuations in dopamine levels caused by oral administration, a continuous intra-jejunal infusion of Levodopa Carbidopa Intestinal Gel (LCIG) is an effective advanced therapy, as it provides a constant plasma levodopa level (Shackleford et al., 2022). Non-pharmacologically, behavioural approaches such as obstacle training on a treadmill, general exercise or conventional physiotherapy have been shown to be efficacious in reducing FoG symptoms (Kwok et al., 2022).

The pathophysiology and therefore the neuronal correlates of FoG are still not well understood. This is partly because the neuronal correlates of FoG were not measurable in the STN in freely walking patients until recently. Measurements were only possible in virtual reality or while walking on the spot and only few research groups were able to detect proper FoG in their experiments. The results are therefore not fully transferable to real conditions and can only be interpreted under this premise. In addition, it has only been possible to analyse the period immediately before the occurrence of a FoG to a limited extent and thus investigate the transition phase and possible preceding abnormalities. New technical innovations therefore appear promising to provide new insights that will

contribute to a better understanding of FoG. Hitherto, it seems to be a combination of different network failures (Falla et al., 2022). However, there are theories based on the assumption that Parkinson's disease is a complex network disorder that impairs cognitive processes (Uhlhaas & Singer, 2006). Different points within these functional networks play a role in regulation, and the imbalance of one or more of these pivotal points can trigger a significant disruption, potentially resulting in clinical symptoms like freezing episodes (Fasano et al., 2017; Weiss et al., 2015).

Nieuwboer et al. has summarised the triggering factors in four different models (Nieuwboer & Giladi, 2013):

1. The cognitive model posits that FoG results from an inability to resolve conflicting responses, indicative of executive dysfunction. While individuals under normal conditions delay response selection to resolve conflict, those with FoG exhibit faster decision-making but with increased incongruence, leading to the onset of FoG (Vandenbossche et al., 2012).
2. The interference model posits that the simultaneous processing of cognitive and limbic information during a motor task overwhelms the basal ganglia's information processing capacity, disrupting neuronal communication between motor, cognitive, and limbic circuits and ultimately leading to FoG. This disruption increases synchronization within the basal ganglia circuitry, resulting in excessive inhibition of the thalamus and pedunculopontine nucleus (PPN), thereby triggering locomotion interruption (Lewis & Barker, 2009; Lewis & Shine, 2016).
3. The threshold model suggests that as Parkinson's disease progresses, various motor and gait dysfunctions including reduced stride amplitude, impaired gait coordination, and increased variability of step timing accumulate, ultimately reaching a point of motor breakdown (Plotnik et al., 2012).
4. The decoupling model posits that FoG occurs due to a disconnection between the pre-planned motor program and the actual motor response (Jacobs et al., 2009).

Transitioning from the descriptive mechanisms that may lead to FoG to an electrophysiological analysis, it is useful to investigate the activity of the STN as the cornerstone of the locomotor network more in detail.

1.6 The neurophysiological approach to Freezing of Gait

Only little is known about the neurophysiological mechanisms underlying FoG and even less about the neurophysiological patterns preceding a freezing episode, leading to FoG. Neurophysiological studies reported abnormal STN dynamics in patients suffering from FoG (Georgiades et al., 2019; Syrkin-Nikolau et al., 2017). There is evidence that freezers present with increased activity in the lower beta band (12-22 Hz) during walking compared to standing, whereas non-freezers show a reduction in the entire beta band (12-35 Hz). This suggests that insufficient suppression in the lower beta band could trigger a freezing episode (Singh et al., 2013). Further studies confirmed the enhanced beta activity during freezing episodes and even demonstrated increased activity during gait that is more vulnerable to freezing (Chen et al., 2019; Storzer et al., 2017).

In previous studies, our own research group has intensively investigated upper limb freezing (ULF), a phenomenon that occurs with high co-incidence with FoG (Barbe et al., 2014) and appears to share similar spatiotemporal characteristics (Vercruysse et al., 2014). By investigating EEG measurements and repetitive finger tapping, it was observed that finger taps in the transition phase between normal finger tapping and ULF showed reduced beta modulation and instead pathologically increased synchronization in the beta band compared to regular finger tapping, which indicates that the clinical occurrence of ULF is preceded by pathological cortical motor processing (Scholten et al., 2020).

These results raise the question of whether similar abnormalities and mechanisms can also be observed in FoG. Furthermore, it would be interesting to know if similar neurophysiological abnormalities can be detected in the STN, which has recently become an analysable structure thanks to new stimulation devices.

The analysis of the transition phase itself is of great interest, as it appears to represent the beginning of a faulty process that is already detectable at the neurophysiological level but does not yet have a clinical correlate. In addition to providing insights into the underlying mechanisms of FoG, the investigation of this phase could help to predict freezing by identifying preceding markers - potentially useful from a therapeutic perspective for future closed loop strategies.

To investigate the temporal component and the transition phase preceding a freezing episode in more detail, knowing if and how beta activity is modulated over the gait cycle is essential to exactly differ between gait-associated dynamics and abnormal patterns associated with FoG. There is evidence that frequency bands show different gait cycle-locked modulation (Hell et al., 2018; Louie et al., 2022). STN power in alpha, beta, and gamma frequencies appears to increase before and around the point of terminal contact of the foot, in other words, during the double-support phase of the gait cycle (Hell et al., 2018). Another research group tested the hypothesis that beta activity is modulated over the gait cycle and tried to find out whether beta modulation is time-locked to the movement of the contralateral leg or synchronous in both STN. Activity in the upper beta band (20-30Hz) was modulated in each gait cycle, alternately and oppositely in both the left and right STN. In detail, oscillations in the high beta band decreased after ipsilateral heel strike (while the contralateral foot was raised) and increased after heel strike of the contralateral leg. Another interesting finding was that auditory cueing, associated with improvement of patients' gait, went along with enhanced beta modulation (Fischer et al., 2018).
To summarise, current evidence indicates a modulation of the different frequency bands over the gait cycle during normal walking. However, it is difficult to generalize these preliminary insights to real-world walking and FoG which means that patients should ideally be studied while walking freely.

1.7 Experiment and paradigm

Freezing of gait is a debilitating motor symptom in advanced PD patients, leading to massive restriction of patients' mobility, quality of life and resulting in falls, injuries, and hospitalization. The missing understanding of the underlying neurobiological mechanisms thus goes along with unexploited therapeutic options. Novel bidirectional stimulation devices which can record brain activity simultaneously while patients are walking now offer the possibility to access deep brain circuits and analyse neuronal signals in freely moving PD patients. Available since 2020, Medtronic's new Percept™ pulse generator enables for the first time the wireless acquisition of continuous LFP signals from patients outside the research environment, including during normal gait and freezing episodes. It allows clinicians to correlate symptoms such as FoG with oscillatory abnormalities not only intraoperatively or in virtual reality as has been done previously, but in real-to-life scenarios which helps establish biomarkers that precede the worsening of the patient's clinical state - possibly useful for future closed loop models (Jimenez-Shahed, 2021). These new technical achievements offer the opportunity to explore the pathophysiology behind FoG in more detail and thus hopefully improve the therapeutic options for patients in the future.

In our study, we leverage these capabilities to specifically investigate the neuronal characteristics of FoG-specific brain activity in PD patients, implanted with the bilateral STN-DBS Neurostimulator Medtronic Percept™.
We hypothesize that,

- Freezing of gait is measurable by LFPs in the STN in freely moving patients
- Freezing of gait is distinguishable from normal walking and voluntary stops based on LFPs in the STN
- the transition phase, the time immediately before FoG occurs, already shows neurophysiological abnormalities which can be recorded by LFPs in the STN and differ in the activity patterns before an arbitrary stop – as previous studies of our research group have shown that an upper limb freezing episode (comparable to FoG, only presented on the upper limb)

is preceded by reduced beta band power modulation and increased phase synchronization (Scholten et al., 2020).

2 Materials and Methods

Parts of the following methods presented here have already been published as ‘Supraspinal contributions to defective antagonistic inhibition and freezing of gait in Parkinson’s disease’ in Brain, in addition to this dissertation (Klocke et al., 2024).

2.1 Patients

We studied advanced PD patients, diagnosed according to the UK Parkinson Disease Brain Bank criteria (Hughes et al., 1992) who were classified as freezers according to established criteria published elsewhere (Snijders et al., 2012) and treated with bilateral STN-DBS (Medtronic Percept™ PC Neurostimulator). Patients were recorded at least 6 months after implantation to avoid influence of the stun effect (Tykocki et al., 2013). This effect arises from the acute intraoperative penetration of DBS implantation, which initially results in improvements in motor scores (Mann et al., 2009). Patients had to have electrode contacts in the subthalamic nucleus with sufficient signal quality of the STN-LFP during the screening session. Patients suffering from dementia or cognitive impairment as reflected by Montreal Cognitive Assessment (MoCA, < 17 points) were excluded from the study, as well as patients with a current moderate or severe depressive episode as assessed by the Beck’s Depression Inventory II (BDI II ≥ 24 points). Furthermore, independent walking of the patient was required and therefore orthopaedic or neurological conditions limiting the patient’s self-dependent gait led to exclusion from the study.

For clinical characterisation and verification of inclusion and exclusion criteria, a screening session took place the evening before the experiment when the patient was under current medication and stimulation (MedON, StimON). All patients underwent clinical examination, including the Movement Disorders Society Unified Parkinson’s Disease Rating Scale (UPDRS), Freezing of Gait Assessment Course (FOG-AC), Berg Balance Scale (BBS) and neuropsychological tests. Some of the tests were repeated on the next day, during the experiment, to obtain values in the medication OFF and stimulation

OFF state (MedOFF, StimOFF). A detailed list of the clinical data can be found in **Table 1.**

Recordings were collected after overnight withdrawal from dopaminergic medication (MedOFF) in the University Hospital of Tuebingen, Tuebingen, Germany. The Human Ethics Research Committee of the University of Tuebingen approved this study (*166/2020BO1)* and written informed consent was obtained from all patients according to the Declaration of Helsinki.

Table 1. Details of patients included.

Clinically affected hemibody was assessed based on MDS-UPDRS III items 3.3-3.9 during MedOFF/StimOFF; Levodopa equivalent dose was calculated according to Schade et al. (2020);† Based on patient history, initial PD symptoms started in the left hemibody – the right STN was therefore chosen as the disease dominant STN; * NFOG-Q: Patients are interviewed about the last few months which is why they may not have experienced FoG due to effective therapeutic management. BDI = Beck's Depression Inventory II; E = equivalent type; F = Female; FOG-AC = Freezing of Gait Assessment Course at Baseline; L = Left; LEDD = Levodopa equivalent daily dose; M = Male; MDS-UPDRS-III = Movement Disorder Society Unified Parkinson's Disease Rating Scale; n.a. = Data not available; motor examination; MoCA = Montreal Cognitive Assessment; NFOG-Q = New Freezing of Gait Questionnaire; R = Right; SEM = Standard error of the mean.

ID	**Sex/Age at onset,** *years*	**Disease duration at recording,** *years*	**Time since implantation,** *months*	**Subtype**	**MDS-UPDRS III** *MedON/StimON*	**MDS-UPDRS III** *MedOFF/StimOFF (at recording)*	**MDS-UPDRS III hemibody** *L / R*	**LEDD** *mg/d*	**NFOG-Q**	**FOG-AC** *MedON/StimON*	**MoCA**	**BDI**
01	M / 53	16	45	E	31	59	19 / 20	989	0*	0	27	9
05	F / 53	13	56	E	22	50	19 / 16	500	13	0	23	14
09	M / 61	11	10	E	25	55	17† / 17	596	n.a	4	25	20
10	M / 32	20	130	AR	37	61	17 / 22	513	20	2	29	13
11	F / 49	19	69	AR	17	33	9 / 13	1230	0*	0	28	15
13	M / 62	10	8	AR	32	26	11 / 6	556	23	n.a.	29	11
14	M / 63	9	10	E	17	44	12 / 15	600	17	2	26	10
15	F / 58	4	14	AR	28	46	16 / 14	554	19	12	29	14
17	M / 61	9	11	E	34	68	25 / 17	540	19	3	24	7

18	F / 41	22	8	AR	9	18	6 / 7	795	12	0	28	12
19	F / 66	8	27	A R	21	49	18 / 11	795	22	10	29	7
20	F / 53	13	8	E	31	59	24 / 13	780	7	4	27	7

Table 2. Additional motor, emotional and cognitive characteristics of patients included.
MDS-UPDRS = Movement Disorder Society Unified Parkinson's Disease Rating Scale; HADS = Hospital Anxiety and Depression Rating Scale; n.a. = Data not available.

ID	MDS-UPDRS *MedON/StimON*				Trail Making Test *MedON/StimON*		HADS *MedON/StimON*		Berg Balance Scale *MedON/StimON*	Push and Release Test *MedOFF/StimOFF*
	IA	IB	II	IV	Part A	Part B	Anxiety Score	Depression Score		
01	0	6	11	9	37	108	1	1	56	3
05	3	6	15	2	68	150	9	1	53	3
09	n.a.	n.a.	n.a.	n.a.	39	158	n.a.	n.a.	49	3
10	2	1	13	10	34	57	3	8	50	3
11	0	6	6	15	40	45	8	7	54	3
13	3	8	18	9	40	106	1	1	52	1
14	6	11	17	8	95	147	2	3	48	2
15	5	14	16	1	32	62	13	6	51	4
17	1	0	10	0	58	156	0	1	53	3
18	2	8	8	8	46	88	8	2	54	3
19	0	7	11	5	32	61	2	2	49	n.a.
20	2	1	8	4	32	80	3	5	55	4

2.2 Final cohort

Informed consent and signatures were obtained from 20 patients who agreed to participate in the study. After screening these patients for eligibility, two patients did not meet the specified inclusion/exclusion criteria (ID02: BDI ≥ 24; ID04: LFP sensing not possible due to compatibility issues with pre-existing lead extension cable). As a result, the remaining 18 patients were enrolled in the study and participated in the experimental recording sessions. Among these, one patient discontinued the recording due to fatigue during the medication off-state and did not complete any of the experimental gait tasks (ID12). An additional five data sets were lost for analyses due to malfunctioning of inertial sensors (ID03, ID06 - ID08, ID16). Consequently, the final analysis was conducted on a cohort of 12 patients with complete data sets (**Figure 3**)

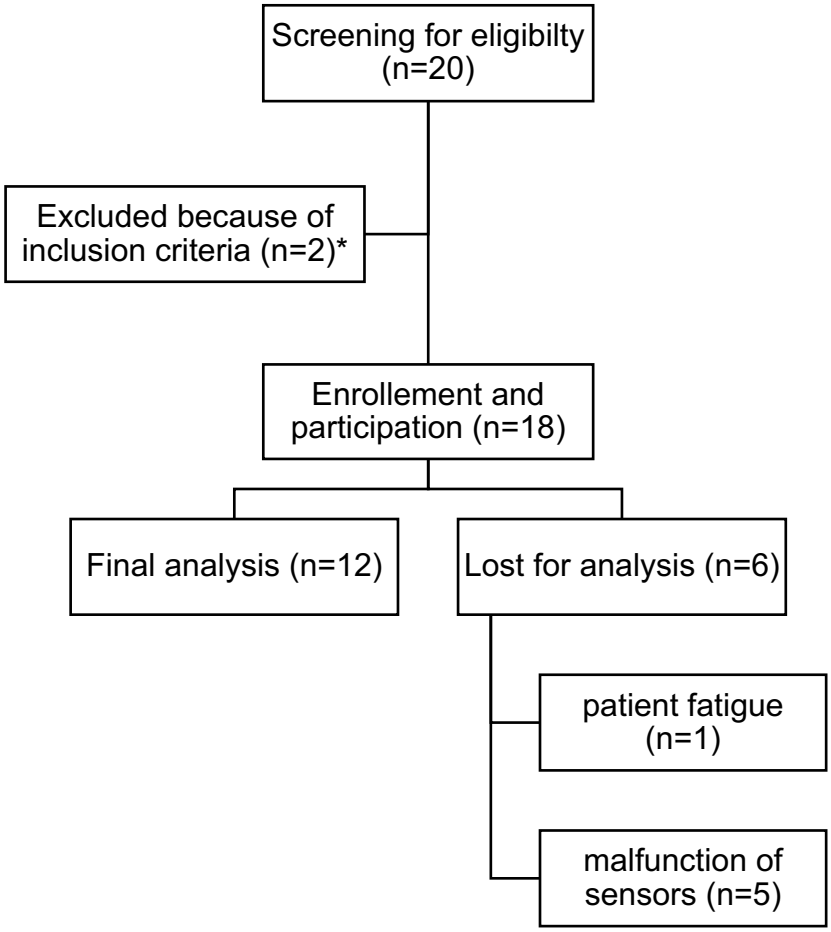

Figure 3. Consort diagram.
* ID02: To many points in the BDI (Beck's Depression Inventory), ID04: Incompatibility of the existing cable and measuring method.

2.3 Surgical procedure and electrode position

All patients included in the analysis cohort had previously undergone implantation of STN stimulation devices (**Table 4**). These devices were either lead model 3389 (n=4), model 3387 (n=1), or the more recent SenSight™ models B33005 (n = 4) and B33015 (n = 3), (Medtronic Inc., MN, USA). Both the 3387 and 3389 models are equipped with four platinum iridium cylindrical contacts, each measuring 1.5 mm in length. The contacts on the 3387 model are placed 1.5 mm apart, while on the 3389 model, they are spaced 0.5 mm apart. The SenSight™ directional lead model shares similar specifications, except for a slightly larger diameter of 1.36 mm and an electrode configuration of 1-3-3-1. The individual contacts on the SenSight™ lead can be either 1.5 mm or 0.5 mm in length. For consistency, the contacts on all leads were conventionally labeled, with the lowermost ones designated as 0 and the uppermost ones as 3 on each side.

The primary objective of the procedure was to specifically target the posterolateral segment of the STN, known for its involvement in motor functions. Additionally, the depth at which the electrodes were eventually placed was adjusted to accommodate patients primarily experiencing gait and postural symptoms. For these patients, the lowermost contacts of the electrodes were positioned at the lower boundary of the STN eventually reaching the SNr region (Weiss et al., 2013). It is important to emphasize that while there were variations in the depth of electrode placement among patients, the surgical trajectory leading to the final target within the STN remained consistent, regardless of the specific clinical phenotype (Milosevic et al., 2020). Prior to the surgical procedure, patients underwent whole brain magnetic resonance imaging (MRI), including pre-operative axial 3D-T1, T2 and susceptibility weighted (SWI) MRI images used for stereotactic targeting.

By employing a combination of pre-operative MR images and post-operative CT images, the localization of contacts was evaluated using an automated fusion algorithm known as iPlan 3.0 stereotaxy, developed by BrainLab Inc. in Munich, Germany. This algorithm was used to reconstruct the placement of the DBS

electrode. The coordinates of each bipolar sensing contact on each electrode were recorded in reference to the AC-PC line. Specifically, these coordinates represent the lateral position (x) relative to the midline in millimeters, the posterior position (y) relative to the mid-commissural point, and the inferior position (z) relative to the inter-commissural plane (**Table 5**). We successfully verified the locations of sensing contacts in all patients except for one (ID15) whose left stimulation electrode did not traverse the STN. Since this contact did not correspond to the disease dominant STN, it was excluded from subsequent analysis. Averaged localization of the centre of gravity of the bipolar sensing contacts relative to the midcommisural point are shown in **Table 3**.

Table 3. Averaged stereotactic coordinates of active electrodes.
Coordinates are shown in mm as mean ± SD in relation to the AC-PC line (mm) lateral to the midline (x), posterior to the mid-commissural point (y) and inferior to the inter-commissural plane (z).

	x	*y*	*z*
Left Side	12.4 ± 1.8	3.1 ± 1.8	4.1 ± 2.4
Right Side	11.1 ± 1.7	3.0 ± 1.7	3.6 ± 2.6

Table 4. Stimulation devices and implantation details.

ID	Implantation Site	Electrode Right STN	Electrode Left STN
01	Left Infraclavicular	Model 3389	Model 3389
05	Left Infraclavicular	Model 3389	Model 3389
09	Right Infraclavicular	SensightElectrode	SensightElectrode
10	Left Infraclavicular	Model 3389	Model 3389
11	Left Abdominal	Model 3389	Model 3389
13	Right Infraclavicular	SensightElectrode	SensightElectrode
14	Right Infraclavicular	SensightElectrode	SensightElectrode
15	Right Infraclavicular	SensightElectrode	SensightElectrode
16	Left Infraclavicular	SensightElectrode	SensightElectrode
17	Right Infraclavicular	SensightElectrode	SensightElectrode
18	Right Infraclavicular	SensightElectrode	SensightElectrode
19	Right Infraclavicular	Model 3387	Model 3387
20	Right Infraclavicular	SensightElectrode	SensightElectrode

Table 5. Contact details of all patients included.
*For this electrode the position in the STN could not be confirmed.

ID	Contact	Direction	Medio-lateral (x)	Direction	Anterior-posterior (y)	Direction	Superior-inferior (z)	Direction
1	1	Left	11.13	Left	4.66	Posterior	6.22	Inferior
	3	Left	12.18	Left	1.67	Posterior	2.49	Inferior
	1	Right	10.75	Right	3.86	Posterior	4.69	Inferior
	3	Right	11.95	Right	0.95	Posterior	0.83	Inferior
5	0	Left	11.89	Left	4.22	Posterior	6.38	Inferior
	3	Left	14.22	Left	0.81	Posterior	0.19	Superior
	0	Right	9.31	Right	5.48	Posterior	2.93	Inferior
	2	Right	10.7	Right	2.31	Posterior	0.02	Inferior
9	1	Left	12.5	Left	2.81	Posterior	5.43	Inferior
	3	Left	15.27	Left	0.56	Posterior	1.23	Inferior
	1	Right	11.74	Right	2.57	Posterior	4.2	Inferior
	3	Right	13.18	Right	0.39	Posterior	1.12	Inferior
10	0	Left	10.4	Left	0.97	Posterior	7.8	Inferior
	2	Left	11.38	Left	0.61	Anterior	4.76	Inferior
	0	Right	11.91	Right	4.56	Posterior	6.48	Inferior
	2	Right	13.39	Right	1.67	Posterior	2.54	Inferior
11	1	Left	9.7	Left	6.13	Posterior	6.18	Inferior
	3	Left	10.76	Left	4.49	Posterior	3.31	Inferior
	1	Right	9.91	Right	4.72	Posterior	3.97	Inferior
	3	Right	11.55	Right	1.5	Posterior	0.69	Inferior
13	0	Left	11.79	Left	6.36	Posterior	5.72	Inferior
	2	Left	14.01	Left	3.39	Posterior	1.13	Inferior
	1	Right	11.98	Right	5.96	Posterior	3.51	Inferior
	3	Right	12.3	Right	4.26	Posterior	1.71	Inferior

14	1	Left	9.23	Left	3.93	Posterior	6	Inferior
	3	Left	11.61	Left	1.63	Posterior	2.31	Inferior
	1	Right	10.29	Right	3.21	Posterior	4.86	Inferior
	3	Right	13.41	Right	0.55	Posterior	1.79	Superior
15	1*	Left	13.83	Left	3.14	Posterior	6.67	Inferior
	3*	Left	16.12	Left	1	Posterior	1.25	Inferior
	1	Right	10.21	Right	2.34	Posterior	4.78	Inferior
	3	Right	12.84	Right	0.61	Posterior	1.45	Superior
17	1	Left	12.95	Left	3.8	Posterior	4.23	Inferior
	3	Left	15.49	Left	1.67	Posterior	1.27	Inferior
	0	Right	7.56	Right	5.05	Posterior	8.65	Inferior
	2	Right	10.18	Right	3	Posterior	3.16	Inferior
18	1	Left	10.98	Left	4.36	Posterior	6.25	Inferior
	3	Left	12.13	Left	2.87	Posterior	3.05	Inferior
	1	Right	8.45	Right	3.61	Posterior	7.15	Inferior
	3	Right	10.91	Right	2.3	Posterior	2.4	Inferior
19	0	Left	11.99	Left	5.74	Posterior	4.9	Inferior
	2	Left	13.22	Left	2.37	Posterior	0.39	Inferior
	0	Right	11.39	Right	3.51	Posterior	6.75	Inferior
	3	Right	13.85	Right	2.01	Anterior	0.13	Superior
20	1	Left	11.15	Left	2.48	Anterior	7.8	Inferior
	3	Left	12.79	Left	5.18	Posterior	4.6	Inferior
	8	Right	8.64	Right	5.59	Posterior	9.25	Inferior
	11	Right	10.46	Right	2.69	Anterior	4	Inferior

2.4 Experimental protocol

Patients were investigated in the morning at least 12 hours after their last dose of dopaminergic medication and at least twenty minutes after turning off the stimulation, providing a washout-period between DBS ON- and OFF-state to reduce the effects of the preceding setting (S. Little et al., 2016). Patients were recorded in a sequence of different conditions. First, 'Sitting' with eyes open for 120 s. Then 'Standing' with eyes open for 120 s, followed by the 'Walking' tasks. Between each task, the patient could take a short break. For the walking conditions, patients walked back and forth at a self-selected speed in a 15 m long and 2.5 m wide corridor, which was additionally narrowed by two obstacles (ca. 1 m wide) to help trigger FoG. Firstly, 360 s of regular 'Walking' was recorded. Afterwards, the subjects were instructed to make multiple voluntary stops while walking, stand still for a few seconds and to tell the instructor, that it was a self-selected 'Stop'. This procedure – as one of several criteria - helped distinguish 'Stop' from 'FoG' in the later evaluation. In a final gait test, patients had to walk again for 360 s while simultaneously performing a serial subtraction task (cognitive interference). Throughout the entire experiment, a 2D colour video camera (Sony Handycam DCR-HC52, resolution: 0,7MP) was set up to film the experiment while kinematics, LFP and electroencephalography (EEG) were measured synchronously. A setup of the whole experiment is shown in **Figure 4.**

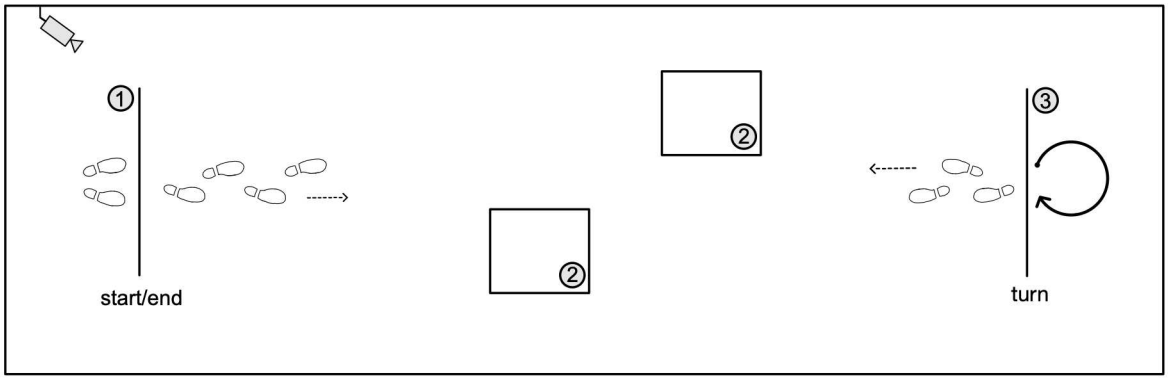

Figure 4. Experimental setup.
The patient begins at position (1) and walks along the hallway, navigating through two obstacles at position (2), and turns around at the marked line (3). He then retraces the same path back to position (1), turning around again, and continues this cycle until the given time expires.

2.5 Data acquisition

2.5.1 Overview of collected data traces and data alignment

For every single condition (Sitting, Standing, Walking, Walking with Stops and Walking with interference) a new recording was started. First, the EEG recording was switched on, which was automatically synchronised to the video. Then the IMUs were turned on and the last data track were the LFPs. Synchronisation of gait kinematics and EEG data was achieved by a custom-built setup, which made it possible to visualise the starting point of the kinematics in the EEG (M1).

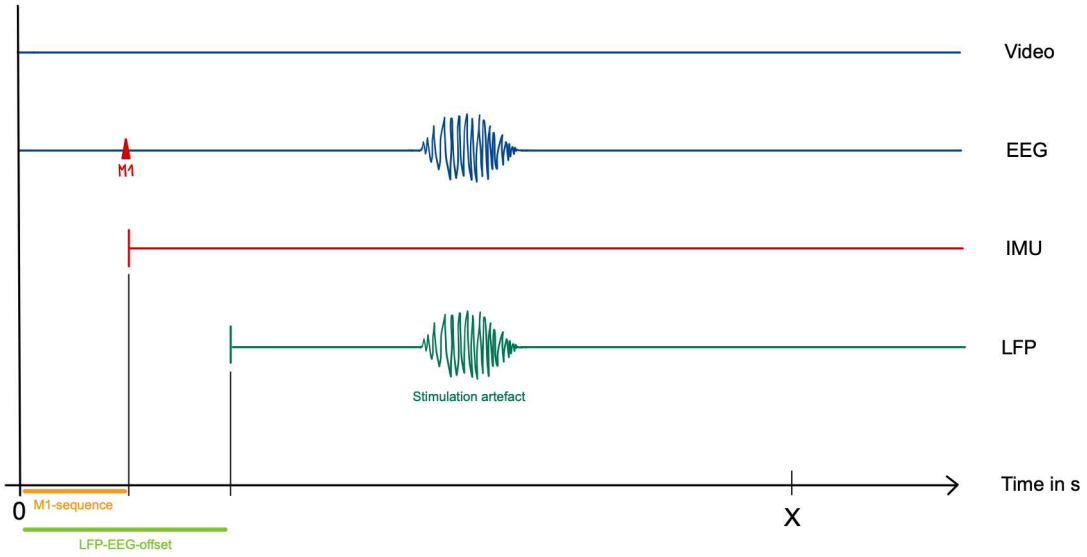

Figure 5. Data traces collected in each experiment.
For each patient, we simultaneously recorded an electroencephalogram (EEG), local field potentials in the STN (LFP), and kinematic data (IMU = inertial measurement units), along with a video.

To synchronize the EEG (and thus as part of this also the ECG signal) and LFP data, a ~5s stimulation train was delivered at the beginning of each recording (1mA, 125 Hz, 100 µs; 'ramping' option deactivated) and its corresponding patterns were used for alignment. When the stimulation was switched on, associated abruptly starting and ending oscillations frequency of the stimulation could be detected in the EEG. In the LFP dataset, the onset and termination of stimulation were represented by biphasic ~0.5 s long transition artefacts of high amplitude and opposite polarity (**Figure 6**). The transition artefact, visible in the

LFP dataset, when the stimulation was turned off, was used for alignment (Thenaisie et al., 2021). It begins with a voltage drop, which in turn is accompanied by the abrupt end of the artefact signal in the EEG. Slight temporal shifts, but usually not exceeding 20 ms, can occur due to inaccuracies in the manual extraction of the time points of both signals.

By first synchronizing the EEG signal with the IMU signals and subsequently with the LFP recordings, we achieved precise temporal alignment of all signals. Generally, any temporal discrepancies in the alignment did not surpass 20ms.

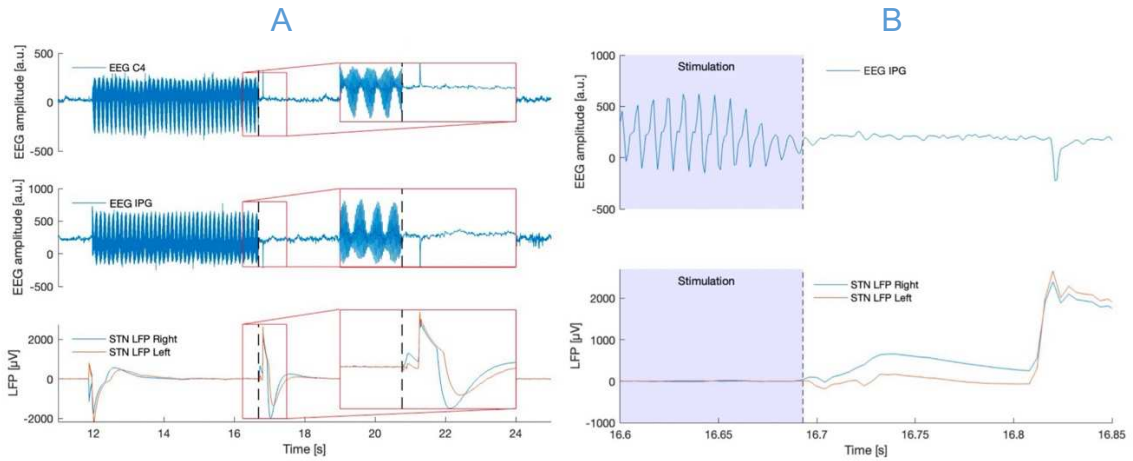

Figure 6. Alignment of LFP and EEG recordings shown in patient 09 (Klocke et al., 2024).

(A) A DBS artefact was introduced by a short stimulation period (1 mA, 125 Hz, 100 µs) and recorded by BrainSense™ streaming. The EEG recording depicts bursts of activity linked to stimulation, while the LFP recording portrays the initiation and conclusion of deep brain stimulation through distinct high-amplitude transitional artefacts **(B)** The conclusion of the final stimulation pulse noted in the EEG recording (indicated by a vertical dashed line) aligns with the initiation of the transition artefact. This deflection can be observed around 120 ms after stimulation in both the LFP and EEG traces, facilitating precise temporal synchronization.

2.5.2 Kinematics

Movement parameters were recorded using wearable inertial measurement units (IMU, Opal, APDM Inc., Portland, OR, USA), which were positioned in a standardized manner for all subjects and tasks on both left and right ankles and on the lumbar spine (L5). In every sensor there was a three-axis accelerometer, a gyroscope and a magnetometer with X-, Y- and Z-axes pointing in the patients' viewing direction downward, to the right and forward, respectively. Data from the sensors were collected at 128 Hz (accelerometer range: ±6 g, gyroscope range: ±200 degree per second, magnetometer range: ±6 Gauss) and wirelessly and in real time streamed to a portable computer via an Access Point (Mobility Lab, APDM Inc., Portland, OR, USA). Data were exported in the hierarchical data format (HDF5).

Gait cycles were determined using the accelerometer signal along the anterior-posterior plane (x-axis) and the gyroscope signal in the medial-lateral direction (y-axis) with angular velocity represented in the sagittal. Corresponding to gait cycles which were defined as the period between the time points of two succeeding heel strikes (HS) identified in the accelerometer signal (x-axis) of the foot, obtained gait events were chosen. Those are Mid-Swing (MS), defined by the peak-angular velocity assessed by the gyroscope in the sagittal plane, toe-off (TO), defined as minimum acceleration in the anterior-posterior direction before MS and HS as the minimum acceleration after MS **(Figure 7)** (Scholten et al., 2017). Gait cycles lasting more than 2.5 seconds were excluded.

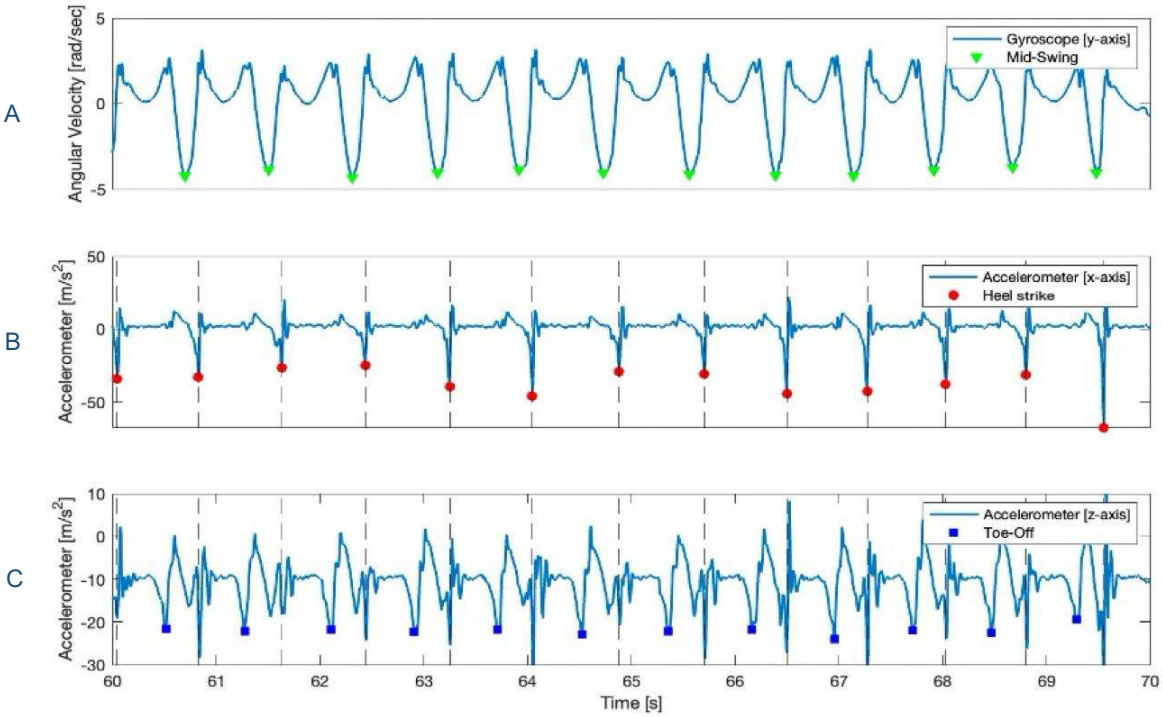

Figure 7. Analysis of the accelerometer and gyroscope.
(A) The Mid-Swing was detected by the peak-angular velocity in the sagittal plane, marked with green triangles. **(B)** The heel strike was identified in the x-axis of the accelerometer signal as the minimal acceleration after Mid-Swing, marked with red points. **(C)** In the z-axis, the Toe-off was identified as the minimum acceleration before Mid-Swing, indicated by the blue boxes.

2.5.3 Electroencephalography

During all tasks cortical electrophysiological activity was recorded using a wireless 48-channel scalp EEG (Brain products, MES Electronics, Gilching, Germany). EEG electrodes were positioned based on the 10-20 electrode system using an EEG cap (EASYCAP with classic actiCAP electrode holders, EASYCAP GmbH, Woerthsee-Etterschlag, Germany).

EEG electrodes were referenced to the right earlobe and a ground electrode was positioned at FPz. To record EMG data, additional electrodes (channels 49-56) were attached in a bipolar configuration on the tibialis anterior and medial gastrocnemius muscles of each leg. Another two more electrodes (channels 57-58) were applied on top of the IPG to capture DBS stimulations and electrocardiography signal (ECG). Data acquisition was synchronized to the internal clock of the device. Signals were acquired with a sampling frequency of

1000 Hz and impedances were kept below 5 kOhm. Raw data files were exported in BrainVision data format.

The EEG and EMG data were not relevant to the research question of this doctoral thesis but were collected to synchronise the data and for later potential analyses of the research group, which is why they are only briefly mentioned here.

2.5.4 Electrocardiography

To capture electrocardiography (ECG), two electrodes (part of the multichannel EEG system, as described above) were placed over the chest next to the IPG (Brain products, MES Electronics, Gilching, Germany). This signal was later used to control the quality of the LFP signal regarding potential ECG artefacts.

With the two electrodes we additionally recorded the DBS stimulation artefact, which was later used to align the data.

2.5.5 Local field potentials

LFPs were captured using the 'BrainSense^{TM} *streaming mode*', which limits sensing to a single bipolar contact pair for each STN. Prior to the initial recording session for each subject, we employed the Percept PC sensing feature in 'BrainSense^{TM} *survey mode*' and visually assessed the power spectral density (PSD) of each contact pair in the MedOFF/StimOFF state. The contact pair that exhibited the highest peak power in the beta range during resting state (while Sitting), as observed on the Clinician programmer tablet (CT900D, Medtronic Inc., MN, USA), was selected and maintained consistently for all subsequent experiments (**Table 6**).

In addition, we ensured that the selected contact pair was not categorized as an 'artefact' by the system and that neighbouring contacts did not exhibit significantly distinct frequency bands and modulations (Thenaisie et al., 2022). We adopted this approach considering the well-established observation that the highest beta activity within the subthalamic region is localized to the STN, specifically its dorsal "motor" region. This representation has been affirmed and reproduced through

intra-operatively microelectrode recordings of neuronal discharge and LFPs in PD patients. (Chen et al., 2006; Eusebio et al., 2011; Kolb et al., 2017; Kühn et al., 2005; Litvak et al., 2021; Tamir et al., 2020; Trottenberg et al., 2007; Weinberger et al., 2006; Yoshida et al., 2010; Zaidel et al., 2010). Subsequently, LFPs were captured using a bipolar recording channel (contact pairs 0-3, 1-3, or 0-2), at a sampling rate of 250 Hz. These recordings were then downloaded from the tablet and saved in a Java Script Object Notation (JSON)-format file for subsequent offline analysis.

Table 6. Patients' sensing details.
L = Left; R = Right; s = seconds, * For ID01, no beta peak was available, which is why a peak frequency within the alpha range was chosen (right STN).

ID	**Selected Contacts**	**Peak Frequency,** *Hz*	**Amplitude** *mA*
01	R: 1-3 L: 1-3	8.79* 20.51	0.9 1.24
05	R: 0-2 L: 0-3	19.53 18.55	1.2 0.78
09	R: 1-3 L: 1-3	14.65 18.55	3.93 2.29
10	R: 0-3 L: 0-2	24.41 13.67	0.78 0.56
11	R: 1-3 L: 1-3	18.55 27.34	1.0 0.9
13	R: 1-3 L: 0-2	18.55 18.55	0.92 1.75
14	R: 1-3 L: 1-3	15.63 22.46	0.66 0.9
15	R: 1-3 L: 1-3	18.55 17.58	2.32 0.85
17	R: 0-3 L: 1-3	14.65 12.70	2.14 1.32
18	R: 1-3 L: 1-3	19.53 17.58	1.31 1.05
19	R: 0-2 L: 0-3	12.70 14.65	3.08 0.51
20	R: 0-3 L: 1-3	23.44 18.55	1.47 1.88

2.6 Data analysis

2.6.1 Definition of gait events

All recorded video files were viewed using the VirtualDub 1.10.4 software (https://www.virtualdub.org/) for framewise video annotation. Sequences with start time and end time were extracted out of the video according to the definition of the different sequences such as *walking (Walk)*, *turning*, *self-selected stopping (Stop)*, *freezing (FoG)* and *transition phases* preceding a *FoG (Pre-FoG)* or *Stop (Pre-Stop)* episode. Freezing that occurred during turning or after a self-selected stop in the sense of a start hesitation were not considered. A detailed description of the individual sequences can be found in **Table 7**.

Table 7. Definition of gait events.

Event	Definition
Walking	A sequence of straight continuous walking, without turning motions, freezing or self-selected stop. Start point and end point is the heel strike (HS) of the right foot, containing all gait cycles in between.
FoG	Only FoG during straight line walking was considered. It was evaluated according to the definition of Nutt et al. (Nutt et al., 2011), described in detail in the introduction of this dissertation. Therefore, two independent raters selected sequences in the videos where forward progression was completely disrupted or severely impaired (Nutt et al., 2011). Only FoG, which was identified as such from both, was considered. They also classified whether the episode was predominantly akinetic or trembling-in-place like (Cockx et al., 2023). To further support the selection of freezing episodes based on the videos, we tried to use additional kinematic criteria. Therefore, we determined the Freeze Index (FI) for each FoG event, defined as the square of the area under the curve of the power in the 3-8 Hz band (freeze band), divided by the square of the area under the curve of power in the 0.5-3 Hz band (locomotor band) belonging to the leg's vertical acceleration signal. For each recording, a 4-s Hanning window with 50% overlap (Welch method) was used with the data rescaled to the range of 0 and 1. A freeze threshold for each subject was calculated as the mean ± 1 SD of the peak FI from nine epochs of Standing to differentiate between FoG and activity of volitional Standing (Mancini et al., 2017; Moore et al., 2008). Additionally, we assumed that FoG without an increase of FI might occur, especially in the akinetic type. For those few trials we evaluated the preceding gait cycles regarding cadence increase or consecutive amplitude reduction in the steps. The sequence effect derived from this indicates that FoG is more likely than, for instance, voluntary stops (Jorik Nonnekes et al., 2019). Together, all FoG episodes without FI increase and without observable sequence effect were excluded from analysis.

	The exact starting point was set to the last normal HS of either the right or left leg before FoG occurred. The end was defined as the HS initiating the first gait cycle after overcoming freezing and reinitiating or unaffected walking. Only episodes lasting for at least 1000 milliseconds were evaluated.
Stop	A voluntary stopping of the patient. At the beginning of the session, patients were instructed to consciously stop while straight line walking, stand still for a few seconds before reinitiating gait and verbally state that they had stopped voluntarily, recognisable later in the video. To support the video-based definition of our stops and to ensure that we clearly separated FoG and Stop episodes, we further analysed the energy spectrum and heart rate of the episodes. The energy spectrum for FoG and Stop episodes was calculated using the vertical linear acceleration of the foot. FoG episodes showed higher power in the 'freezing band' (3-8 Hz) compared to Stop episodes and were characterised by a constant heart rate, while stops showed a distinct drop in heart rate (Cockx et al., 2023). Moreover, we discarded all Stops that were closer than two gait-cycles to a turn or three gait-cycles to a freezing episode. Start of the self-selected Stop was defined as the HS of the foot leading to a closed standing position. The end of the Stop was chosen as the toe-off of the foot making the first step after the standing time, initiating Walking. Only Stops with a duration over 1000ms were included and we analysed the first 1000ms of each Stop.
Pre-FoG	A transition phase preceding the freezing episodes was defined as the last three gait-cycles before the start of the event. In case of slow walking patients, we included only gait cycles occurring 3000ms before FoG onset. We made this choice based on past research about upper limb freezing, showing that changes leading to upper limb freezing had abnormal brain activity up to three tap cycles before the freeze (Scholten et al., 2020).
Pre-Stop	According to Pre-FoG, the transition phase of a self-selected Stop was defined as the last three gait-cycles before stopping. In case of slow walking patients only gait cycles occurring 3000ms before Stop onset were considered.

The selected time points of determining the specific sequences were then transferred into MATLAB (v2022a, MathWorks, Nattick, MA, USA) and associated with exact gait events from the kinematics, respectively **(Figure 8**).

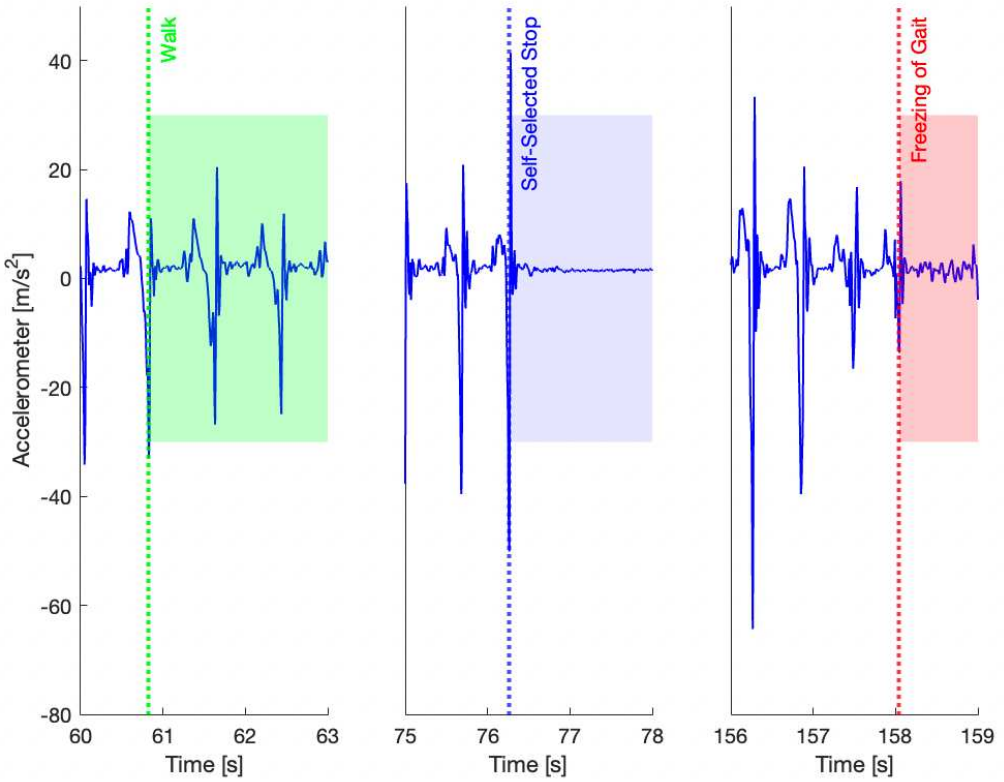

Figure 8. Identification and Segmentation of Gait Sequences: Reflections of Definitions in Kinematic Data.
The different sequences like Walking, Self-selected Stop, and Freezing of gait were identified within the video according to the specific definition (**Table 7**). The corresponding heel strikes to the noted starting and end time points were extracted, and the kinematics divided into different epochs.

2.6.2 Gait Characteristics: Spatial and Temporal Aspects

We computed both spatial and temporal gait parameters for each subject and gait condition in our study using the MobilityLab algorithm (APDM Inc. Portland, OR USA): cadence (steps/min), mean step time (s), relative stance time (in %, indicating the time from the initial heel strike to the toe-off of the same leg relative to the stride time), relative swing time (in %, representing the time from toe-off to the following heel strike of the same leg relative to the stride time), stride velocity (m/s), stride length (m) and peak angular velocity of the shank (°/s; the maximum angular velocity during the swing phase in the sagittal plane).

To ensure the analysis accurately represents the intrinsic characteristics of regular gait, we employed a median filter to remove outliers exceeding or falling below three standard deviations from the median value (Hausdorff et al., 2003).
Our reporting of gait parameters is structured according to the distinction between the leg predominantly impacted by the disease (disease dominant leg) and the less affected leg (non-disease dominant leg) during regular gait, as determined by the hemibody MDS-UPDRS III score (specifically, items 3.3-3.9 during MedOFF/StimOFF). When comparing gait parameters between regular gait and the Pre-FoG and Pre-Stop conditions, we exclusively considered data from the disease-dominant leg.
Gait cycles at the initiation of gait and those occurring three seconds prior to FoG or Stop as well as the first step before and after a turn were excluded from the analysis.

2.6.3 Preprocessing of LFP data

All data analyses were conducted using MATLAB (v2022a, MathWorks, Natick, MA, USA). Initially, both LFP and IMU data were resampled to a frequency of 1000 Hz to match the EMG and ECG reference signal. Subsequently, the LFP signals underwent high-pass filtering at 1 Hz using a 6th order Butterworth filter to eliminate low-frequency noise. Furthermore, each LFP recording was subject to thorough visual inspection and extensive exploration to identify and address ECG- and gait-related artefacts.

2.6.3.1 Gait-related artefacts

Previous studies investigating gait-related power modulation have predominantly relied on ambulatory EEG recordings. However, these EEG recordings have been susceptible to artefacts, such as those caused by heel strike-related mechanical perturbations or cable swingings which have posed analytical challenges (Kline et al., 2015; Nordin et al., 2018). Conversely, less attention has been devoted to addressing gait-related artefacts in recordings of LFPs obtained

from DBS electrodes. Nevertheless, we recognize the importance of rigorously controlling for these artefacts in LFP recordings.

In studies involving mobile PD patients engaged in walking experiments, the presence of gait-related artefacts has been a significant concern. For example, earlier research using EEG recordings reported the occurrence of broad-band frequency artefacts that were synchronized with heel strikes (Kline et al., 2015). Similarly, LFP recordings obtained using the previous Medtronic Activa PC+S® system during natural gait revealed low-frequency power modulation in both STN, regardless of laterality (Hell et al., 2018). This observation raised questions regarding whether these modulations might be attributable to artefacts rather than genuine neural activity. Unlike oscillatory neural activity, which typically does not exhibit consistent changes across broad frequency bands at a given time point, non-oscillatory, transient signals like gait-derived artefacts can display such patterns (Jacobsen et al., 2021).
Despite their potential to confound results, gait-related artefacts have been addressed rigorously in only a limited number of studies. Therefore, prior to further steps, we conducted a series of control analyses to ensure the absence of heel strike-related artefacts that could have compromised our data.

We initiated the analysis by selecting sequences of regular Walking and examined the raw LFP signals from both STNs. Simultaneously, we overlaid the time points corresponding to right and left heel strikes with the accelerometer signal from both feet to identify any substantial deflections in the LFP recordings that coincided with heel strike events (**Figure 9**).

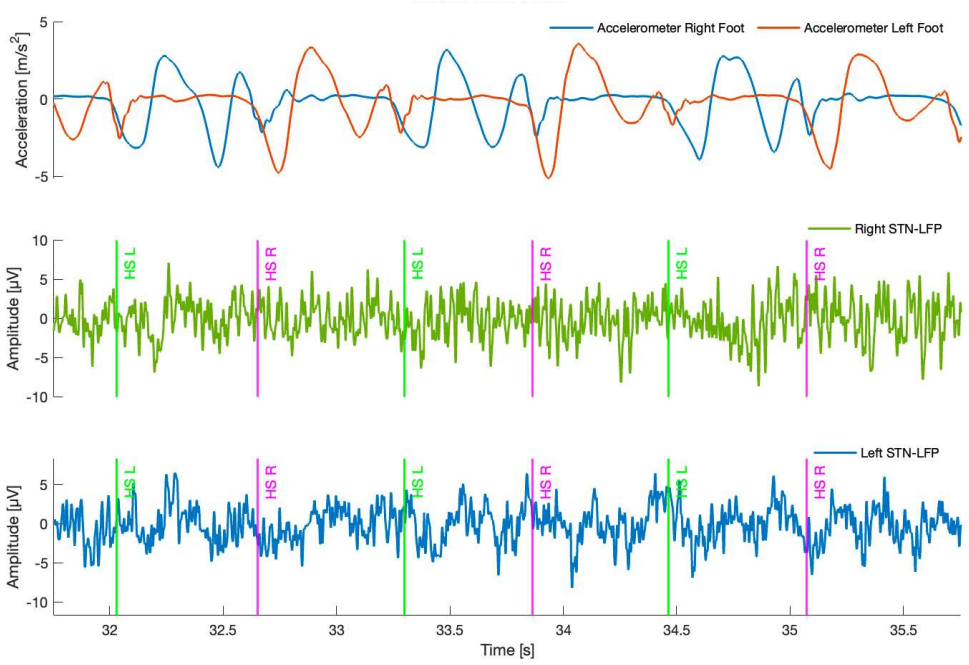

Figure 9. Example of synchronized kinematic data and raw LFP time series during regular gait.
The upper panel shows the accelerometer of the right (blue) and left (red) foot. The lower panels show the raw LFP signal of the right STN (in green) and the reft STN (in blue). Time points of heel strikes in the LFPs are indicated by vertical lines - HS R: Heel strike of the right foot, HS L: Heel strike of the left foot. No heel strike-related Amplitude changes can be found here (dataset of ID10 - Walk).

Following a careful review of the raw STN time series, we examined the time-frequency domain using Morlet continuous wavelet transformation (CWT) in the next step. Leveraging the heel strike time points, we extracted individual gait cycle epochs from the CWT matrix, spanning from left heel strike to the subsequent left heel strike (full gait cycle). These epochs were then resampled up to 1000 data points, each corresponding to a time bin representing 0.1% of the gait cycle to allow comparison across a multitude of gait cycles.

To visualize fluctuations in power concerning the baseline frequency spectrum (referred to as event-related spectral perturbation, ERSP), we subtracted the average frequency spectrum of the entire gait cycle from each gait cycle's CWT matrix at each time point. The resulting matrices were averaged within each subject to generate an average time-frequency plot. We systematically searched

for broad band power increases that aligned with the heel strikes of either foot **Figure 10**.

Upon comprehensive examination of all ERSPs in patients and trials involving regular gait activity, we did not observe any significant broadband power increases attributable to heel strike motions. The absence of gait-related artefacts may be due to differences in recording modalities, as LFPs are recorded directly from neuronal tissue in subcortical layers, whereas EEG is typically measured at the scalp, resulting in different signal-to-noise ratio.

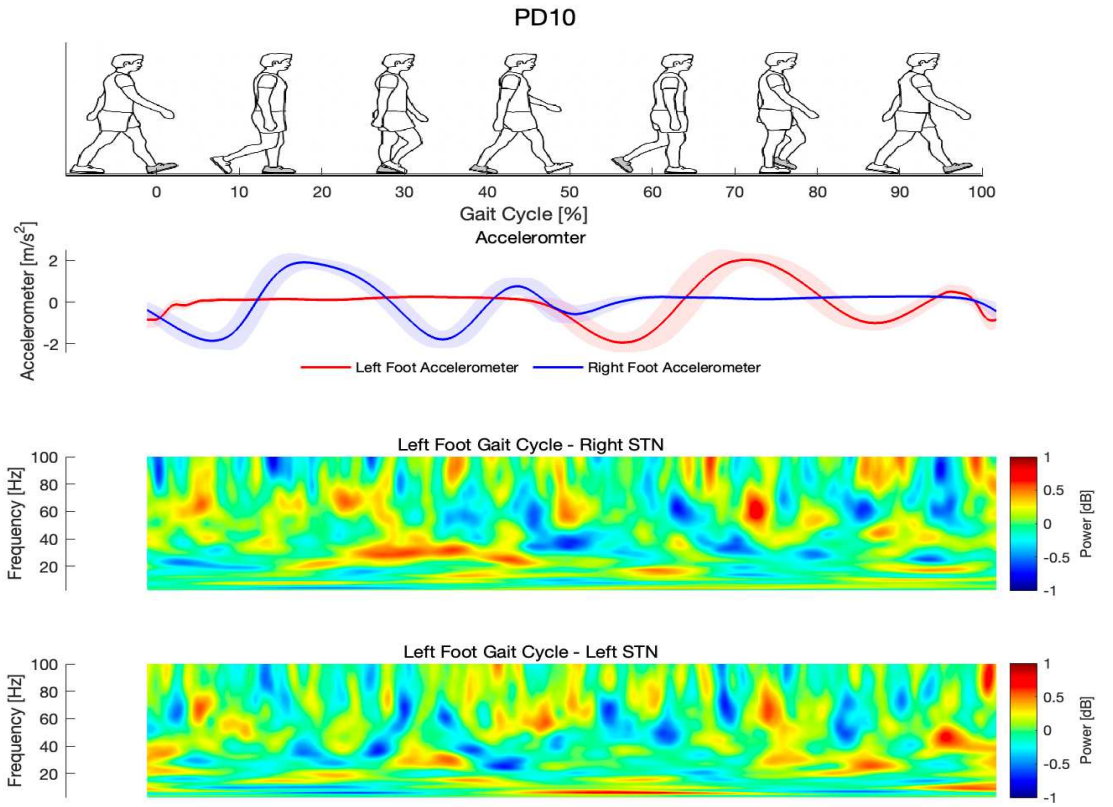

Figure 10. Exemplary control for movement-related artefacts in a representative patient (ID10).
At the top of the figure, a complete gait cycle is displayed (in this case, for the left leg). The second uppermost panel shows the average gait cycle computed from heel strike to heel strike (mean ± standard deviation) for the left foot accelerometer signal (red), alongside the contralateral right leg (blue). The lower two panels each display the corresponding ERSP plot for the right and left STN, respectively. Notably, there is no evidence of gait-related artefacts which would present as broad band activations corresponding to a heel strike.

2.6.3.2 Electrocardiography related artefacts

To obtain a pure electrical signal of brain activity, it is necessary to check whether other sources of electrical activity are influencing the measurement. Since the human heart contracts as a result of electrical excitation, we checked our data for ECG artefacts (Neumann et al., 2021).

Previous reports using the Medtronic Percept device have noted the presence of ECG artefacts when stimulation is turned on, especially with left subclavicular implant locations (see **Table 4** for implant location of our cohort) due to the greater proximity of the device to the cardiac dipole (Neumann et al., 2021; Thenaisie et al., 2021). To address this, we first conducted a thorough visual inspection of each LFP dataset to identify potential ECG artefacts. To determine R-peaks - corresponding to a QRS complex - in the externally recorded ECG signal, we set a threshold at 2.5 times the standard deviation of the entire signal after z-scoring ($X-\mu/\sigma$) the data. These peaks also had to be at least 500 ms apart, equivalent to a heart rate of 120 beats per minute. To account for negative QRS complexes, we repeated the procedure after multiplying the signal with -1, and the peaks with the highest mean were used to determine the orientation of the QRS complex. Afterwards, we estimated the timestamps of potential R-peaks in the LFP dataset using the identified R-peaks in the ECG signal (**Figure 11**).

Considering the recurring nature of ECG artefacts within the LFP dataset due to the quasi-periodic pattern of QRS waves, we labeled LFP datasets as "contaminated with ECG artefacts" if they met specific criteria. These criteria included multiple consecutive R-peaks in the LFP dataset coinciding with those detected in the external ECG signal, a minimum of one R-peak every three seconds, and a heart rate of at least 40 beats per minute (Stam et al., 2023).

We identified ECG artefacts in all recordings of ID10, classified as minor due to their low amplitude contamination, where the tip of the QRS complex remained close to the level of neural activity (Neumann et al., 2021).

The algorithm developed by Stam and colleagues (Stam et al., 2023) detects the locations of the QRS complexes using the supplied ECG reference signal. It then

scans the LFP signal for potential deflections at these time points. Once R-peaks are identified in the LFP recording, epochs are created, including a window of 250 ms before and 400 ms after the R-wave, encompassing the PQRST complex. These epochs are averaged to create an initial template, which is further optimized for each epoch to minimize the sum of squared errors between the original LFP signal and the initial PQRST template (**Figure 12**).

In the final step, the epoch-specific optimized template is subtracted from the corresponding epoch in the original LFP signal. This process results in a cleaned LFP signal without ECG artefacts (Stam et al., 2023). Analysis of the entire time series in the frequency domain using continuous wavelet transformation revealed decreased power in the low-frequency ranges (**Figure 12**).

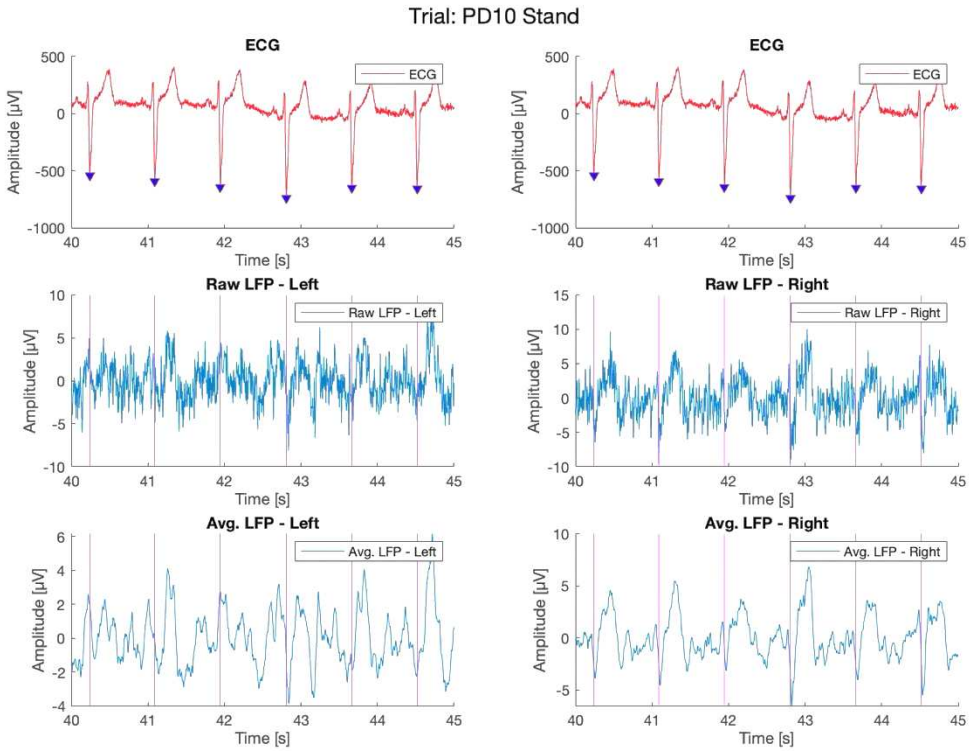

Figure 11. Example of ECG artefacts in the LFP signal of ID10.
R-peak timestamps were identified in the ECG recordings and marked with blue triangles. The corresponding time points and thus time points for possible ECG artefacts in the LFP signal were marked with purple lines. To facilitate detection during the visual inspection of the data, the LFP signal was averaged using a moving average filter (50ms).

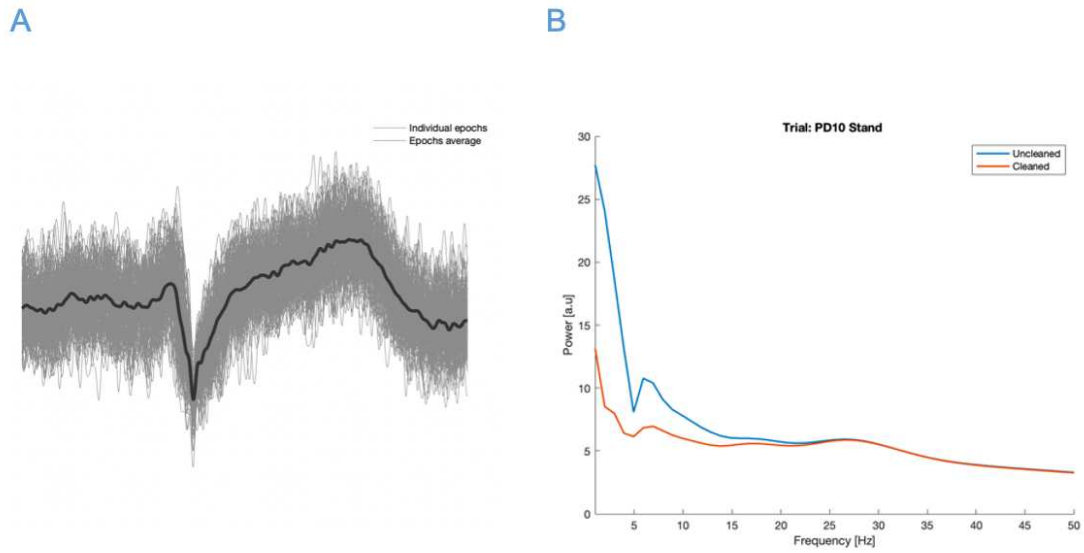

Figure 12. Intermediate steps of the artefact subtraction.
In (A), all individual epochs are displayed including the resulting average for the initial template (black). (B) LFP of ID10 before (blue) and after subtraction (red) of the template (Klocke et al., 2024).

2.6.4 Frequency domain analysis during different conditions

For analyzing signals like brain activity, there are different options regarding time frequency analyses. Fourier transformation is common but assumes signal stationarity. Short-term Fourier transform (STFT) and wavelet transform (WT) address this problem, but STFT has limited frequency resolution because it restricts frequency analysis to the window's width and can distort signal properties. WT offers flexibility but is computationally demanding. For intricate analysis, the continuous wavelet transform provides high-resolution time-frequency representation with near-continuous discretization, making it a powerful tool for real world data analysis (Arts, Lukas, 2022, Lachaux 2002).

To visualize the power spectra of our data, we initially transformed the continuous STN recordings corresponding to the disease dominant STN using complex Morlet continuous wavelet transformation (CWT).
The CWT utilized wavelets spanning 6 cycles with frequencies spaced between 1 and 60 Hz (frequency resolution 1 Hz) (Matlab function: cwtft).

Next, we segmented the resulting CWT matrix into individual epochs by utilizing the respective starting and ending points of the events of interest, preserving their spectral distribution. In the case of a FoG/Stop episode, we decided to use the entire duration of the event to comprehensively capture spectral changes.

To ensure consistency and minimize the influence of electrode proximity and local tissue properties on absolute power, we computed relative power. This involved averaging across the time domain and then normalizing each spectrum by its own overall mean power across frequencies. We excluded low frequencies (up to 10 Hz) and other frequencies potentially contaminated by technical artefacts related to the sensing equipment (33–37 Hz, 48–52 Hz, >90 Hz) (Singh et al., 2013; Neumann et al., 2016; Storzer et al., 2017). Frequency domain spectra were log-transformed and compared to the baseline 'Standing'. Therefore, the Standing signal was partitioned into windows lasting 2 seconds each. Power spectra were computed for each window, underwent visual examination to identify any potential artefacts and subsequently averaged across nucleus and all windows.

2.6.5 Event-related Time-Frequency Analysis

To account for variations in the duration of gait cycles, we applied a time-warping technique to each gait cycle's time-frequency matrix at each frequency. This process created epochs with equal lengths that allowed epochs of different original lengths to be compared. After time-warping, each epoch contained 1000 samples which represented the relative progression of the gait cycle from 0% to 100%.

For episodes of FoG and Stop, we selected an epoch of 1000 milliseconds following their defined onset. This choice was made because we were specifically interested in observing immediate changes in the spectral characteristics.

During the transitions, such as Pre-FoG or Pre-Stop, we averaged the gait cycles to produce an average spectrogram for each transition phase.

To quantify the changes, we calculated the mean percentage change from the baseline. This involved normalizing the absolute power values by first subtracting

the baseline power, followed by division of the corresponding subject-specific STN resting (Standing) baseline values, multiplied by the factor 100.

$$\frac{power\ -\ baseline\ power_{standing}}{baseline\ power_{standing}}\ x\ 100$$

This normalization allowed us to assess how the spectral features changed relative to each subject's individual baseline. After the process of normalization, time-frequency matrices were averaged across all trials, resulting in a grand average spectrogram.

2.7 Statistics

For the statistical analysis of our data, we started with the investigation of alterations in spectral activity across various contexts: Walking, transition periods (Pre-FoG and Pre-Stop), FoG episodes, and stops. Subsequently, we investigated how spectral characteristics differed from their respective baseline values 'Standing' during episodes of 'FoG', 'Stop', and their transition phases.
Statistical analyses for demographic, kinematic, and clinical data were carried out using built-in functions in Matlab. Unless stated otherwise, all data are presented as mean ± standard deviation (SD). Prior to pairwise comparisons, data underwent assessment for normality using the Kolmogorov-Smirnov test with a 95% confidence interval (CI). Depending on the results, data were subjected to independent samples t-tests (parametric) (paired samples t-test where indicated) or to Wilcoxon signed-rank tests if the assumption of normality was violated (nonparametric). Statistical significance was determined at a threshold of $p < 0.05$.

2.7.1 The multiple comparison problem

The multiple comparisons problem is a challenge encountered in the statistical analysis of EEG data but also in LFP data for example (Maris & Oostenveld, 2007). It arises because EEG-data/LFP-data are inherently multidimensional, with a spatiotemporal structure that includes data from multiple channels and multiple time points. Essentially, the multi comparisons problem arises because

when one is trying to detect an effect of interest - such as a difference between experimental conditions - across all possible combinations of channels and time points, a large number of statistical comparisons is necessary, often in the order of several thousands. This can lead to an increased likelihood of making false positive conclusions (Maris & Oostenveld, 2007). In this context, nonparametric statistical testing offers a solution to address the multi comparisons problem by conducting permutation tests (Maris & Oostenveld, 2007).

The process of cluster-based permutation analysis can be divided into two major parts, the first of which is the formation of clusters. Therefore, the initial samples are compared using an appropriate statistical test (e.g., t-test for independent samples). Samples with t-values above a defined threshold are grouped into clusters. The t-values within a cluster are summed up yielding the cluster size(s) and the largest cluster is used for the nonparametric test statistic. In a second part, the data being part of the cluster now are shuffled (Resampling) and the same process is repeated up to n times in a Monte Carlo simulation. This finally results in a distribution of t-values. Based on the distribution of t-values, it can be determined how likely it is that the t-value observed in the original data for a cluster is due to chance. If $p < 0.05$, a significant difference can be assumed (Maris & Oostenveld, 2007).

To study the frequency domain spectra and time frequency spectral modulation during different conditions, we used non-parametric cluster-based permutation testing, implemented in Fieldtrip. Therefore, our clusters were built out of two or more adjacent time-frequency samples with a P-value below 0.05 (two-sided) based on their spatial, spectral, and temporal proximity. We performed 1000 cycles during the permutation process. As a threshold to identify significant clusters in the original data, we used the 95^{th} percentile of the permuted t-value distribution.

3 Results

3.1 Patient details and localisation of contacts

A total of 12 datasets were analysed in the study. An overview of the demographics and clinical parameters from the related patients can be found in **Table 8**. The patient in the analysis cohort had an average age of 67.26 ± 5.85 years and an average disease duration of 12.83 ± 5.21 years. An average result in the MDS-UPDRS III Score in MedON and StimON of 25.33 ± 7.97 compared to 47.33 ±14.40 in MedOFF and StimOFF condition shows a marked improvement of motor symptoms, indicative for L-Dopa sensitive, idiopathic PD and correct electrode position for effective DBS.

Table 8. Clinical details.
Values are given as mean ± SD (Standard deviation) unless stated otherwise. BDI: Beck Depression Inventory; FOGQ: Freezing of Gait Questionnaire; MDS-UPDRS: Movement Disorder Society-Unified Parkinson's Disease Rating Scale; MoCA: Montreal Cognitive Assessment; FOG-AC: Freezing of Gait Assessment Course

No. of patients	**12**
Sex (Male/Female)	6 / 6
Age at experiment	67.26 ± 5.85
Age at time of surgery, *Years*	64.52 ± 8.09
Age at disease onset, *Years*	54.33 ± 9.50
Disease duration, *Years*	12.83 ± 5.21
Years since implantation	2.67 ± 3.09
Dose of levodopa equivalent medication, *mg/d*	681.92 ± 211.20
MDS-UPDRS III Score, MedOFF/StimOFF	47.33 ± 14.40
MDS-UPDRS III Score, MedON/StimON	25.33 ± 7.97
MDS-UPDRS III Score, MedOFF/StimOFF - hemibody Left	16.08 ± 5.71
MDS-UPDRS III Score, MedOFF/StimOFF – hemibody Right	14.25 ± 4.53
MDS-UPDRS III Score, MedOFF/StimOFF – disease dominant hemibody	17.25 ± 5.29
MDS-UPDRS III Score, MedOFF/StimOFF – non-disease dominant hemibody	13.08 ± 4.40
FOG-AC MedON/StimON	3.36 ± 3.91
FOGQ Score	14.58 ± 7.96
MoCA Score	25.8 ± 3.6
BDI	12.2 ± 4.5

3.2 Comparison of patients exhibiting or not exhibiting Freezing in the experiment

Our cohort consisted of 12 freezers (Snijders et al., 2012), 11 of which were 'definite freezers' who showed FoG either in the clinical assessment or during the experiment and one 'probable freezer' (ID18) who only reported off-related freezing by history. During the experiment, only a subset of patients showed freezing while straight line walking, which led us to compare these two subgroups. Interestingly, the two groups differed in certain aspects. On average, patients showing FoG during straight-line walking in the experiment tended to be younger (mean: 64.4 vs 69.3 years) and had a shorter disease duration compared to those

not exhibiting any FoG (mean: 11.0 vs 14.1 years). However, patients who showed FoG achieved higher scores in recorded assessments such as NFOGQ (mean N-FOG scores: 16.6 vs 11.7 points), MDS-UPDRS III Med ON/Stim ON (mean: 29.4 vs 22.4 points), and MedOFF/StimOFF (mean: 55.6 vs 41.4 points) (**Figure 13**). Both groups showed similar results in cognitive and psychometric tests (mean MoCA scores: FoG exhibiting group 27.0 vs No-FoG-exhibiting group 26.7 points; mean Beck's Depression Inventory II scores: 10.2 vs 12.6 points).

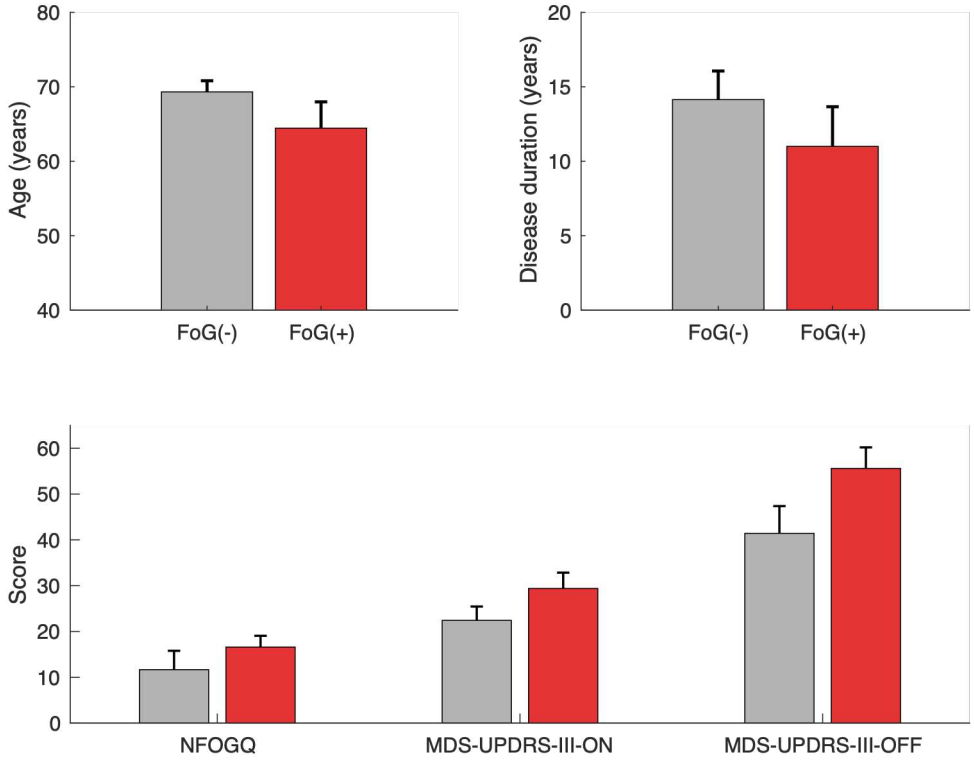

Figure 13. Clinical test results of patients showing and not-showing Freezing of Gait during straight-line walking in the experiment.
The mean values and the standard error of the mean of the respective group are shown, red bars show the results of patients exhibiting FoG (+), grey bars of the patients not exhibiting FoG (-) during straight line walking. ON means MDS-UPDRS III Score was evaluated during Med ON/Stim ON and OFF means patient was in MedOFF/StimOFF.

3.3 Disease-dominant STN

To determine the disease-dominant STN on which all subsequent analysis were performed, we used the MDS-UPDRS Score, item 3.3-3.9. We built hemibody scores (right or left) to identify the more affected side and the contralateral STN accordingly was defined as the disease dominant STN (**Table 1**). Among the specified STN's, 5 were on the right and 7 on the left.

The results showed that the disease dominant side had a mean MDS-UPDRS III score of 17.25 ± 5.29, while the non-dominant side had a mean score of 13.08 ± 4.40 (**Table 8**). This difference was statistically significant based on a paired samples t-test ($p < 0.01$).

3.4 Spatial and temporal gait parameters of the different conditions

In our study we focused on analysing gait cycles contralateral to the disease dominant STN. Our analysis included a total of 1119 regular gait cycles, with a median cadence of 101 ± 24 steps per minute and an average stride length of 0.88 (± 0.13) m with the disease dominant leg (**Table 10**).

We observed 42 episodes of FoG in 5 out of the 12 subjects, with a median count of 6 [IQR = 2,17] episodes with a median duration of 8.2 [IQR = 3.6, 10.2] s. Furthermore, we noted 88 instances of self-selected stops in 10 out of the 12 subjects, with a median count of 9 [IQR = 7, 10] stops and a median duration of 2.5 [IQR = 1.7, 2.6] s per subject (**Table 9**).

Additionally, we recorded 75 Pre-FoG gait cycles (median per subject 13 [IQR = 11, 21] with a median cadence of 116 ± 13 steps/min per subject) and 156 Pre-Stop gait cycles (median per subject 17 [IQR = 9, 18]) with a median cadence of 104 ± 36 steps/min (**Figure 15**).

When comparing stride length between Walking and the transition phases, there is a tendency for stride length to be shorter in Pre-FoG compared to Walking ($p= 0.063$), but not compared to Pre-Stop (**Figure 14**).

Table 9. Recorded events during all experiments.
IQR = Inter quartile range.

	Walking	Pre-Stop	Pre-FoG	Stop	FoG
	(gait cycles)				
Number of patients	12	10	5	10	5
Recorded events	1119	156	75	88	42
Events per subject Median (IQR)	96 (62,180)	17 (9,18)	13 (11,21)	9 (7,10)	6 (5,13)
Duration in *s* Median (IQR)	-	-	-	2.5 (1.7, 2.6)	8.2 (3.6, 10.2)

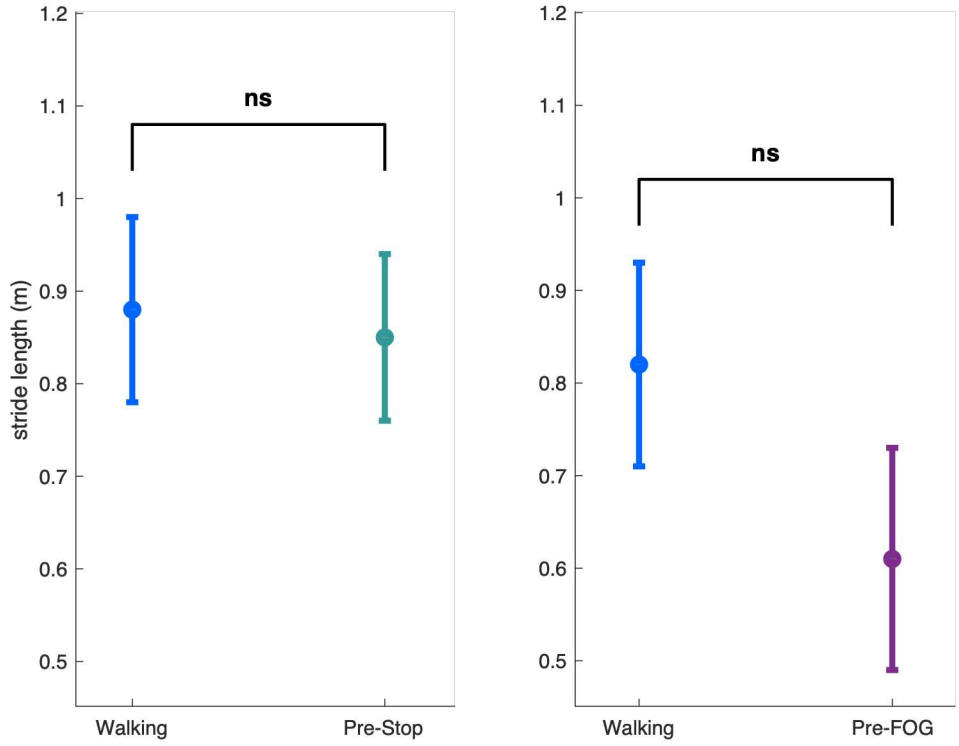

Figure 14. Comparison of stride length under different conditions.
The mean values of the disease-dominant leg, indicated by dots, and the standard deviations are displayed. Blue represents Walking, turquoise denotes Pre-stop, and purple indicates Pre-freeze (p = 0.063 Walking vs Pre-FoG, indicated by ns = not significant).

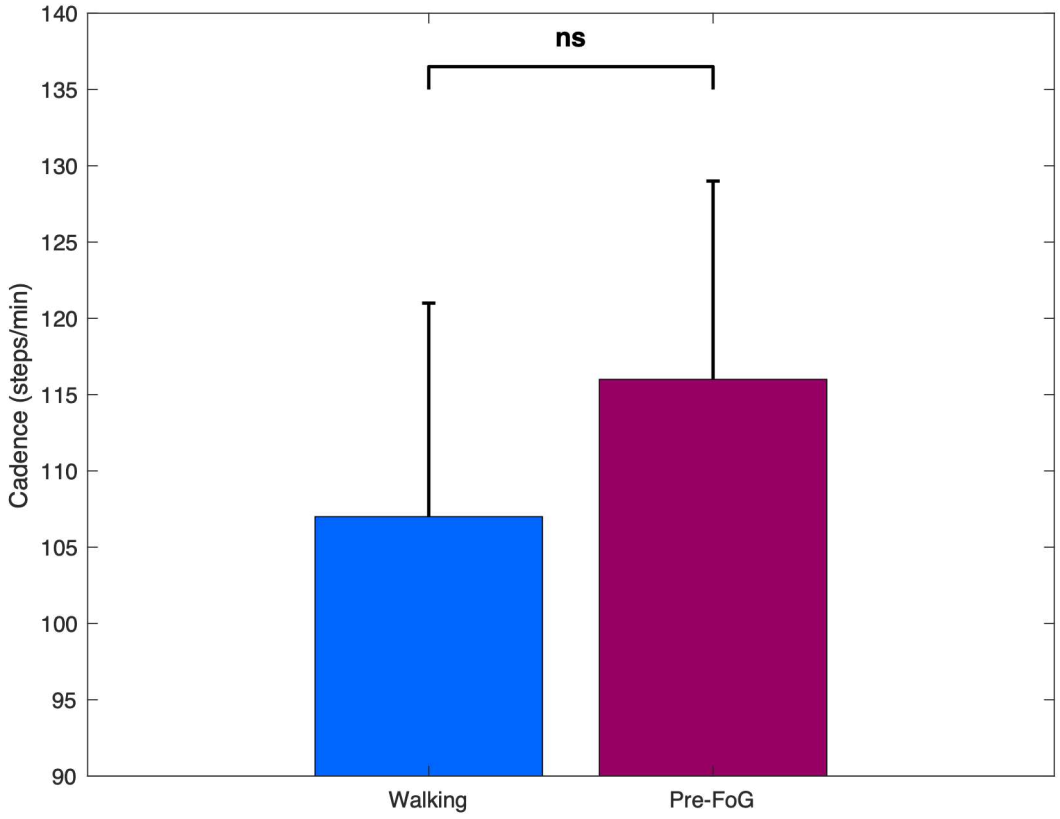

Figure 15. Comparison of Cadence during different conditions.
In the transition phase of FoG a higher Cadence can be observed compared to Walking (p = 0.063)

Table 10. Spatial and temporal gait parameters.
p-values were computed with paired-samples t-test (normally distributed data) or two-tailed Wilcoxon-signed rank test (normally distributed data). D = Disease dominant leg according to disease dominant hemibody MDS-UPDRS III scores, ND = non-disease dominant leg, p = p-value, SD = Standard deviation.

Parameter	**Grand average (mean ± SD)**								
	12 subjects (all patients)			**10 subjects (patients with stops)**			**5 subjects (Freezer)**		
	Walking (D)	**Walking (ND)**	***p***	**Walking (D)**	**Pre-Stop (D)**	***p***	**Walking (D)**	**Pre-FoG (D)**	***p***
Cadence (steps/min)	101 ± 24		-	99 ± 23	104 ± 36	0.652	107 ± 14	116 ± 13	0.063
Stride velocity (m/s)	0.72 ± 0.13	0.73 ± 0.13	0.320	0.71 ± 0.14	0.71 ± 0.17	0.426	0.72 ± 0.09	0.58 ± 0.08	0.063
Stride Length (m)	0.88 ± 0.13	0.87 ± 0.13	0.465	0.88 ± 0.10	0.85 ± 0.09	0.164	0.82 ± 0.11	0.61 ± 0.12	0.063
Step time (s)	0.65 ± 0.16	0.62 ± 0.14	0.175	0.66 ± 0.18	0.65 ± 0.16	0.910	0.59 ± 0.05	0.56 ± 0.04	0.063
Stance time (%)	64.39 ± 4.86	66.71 ± 3.38	0.032	65.59 ± 4.06	65.63 ± 6.06	0.910	62.61 ± 4.09	65.07 ± 3.06	0.313
Swing time (%)	35.60 ± 4.86	33.29 ± 3.38	0.032	34.41 ± 4.06	34.37 ± 6.06	0.910	37.39 ± 4.09	34.93 ± 3.06	0.313
Peak Angular Velocity (deg/s)	221 ± 33	248 ± 38	0.042	224 ± 34	213 ± 34	0.004	208 ± 30	180 ± 31	0.063

3.5 Subthalamic Activation patterns during regular gait

3.5.1 Oscillatory activity during Walking

To elaborate on changes in time-frequency activation and synchronization, we first compared the two conditions: Sitting and Standing and observed a reduction of activity in Standing in the theta, alpha and beta bands ($p < 0.05$; non-parametric cluster-based permutations) compared to Sitting. Using Standing as a baseline condition, Walking resulted in a significant suppression of activity in the 8-32 Hz range (**Figure 16**). The significant suppression during Walking compared to Standing could be further analysed for the different frequency bands by comparing the relative power of subject averages. Using the Wilcoxon signed-rank test (data not normally distributed, Kolmogorov-Smirnov $p < 0.05$), we found a significant difference in the alpha ($p = 0.0425$), low beta ($p = 0.0161$), and high beta band ($p = 0.0342$) between Standing and Walking (**Figure 17**).

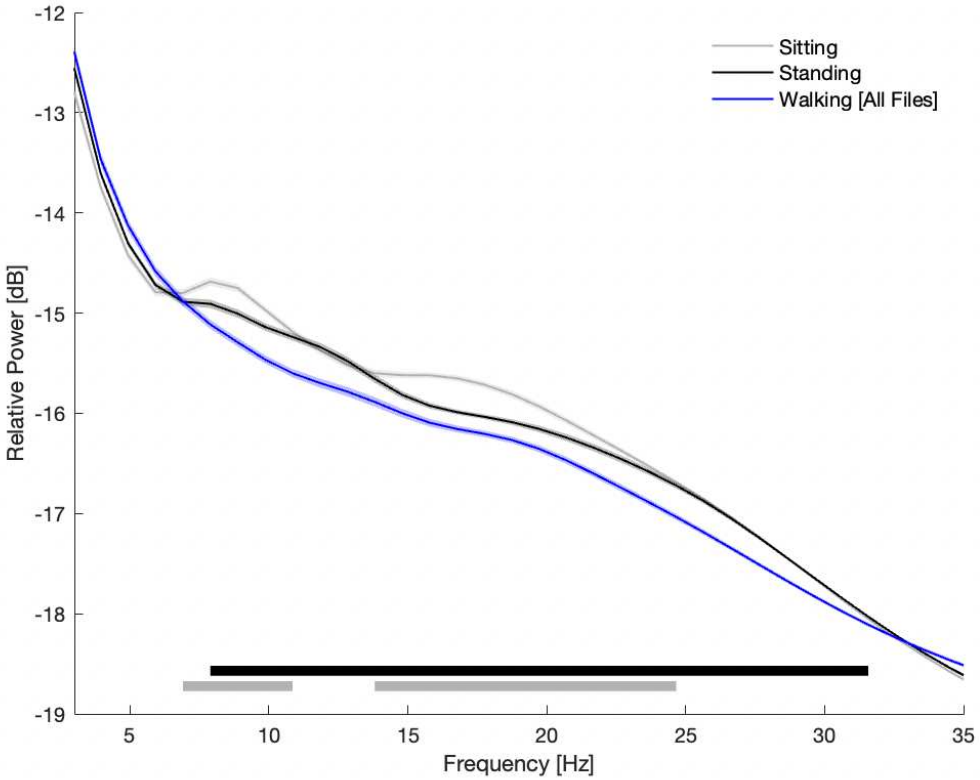

Figure 16. Frequency domain spectrum of the disease-dominant STN in Sitting, Standing and Walking.
The relative power of Standing is assessed in comparison to epochs of Walking and Sitting. Employing cluster-based permutation testing, significant differences ($p < 0.05$) are denoted by horizontal bold bars, with black bars indicating comparisons between Standing and Walking, while grey bars represent comparisons between Sitting and Standing.

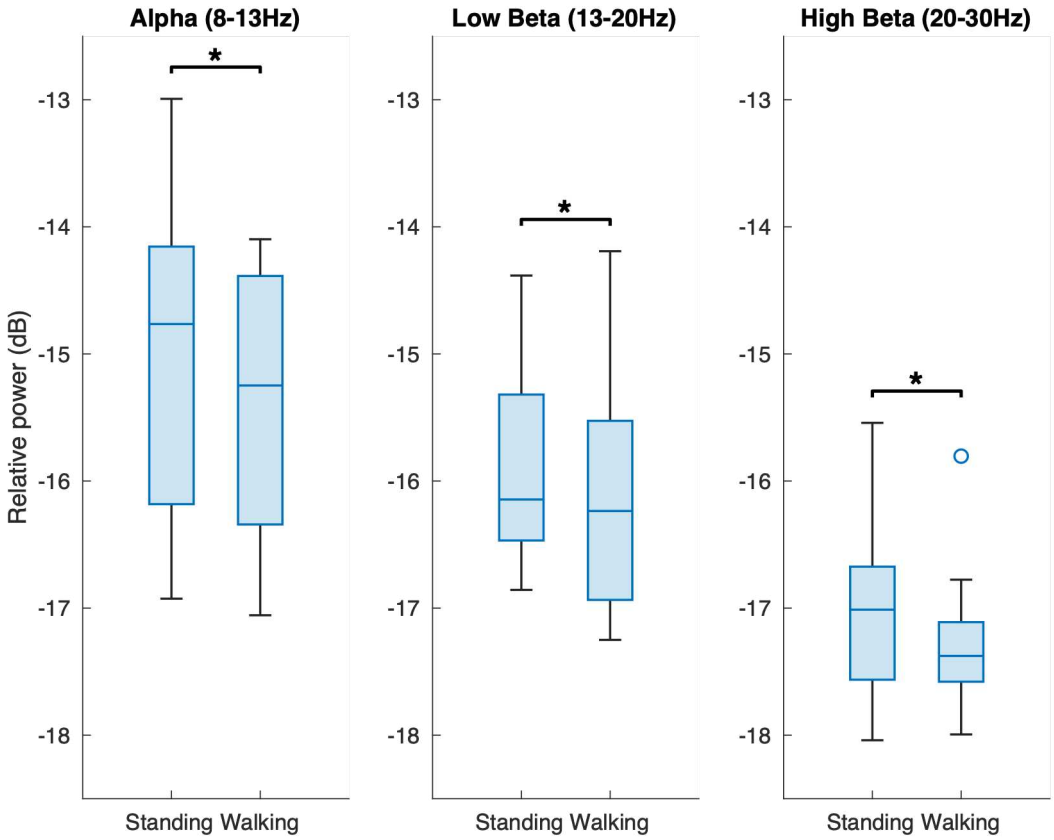

Figure 17. Comparison of relative power between Standing and Walking in the alpha, low and high beta frequency bands.
Relative power shows an attenuation in the alpha, low beta and high beta bands during Walking compared to Standing. Wilcoxon-signed rank test showed a significant difference for each frequency band (alpha: $p = 0.0425$, low beta: $p = 0.0161$, high beta $p = 0.0342$) indicated by the black star.

3.5.2 Modulation of subthalamic activity over the gait cycle

We observed a modulation of the frequencies over the gait cycle in different frequency bands. Compared to baseline (Standing), there was an increase of power in two clusters throughout the entire gait cycle, in the gamma-band (>35Hz) and in the delta- and theta-band (<7Hz). Two clusters of power decrease during Walking could be found, both in the lower beta band (13-20Hz) and in the upper beta band (20-30Hz), as well as in the alpha band (9-12 Hz). The activity in the alpha band was relatively stable throughout the gait cycle, with a brief resynchronization at the time of the contralateral heel strike (~50% gait cycle). Beta band attenuation was more variable, showing the strongest event-related desynchronization before and during both ipsilateral (around 18% gait cycle) and contralateral toe-off (around 67% gait cycle), and (re)synchronization from Mid-Swing to heel strike and double-support phase. The cluster-based permutation analysis unveiled a significant effect of condition ($p < 0.05$).

.

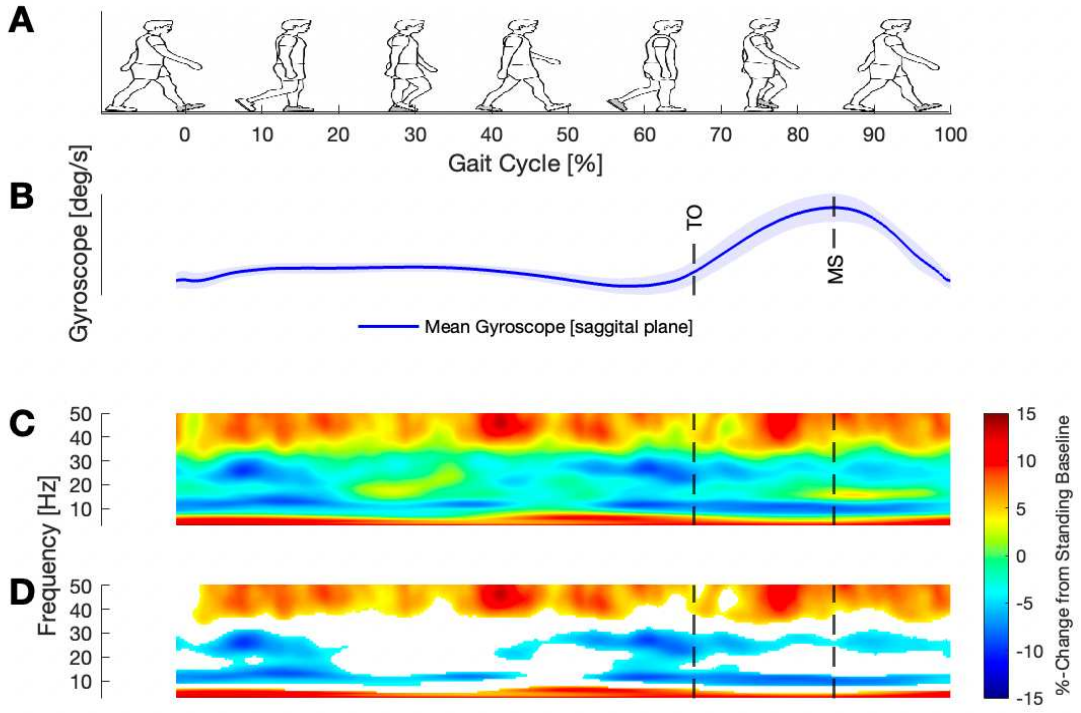

Figure 18.Time-frequency representation of the regular gait cycle.
(A) Illustration of the gait cycle of the left leg, beginning and ending with a left heel strike (0-100%) (B) Gyroscope signal averaged across subjects of the leg contralateral to the disease-dominant STN. Shaded blue area display the ±1 SD from the mean. 'TO' means toe-off which occurs about 66.9% of the gait cycle, 'MS' for Mid-Swing which occurs at 86.5% of the gait cycle. (C) Time-frequency group analysis, normalized to a gait cycle and pooled across all epochs originating from the disease-dominant STN. Changes in power relative to the standing baseline (%) are shown. Throughout the gait cycle, high and low beta as well as alpha power are attenuated to different extents. Gamma power (>35 Hz) and low frequencies (<7 Hz) are increased. (D) Only the significant areas within the alpha-, beta- and gamma band as well as in the low frequencies (< 7 Hz) are shown (Non-parametric cluster-based permutation analysis $p<0.05$). Non-significant clusters are masked.

3.6 Oscillatory activity during and preceding Freezing of Gait

Comparing the frequency-domain spectra of Pre-FoG and FoG with the Standing baseline, the STN activity showed an increase of activity in the lower beta band during FoG from 12-21 Hz and in Pre-FoG from 12-17 Hz (numerical differences that did not reach statistical significance). Significant upper beta band attenuation was found in Pre-FoG (21-27 Hz) and FoG (23-33 Hz) (**Figure 19**).

When comparing mean relative power of FoG and Pre-FoG, a significant increase of low beta band activity during FoG is observable, whereas no change can be seen in the high beta band. Theta and alpha activity show a tendency to decrease during FoG compared to Pre-FoG (**Figure 20**).

In the time-frequency analysis, FoG was characterised by fluctuating power increases in the beta band. The suppression of the alpha and beta bands typical of normal gait was no longer present. However, the differences were not statistically significant in the permutation analysis (**Figure 21**).

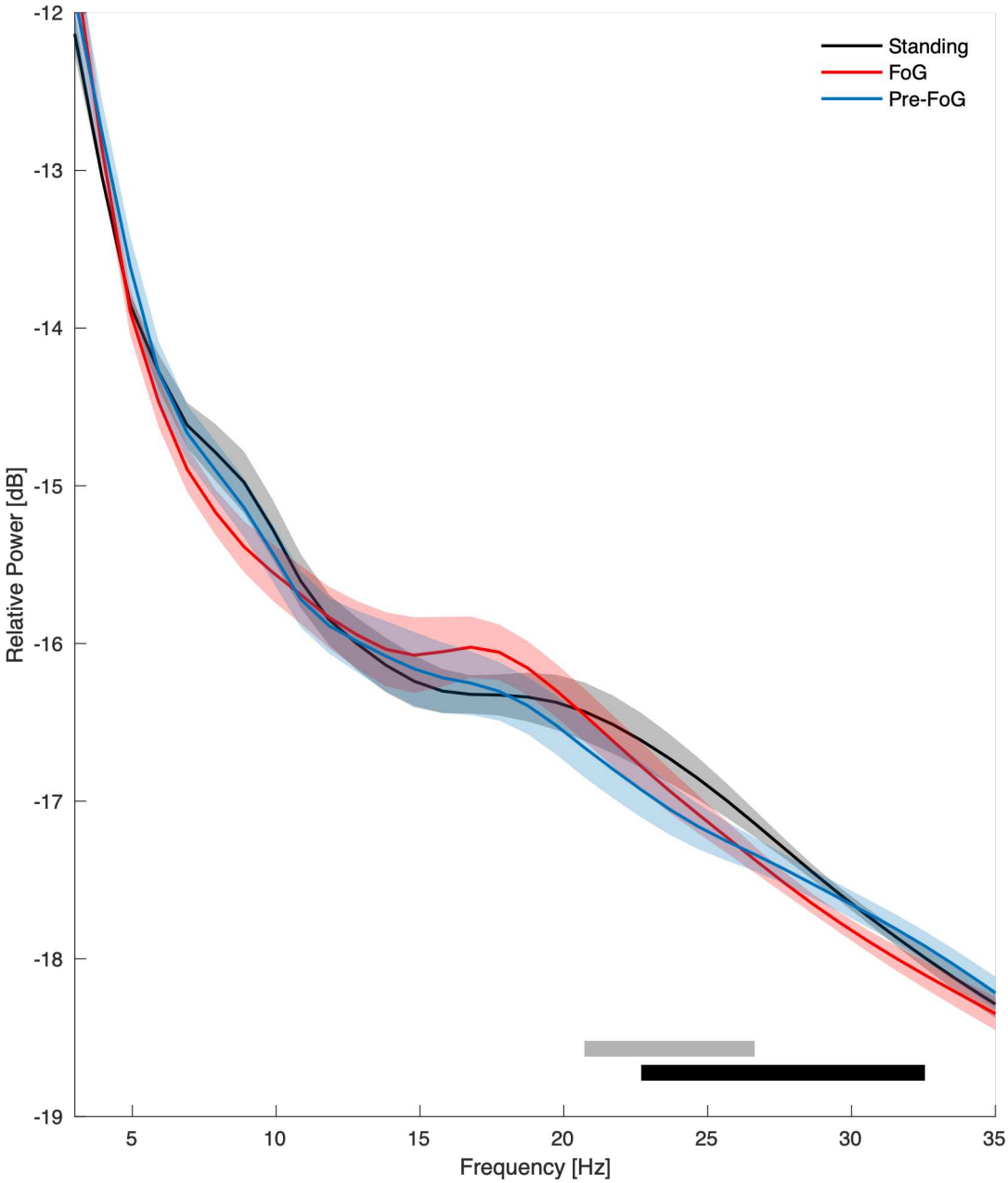

Figure 19. Frequency domains of the disease-dominant STN across different conditions: Standing, Pre-Freezing and Freezing.
Relative power of Standing is contrasted with FoG and Pre-FoG epochs. Through cluster-based permutation testing, significant differences ($P < .05$) are highlighted by horizontal bold bars. Black bars denote statistical significance between Standing and FoG, while grey bars denote significance between Pre-FoG and Standing. Shaded error bars depict the standard error of the mean.

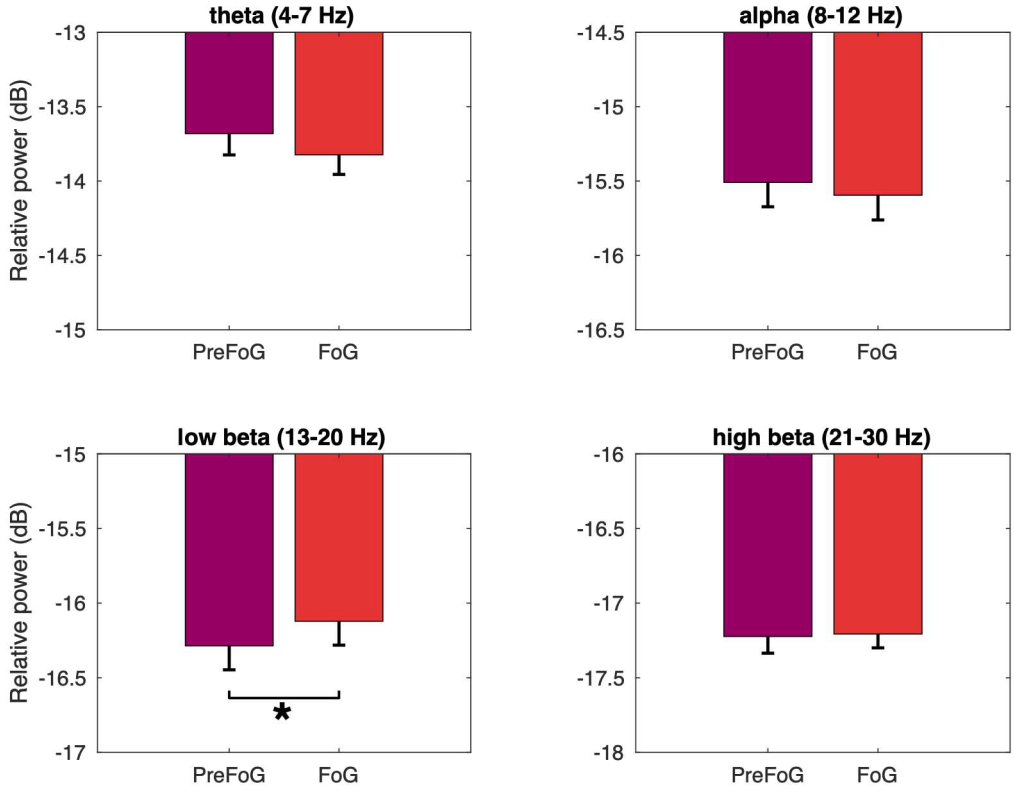

Figure 20. Mean relative power of different frequency bands during different conditions.
Displayed is the mean relative power of Pre-FoG episodes (purple) and of FoG episodes (red). Black lines indicate the standard error of the mean. There is a significant increase comparing FoG to Pre-FoG in the low beta band, marked by a black star ($p = 0.0102$)

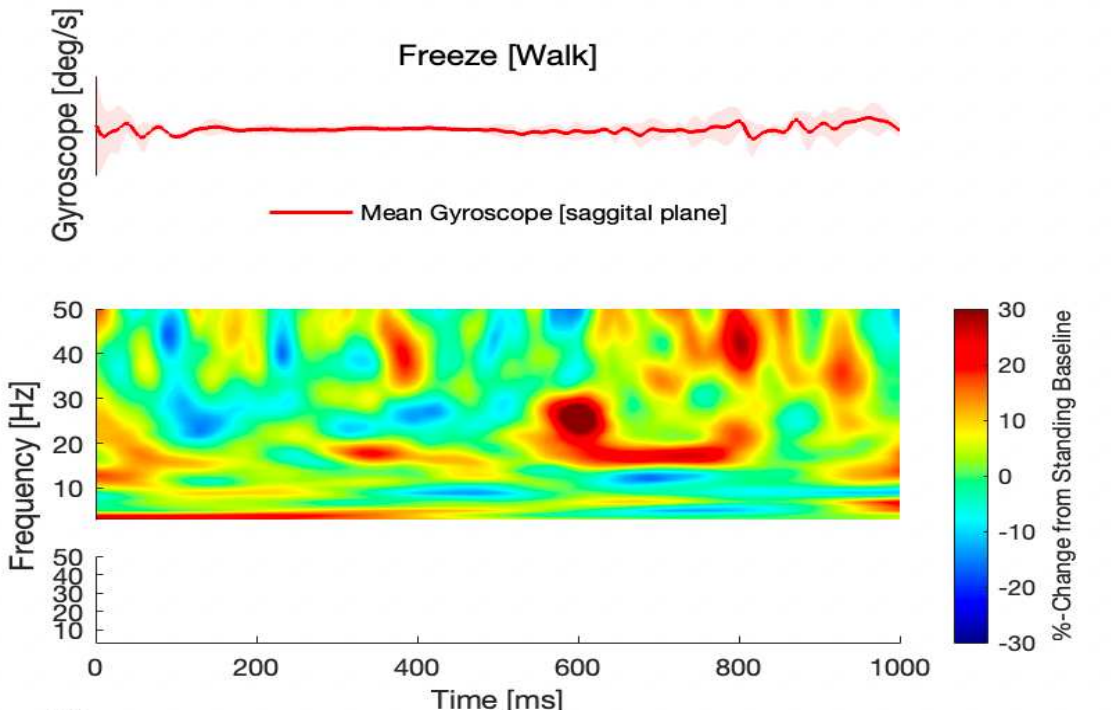

Figure 21. Time-frequency spectrogram illustrating the lack of beta-band suppression during Freezing.
The upper panel shows the average gyroscope signal across subjects from 0 to 1000 ms after onset of freezing. The middle panel displays the group analysis of time-frequency data pooled across all epochs from the disease-dominant STN, showing changes in power relative to the Standing (%). The lower panel highlights significant clusters identified through permutation analysis ($p < 0.05$), with non-significant clusters masked. During FoG, there is a notable absence of lower beta-band attenuation, with intermittent power increases between 15-20 Hz and 14-34 Hz, yet permutation analysis did not reveal any significant effects ($p > 0.05$). No significant alpha-band attenuation is observed.

3.7 Oscillatory activity associated with Stops

When comparing the frequency domains of Stop and Pre-Stop against Standing, there was activity suppression in Stop at 6-13 Hz ($p = 0.002$) compared to Standing. In the transition period before a Stop, we found decreased activity between 7-14 Hz ($p = 0.004$) and 18-26 Hz ($p = 0.002$) compared to Standing (**Figure 22**).

Time-frequency analyses revealed a significant cluster of alpha, low beta and high beta band attenuation ($p = 0.001$) during the first half of the Stop. The decrease in power in the beta band returned to normal, in the sense of a rebound, comparing the second half of the Stop to the first. We found another separate cluster in the second half of the Stop, showing an increase of gamma band activity ($p = 0.001$) (**Figure 23**).

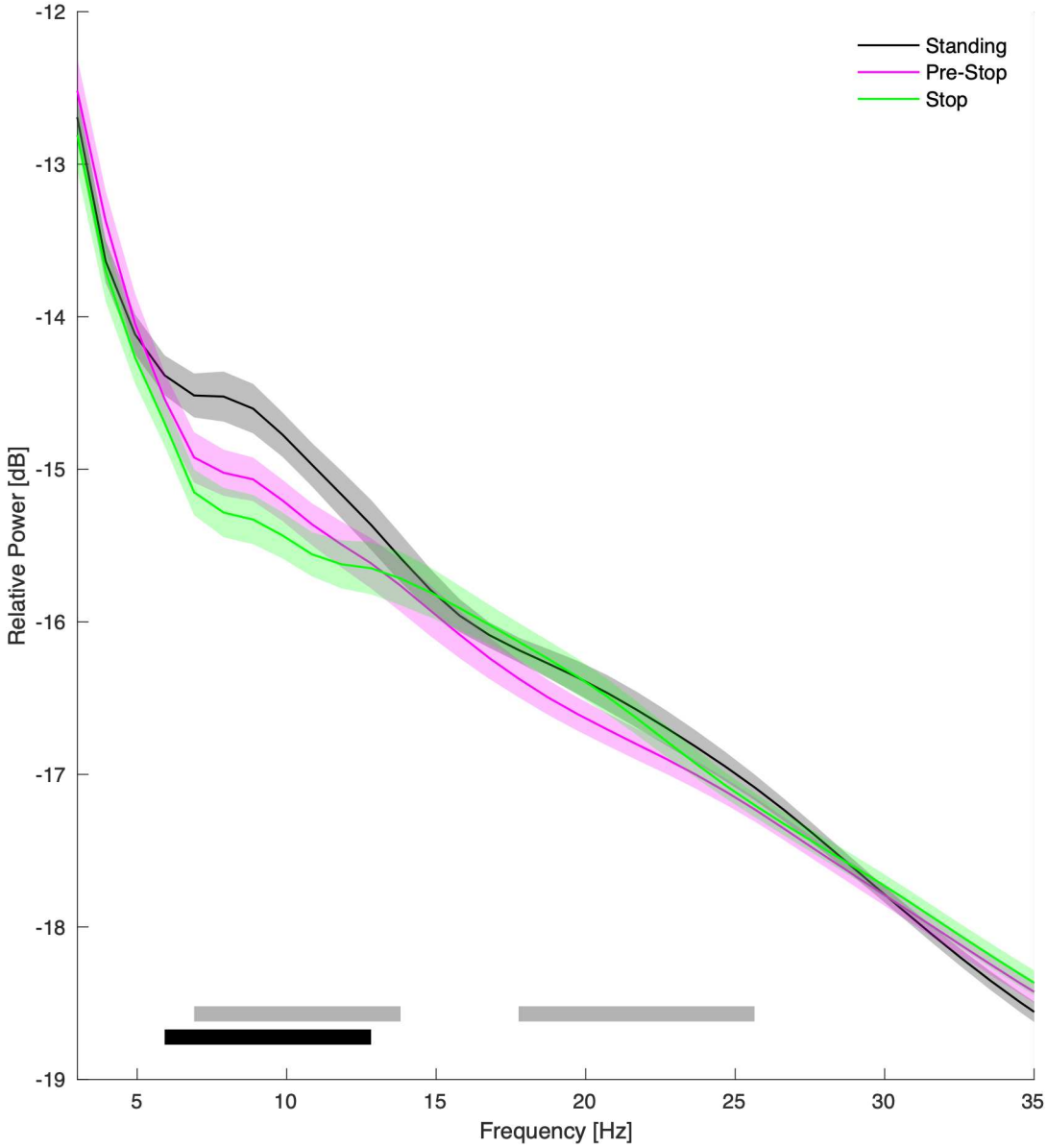

Figure 22. Disease-dominant STN frequency power of standing baseline, stop and Pre-stop.
Relative power of the Standing is contrasted with epochs of Stop and Pre-Stop. Employing cluster-based permutation testing, significant differences ($P < .05$) are indicated by horizontal bold bars. Black bars signify the comparison between Standing and Stop, while grey bars denote the comparison of Pre-Stop and Standing. Shaded error bars illustrate the standard error of the mean (SEM).

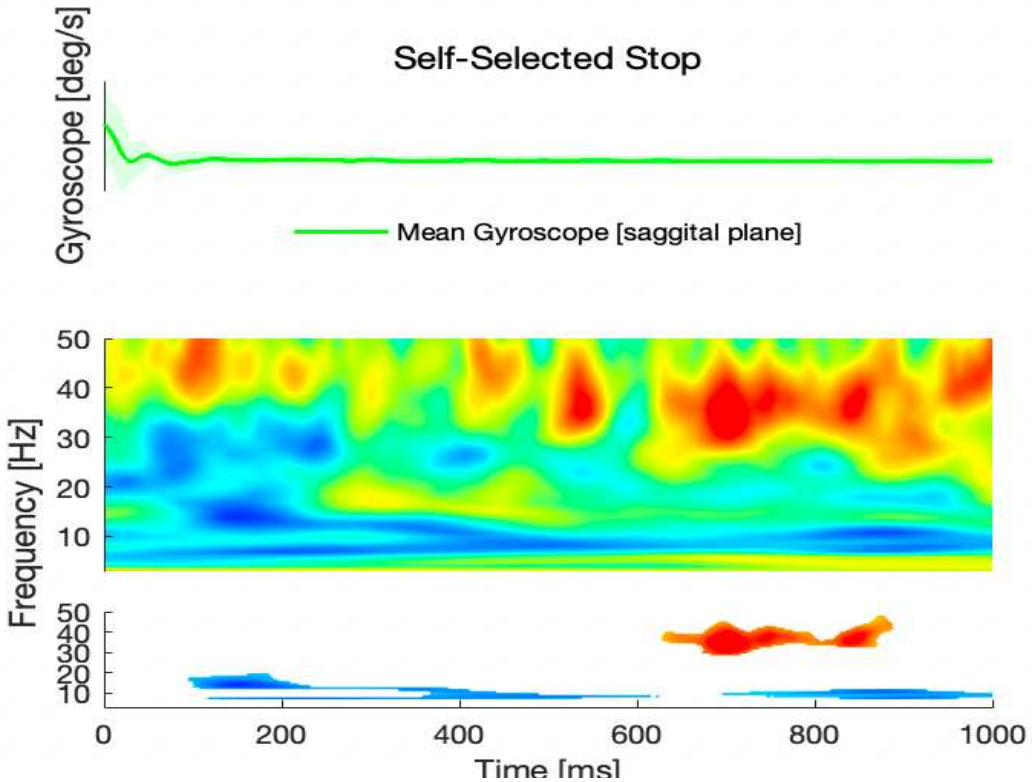

Figure 23. Time-Frequency analysis of self-selected stop.
The upper panel shows the average gyroscope signal across subjects from 0 to 1000 ms after the epoch begins. The middle panel displays the group analysis of time-frequency data pooled across all epochs from the disease-dominant STN, showing changes in power relative to the standing baseline (%). The lower panel highlights significant clusters identified through permutation analysis ($P < .05$), with non-significant clusters masked

3.8 Comparison of the oscillatory activity during transition phases before FoG and self-selected stops

A comparison of the relative power of the transition phases shows higher activity in Pre-FoG than in Pre-Stop, particularly in the alpha and lower beta bands. This comparison is purely descriptive due to the different number of recorded episodes. The pooled data is shown in **Figure 24**.

Descriptively, Pre-FoG showed a numerical increase and fluctuations in alpha-band and low beta-band activity in contrast to Walking, but these observations did not reach statistical significance. In Pre-Stop, the observed suppression of both the lower and upper beta bands was largely preserved compared to Walking. There was a significant attenuation in the alpha band range ($p = 0.001$) during the second half of the gait cycle. Descriptively, there was a decrease in low and high beta band, as well as alpha band activity in the first half of the gait cycle. Additionally, a decrease in theta-band activity was observed at the transition from Pre-stop to stop, which was not seen in Pre-FoG, where an increase in theta band activity was observed (**Figure 25**).

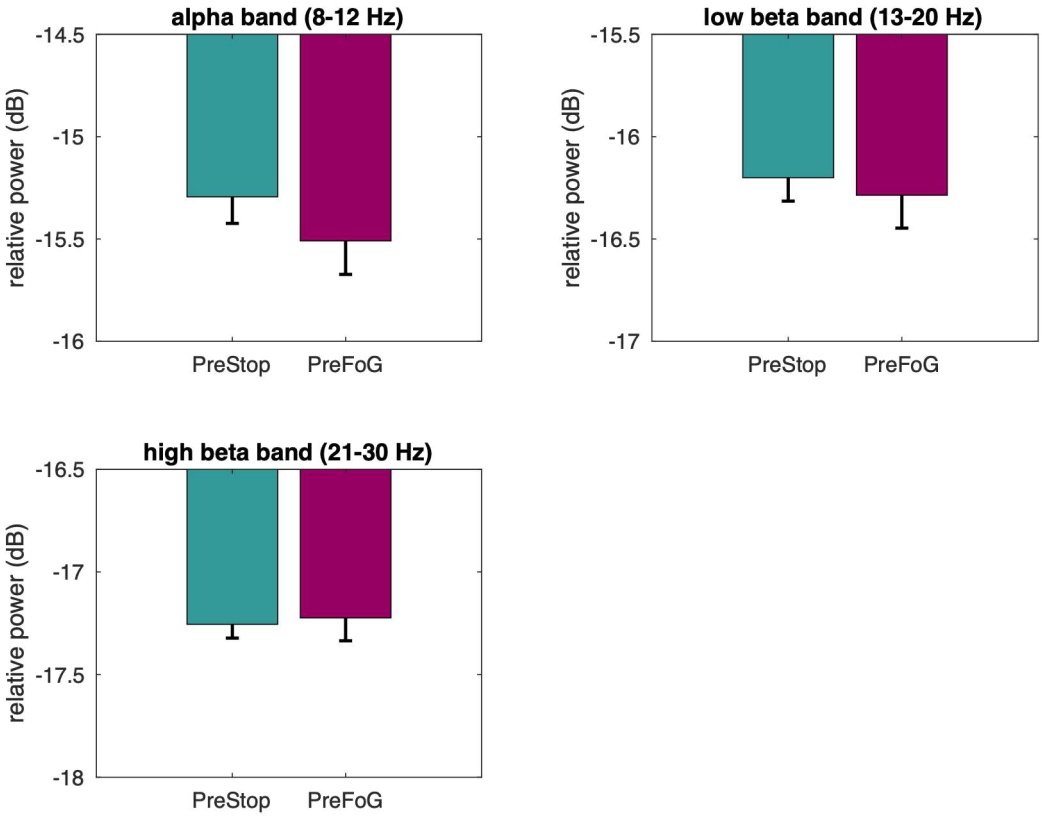

Figure 24. Comparison of relative power between pooled Pre-Stop and Pre-FoG episodes.
Displayed is the mean relative power of all recorded Pre-Stop (turquoise) and Pre-FoG (purple) epsiodes. Black lines indicate the standard error of the mean. No statistical comparison was made due to the different sample sizes.

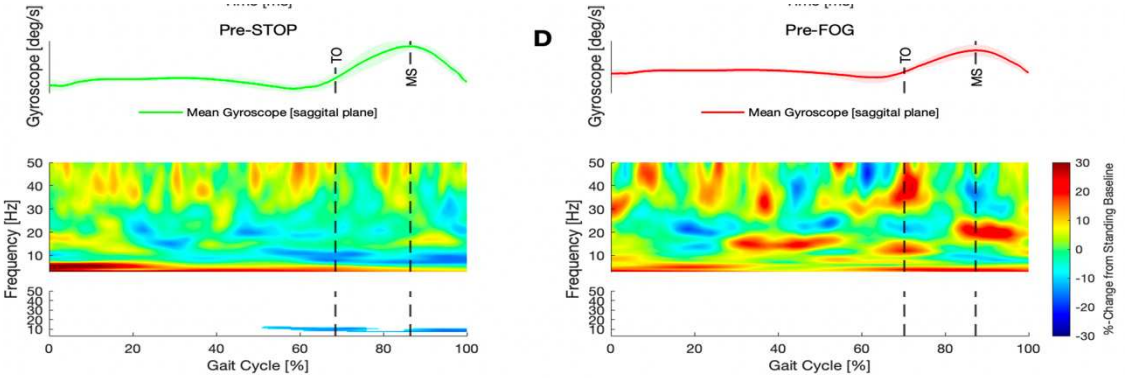

Figure 25. Time-frequency analysis of transition phases.
The upper panel shows the average gyroscope signal across subjects from 0 to 1000 ms after the epoch begins. The middle panel displays the group analysis of time-frequency data pooled across all epochs from the disease-dominant STN, showing changes in power relative to the Standing baseline (%). The lower panel highlights significant clusters identified through permutation analysis ($P < .05$), with non-significant clusters masked.

3.9 Summary of the results

Walking

During Walking, there was a suppression of activity in the 8-32 Hz range, with a significant reduction in alpha and beta power. Regarding gait cycle modulation, time frequency analyses revealed an increased power in the gamma-band (>35Hz) and the delta- and theta-bands (<7Hz) throughout the entire gait cycle. Alpha activity was continuously decreased throughout the gait cycle, with short resynchronization at the time of contralateral heel strike. Beta attenuation, both low (13-20 Hz) and high beta (20-30 Hz), was more variable, showing the strongest event-related desynchronization before and during both ipsilateral and contralateral toe-off and resynchronization from Mid-Swing to heel strike and the double-support phase.

Freezing

STN activity showed a numerical increase of activity in the lower beta band in FoG from 12-21 Hz and a significant decrease in the high beta band. In the time frequency analyses, FoG was characterised by fluctuating power increases in the beta band and the lack of alpha and beta attenuation observable during Walking.

Stop

Stop was characterized by a significant decrease of alpha activity (6-13 Hz). In the time-frequency analyses alpha and beta activity decreased shortly after the beginning of a Stop. Beta activity returned to normal around 380ms after Stop onset in sense of a rebound.

Transition phases

In the frequency domain spectra, Pre-FoG showed an increase from 12-17 Hz (numerical differences that did not reach statistical significance) compared to Standing. Numerical increase and fluctuations in alpha and low beta activity during the gait cycle could be observed in time-frequency analyses. During Pre-Stop, the observed suppression of both the lower and upper beta bands was

largely preserved from Walking. There was a significant attenuation in the alpha band range during the second half of the gait cycle.

4 Discussion

The study focused on analysing activation patterns in the STN during FoG. It revealed distinctions between freezing and the presumable physiological modulation observed during Walking. We detected several anomalies in activation and synchronization patterns that were exclusive to the periods preceding the onset of freezing and its clinical manifestation. Moreover, the research demonstrated that these aberrant activity patterns were specific to freezing and were not observed during voluntary stops. This finding is meaningful as it contributes to the neurophysiological understanding of FoG and could potentially help refine closed-loop DBS models and input variables. By identifying abnormalities in the STN measurable before clinical symptoms appear, we can distinguish between states of inhibited forward progression, such as voluntary stops and freezing, which both occur in a patient's everyday life but have completely different therapeutic consequences.

4.1 Modulation of different frequency bands in the STN as a sign of sufficient gait

Prior to analyzing pathologies related to FoG, we initially investigated the activity of the STN associated with normal gait.

Since aberrant beta oscillation synchrony in the STN is a hallmark of akinesia in Parkinson's disease (Hammond et al., 2007; Little & Brown, 2014) and beta oscillations generally decrease during the planning and execution of movements, a decrease in beta activity seems quite logical and could already be shown in healthy subjects (Seeber et al., 2016) and PD patients (Scholten et al., 2020). We were able to demonstrate a reduction in alpha and beta band power during Walking compared to Standing and Sitting in our patients as well. It goes in line with previous studies which revealed reduced high beta band (20-30Hz) during walking (Hell et al., 2018) and a reduction in beta power within the STN during both bicycling and walking (Storzer et al., 2017), and with a more recent study that was able to distinguish between standing and walking based on beta activity (Canessa et al., 2020). However, not all studies have observed gait related beta power decrease in the STN. For instance, Quinn et al. found no significant

difference in Beta power during forward walking compared to the averaged resting state. Nonetheless, akinetic rigid PD subjects exhibited a tendency towards reduced beta power while walking, contrasting with tremor-dominant patients, whose beta activity was equal to the resting state (Quinn et al., 2015). This variation could be attributed to differences in phenotypes, suggesting that akinetic-rigid PD patients might demonstrate more pronounced gait-related beta alterations, a topic that needs further exploration in future research (Quinn et al., 2015). Another possible explanation could be that simply averaging beta band activity may not be optimal, as previous studies have indicated modulation of STN activity across the gait cycle (Fischer et al., 2018; Hell et al., 2018; Tan et al., 2018) and this simplistic approach may not adequately capture the dynamic nature of this power modulation (Wang & Choi, 2020).

Aligning with the opinion that averaging brain activity over the gait cycle is not sufficient to capture the different parts of a gait cycle and would hinder the detection of pathological clinical gait phenomena like Freezing of Gait, which occur over shorter timeframes, we employed analytical methods with temporal precision. Therefore, we examined the time-frequency representations of STN activity to unveil the modulation of a gait cycle.

We observed frequency modulation across various frequency bands and dimensions throughout the gait cycle. Specifically, we noted an increase in power in the gamma band (>35Hz) during the entire gait cycle compared to standing. We interpret these observations as physiological as they align with findings in individuals with dystonia, who exhibited heightened gamma oscillations during walking compared to sitting in the GPi (Singh et al., 2011), a phenomenon likely applicable to the STN due to their close linkage in the basal ganglia circuits (Singh et al., 2013). This hypothesis is supported by a subsequent study by the same research group focusing on the STN, albeit with a small sample size of six patients (Singh et al., 2013).

Gamma activity has been proposed to have prokinetic effects, as suggested by Brown et al., following findings in rats indicating that such activity may be physiological rather than solely a consequence of Parkinson's disease (Brown,

2003). This prokinetic notion finds support in subsequent studies conducted in the STN in dystonia patients (Geng et al., 2017) and as it was positively correlated with gripping force (Tan et al., 2016). Our own research further corroborates this prokinetic hypothesis, as we observed increased gamma activity during normal walking, which was notably absent during episodes of Freezing. Nonetheless, investigations have revealed a positive association between low gamma activity (31–45 Hz) and the severity of resting tremor (Beudel et al., 2015; Weinberger et al., 2009). This finding prompts us to consider that the enhancement of gamma activity throughout the entire gait cycle, with only trends towards specific gait events rather than distinct peaks, could be influenced by this correlation. Given our sample of 6 equivalent type PD patients— with increased tremor due to dopamine and stimulation deficiency —it suggests the need for further research involving complete tremor-negative patients, or ideally, healthy subjects.

Beta activity has been extensively studied in PD patients, with previous research revealing that beta activity in the STN is not only suppressed during walking as described above but also modulated throughout the gait cycle (Fischer et al., 2018; Hell et al., 2018; Tan et al., 2018). However, some studies only conducted partial evaluations using a stepping-in-place task (Fischer et al., 2018; Tan et al., 2018), while others attributed observed changes to movement-related artefacts (Hell et al., 2018).

Our findings reveal a relatively continuous reduction of alpha band throughout the gait cycle with a brief resynchronization at the time of the contralateral heel strike. The beta band attenuation was more variable, with the strongest desynchronization occurring before and during both ipsilateral and contralateral toe-off, i.e., at the beginning of the swing phase of the respective leg. Before the stance phase was initiated, which means from Mid-Swing to heel strike, resynchronization was observed.

This observation aligns with findings by Fischer et al., who demonstrated pronounced decreases at the time of ipsilateral heel strike when the opposite leg was lifted (Fischer et al., 2018). However, it's worth noting that their recordings were conducted during a stepping-in-place task in a seated position (n=12), thus

lacking a true swing phase of the leg. The research group attempted to ensure the transferability of the data to real walking and observed similar results, albeit in only 3 patients. Furthermore, since we observed relatively similar modulations to those described by Hell et al., namely, more generally, a decrease in alpha and beta band activity associated with swing phases and an increase with stance phases, we consider it unlikely that these modulations are due to artefacts as the authors themselves feared (Hell et al., 2018).

However, to gain more clarity about the significance of individual gait-associated oscillations, further studies are needed, ideally on healthy subjects and because this cohort is hardly available, possibly with other DBS indications and with various purely gait-related experiments.

However, so far, our findings, together with those of other research groups and EEG studies on cortical modulation during gait (Gwin et al., 2011), suggest that precise timing of alpha and beta frequency bands is necessary to coordinate the various components involved in gait. This coordination extends from the cortical motor planning areas, through the basal ganglia, to the mesencephalic motor region medullary and pontine reticular formations, and finally to the spinal cord (Takakusaki, 2017). As part of the basal ganglia, the STN must maintain its own rhythmic timing. In cases of pathological activity or disrupted modulation, the entire system could falter, clinically manifesting as a gait disorder – for example as FoG.

4.2 Freezing and its activation-deactivation abnormalities in the subthalamic nucleus

We observed increased low beta band activity during freezing compared to standing. Notably, a significant increase in low beta activity was evident when comparing FoG to Pre-FoG. This suggests a correlation between low beta activity and the evolution and expression of freezing. These findings are compatible with previous studies reporting heightened beta activity during a freezing episode (Georgiades et al., 2019; Liu et al., 2022) and even during dual task walking which is more susceptible to freezing (Chen et al., 2019). However, other studies have drawn more attention on the lower beta band, which has been shown, for

example, to be increased in freezers during normal walking, whereas a decrease in total beta activity has been observed in non-freezers, highlighting low beta activity as a key component of severe gait disturbance in PD patients (Singh et al., 2013). Our results further support the focus on the lower beta band, going in line with recent evidence indicating that FoG is correlated with low STN beta activity and partial coactivation of the knee extensor muscles, reflecting the inability to shift body weight, as can be the case with freezing (Thenaisie et al., 2022).
Given our observation of a significant decrease in the high beta band during freezing compared to standing, and no rising increase between pre-FoG and FoG, we consider it reasonable to clearly differentiate the beta frequency band when examining freezing - into low and high beta-, as they tend to behave oppositely. Thus, freezing is characterized by a decrease in the high beta band, supporting the hypothesis of high beta being rather prokinetic (Florin et al., 2013; Ozturk et al., 2020).

However, as described above, pure averaging of power does not provide a comprehensive understanding of freezing, as it fails to capture the possible alternating increases and decreases in activity. Therefore, we examined the time-frequency series for a more detailed analysis, revealing prominent fluctuating increases in the beta band during FoG. The observed absence of suppression in the alpha and beta frequency bands, along with the lack of modulation typically associated with normal gait, indicates an inability to achieve the necessary rhythmicity of effective motor control.

Our findings that the STN shows noticeable differences in activation during freezing and no longer exhibits the physiological modulation of normal gait could be a further building block in modeling FoG as the endpoint of a common neural pathway via the STN (Lewis & Shine, 2016). This model suggests that freezing results from impairments in conflict processing. The exact origin of this conflict remains undefined, which does justice to the fact that freezing can arise from a variety of situations and be influenced by different modulators, such as cognitive

processes like interference tasks or increased attention-grabbing events (e.g., cues) (Weiss et al., 2020), as well as anxiety (Giladi & Hausdorff, 2006). When a response conflict occurs, it results in increased activity within the hyperdirect pathway of the basal ganglia, linking the presupplementary motor area and other frontal cortex regions to the STN (Haynes & Haber, 2013). In times of high response conflict, the STN increases its firing rate, which in turn leads to increased activity in the internal segment of the GPi. This subsequently causes reduced activity in the thalamus and increased inhibition of brainstem regions both crucial for controlling normal gait (Frank, 2006; Shine et al., 2013). Thus, an increase in the STN firing rate directly inhibits motor control regions in the brainstem (PPN, MLR), ultimately manifesting as freezing. The reason why the STN increases its oscillatory activity during freezing-inducing conflicts is still not fully understood. One possibility is the ineffective selection of motor plans by the presupplementary motor area (pSMA), resulting in inappropriate information being sent to the STN (Nachev et al., 2008). Since an important task of the STN is to select the timing for motor task execution and prevent premature execution - especially when several motor plans or response options are available - the STN responds to the presence of multiple competing plans by increasing its firing rate. This heightened activity inhibits motor execution until a complete and final plan for the motor task is available.

In the case of a completely conclusive motor plan, as it was the case in our setup of arbitrary stops, the STN would have to reduce its firing rate in the model just described. In our study, this can be observed in the decrease of activity (6-13 Hz) between Stopping compared to Standing. Interestingly, in the time frequency analyses, we observed a suppression of alpha and beta band activity immediately after Stop onset and even before, in the Pre-Stop phase, and there was a rebound of activity at around 300 ms after the Stop onset. It can be interpreted as a Post-movement beta ‘rebound’, a transient increase in beta power observable 300 to 1000 ms after the end of a movement (Kilavik et al., 2013), initially reported for cortical areas, such as motor and somatosensory cortex (Kilavik et al., 2013; van Burik & Pfurtscheller, 1999) and interpreted as a short-term inhibition of the motor cortex networks (Pfurtscheller et al., 2005; Salmelin

et al., 1995). Thus, the theory of increased beta band activity was developed to maintain the 'status quo', i.e. to maintain the current state - sensorimotor or cognitive. A pathologically increased beta activity leads to less flexible behavior and cognitive control (Engel & Fries, 2010). According to this model, the post-movement rebound may be necessary to protect the actual motor state from disruptive factors and a reduction in beta activity before and during a movement enables the motor plan to be initiated in the first place (Barone & Rossiter, 2021). As we saw the movement related beta decrease in our voluntary stops plus the post movement related beta rebound and in contrast the lack of event-related desynchronization of alpha- and beta- band activity in Freezing, we were able to show that these two conditions differ completely in their STN activation patterns and are distinguishable in freely moving patients by LFP measurements.

Altogether, if we see freezing as a phenomenon that occurs when the locomotor network is vulnerable, influenced by various modulators that either decrease or increase its likelihood, and affected by neuronal integration failure (Weiss et al., 2020), all converging to a common ultimate pathway as a bottleneck (Lewis & Shine, 2016), we could suggest that altered activity of the STN acts as a plug clogging this pathway. Pathologically increased beta activity in the STN could be a potential cause and indicator of disturbed movement flow and interruption of the STN's oscillatory dynamics required for physiological gait. These disruptions, already visible as alterations in the last gait cycles before freezing, would ultimately manifest in FoG.

4.3 Freezing as a predictable phenomenon based on STN activity differences emerging even before its onset

We were able to confirm our hypothesis that a change in subthalamic activity is already detectable before freezing is clinically visible. More specifically, we demonstrated that the phase preceding freezing differs distinctly from that before an arbitrary stop. Notably, alpha and low beta activity increased before freezing but decreased before a stop. This discrepancy was not observable in the high beta band, suggesting that changes in alpha and low beta activity should rather

be considered when searching for potential predictors of an upcoming freezing episode.

Our hypothesis was based on our research group's observations of upper limb freezing (ULF) (Scholten et al., 2020). The power modulation of the beta band across finger-tapping cycles decreased in the transition phase preceding a ULF episode and an increase in beta band power was observable (Scholten et al., 2020). Although these measurements were taken using EEG over cortical areas, and ULF and freezing are not identical, similar neurophysiological processes can be assumed due to the close link between the cortex and basal ganglia in movement development. Therefore, it can be concluded that the results are related, and we were able to confirm the observations in the STN.

In the meantime, other research groups have also attempted to shed more light on the transition phase before freezing or to predict freezing. For example, one research group showed an increase in beta activity before freezing in a virtual reality experiment design during DBS implantation surgery (Georgiades et al., 2019). This was measured using extracellular microelectrode recordings of pooled cell body action potentials from multiple subthalamic nucleus neurons. They also compared volitional stopping and freezing in terms of beta modulation using the 99th percentile of beta modulation during normal walking as a threshold. During volitional stopping, beta modulation did not surpass this threshold until the stopping action was executed. In contrast, during freezing, beta power already exceeded this threshold in the moments leading up to a freezing event and peaked much higher at the onset of freezing compared to volitional stopping.

The fact that they observed higher beta activity during volitional stops compared to walking, which we did not, could possibly be explained by the experimental setting. In their case, the stop task was given externally with a stop cue, which differs from our stops where the motivation to stop and the timing were chosen by the patient themselves.

Studies of various cueing mechanisms that show how freezing can be overcome have demonstrated that external stimuli (e.g., hearing a metronome) result in activation of the parieto-occipital cortex (Tosserams et al., 2022). Additionally,

there is evidence that externally influenced movements activate the posterior part of the brain, including the somatosensory, auditory, and visual cortex (Hallett, 2008). Movements that are intrinsically planned by the patient receive their information from the frontal lobe, especially the SMA, the hypothalamus, and the limbic system. For example, activation of the frontal cortex (Tosserams et al., 2022) was observable during internal cueing through silent rhythmic counting by the patient. Since freezing is caused by a lack of intrinsic motor planning due to defective basal ganglia function and lost automation of walking (Redgrave et al., 2010), and a sufficient gait depends on intact executive functions mediated by frontostriatal connections (J. Nonnekes et al., 2019), we consider the comparison of freezing with internally planned stop mechanisms to be more meaningful. This is because we consider more similar cortex areas involved in internally planned stops, compared to those activated during externally induced stops. Regarding the activity of the STN, the intrinsic motivation likely represents a more planned movement execution than an interruption of movement which goes along with beta desynchronization before and rebound after movement execution.
Nevertheless, both results, ours and those of Georgiades et. al. show abnormalities in the STN preceding a FoG even before its onset, which provides more evidence that freezing can be a predictable event using LFPs in the STN.

4.4 Clinical perspective

Considering the paroxysmal occurrence of FoG and our findings of its potential to be predictable due to alterations in the LFPs even before its onset, aDBS should be considered and further investigated as a possible treatment for FoG. Shortly before an episode occurs, which could be recognized by LFP alterations, the stimulation would be briefly adjusted, and a freezing episode prevented.

Current evidence suggests that adapted DBS is as safe and effective as conventional DBS in terms of motor performance (Bocci et al., 2021). It is even better in terms of symptoms control as it adapts stimulation parameters to the patient's clinical state using LFPs as input variables (Arlotti et al., 2016). Utilizing Beta activity as a triggering parameter enhances the efficacy of DBS in improving

motor scores compared to conventional DBS (Little et al., 2013). Moreover, it has be shown to be transferable and well-tolerated in everyday life (Arlotti et al., 2018).

Future studies should explore whether the principle of aDBS is transferable to FoG and if targeted stimulation can alleviate or prevent freezing. We recommend focusing specifically on alpha and low beta band activity, as these appear to be most affected when physiological gait is disrupted by FoG.

The results of our gait kinematic analyses could also contribute to the development of future adaptive DBS systems. For instance, a feedback mechanism from peripheral kinematic sensors could be used as an add-on to the STN measurements, using enhanced cadence or shortened stride length as triggers for stimulation adjustment.

5 Summary

Freezing of gait (FoG) is a debilitating motor symptom in patients with Pakinson's disease (PD), characterized by a sudden inability to walk forward. It is leading to severe impairments of patients' mobility, quality of life and resulting in falls, injuries, and hospitalization. The missing understanding of the underlying pathophysiology thus goes along with unexploited therapeutic options.

Deep brain stimulation devices with sensing capability enable to record oscillatory neuronal activity in patients while walking and exhibiting freezing. This technology allowed us to measure local field potentials (LFPs) with Deep Brain Stimulation (DBS) electrodes in PD patients to investigate subthalamic activity during and preceding a FoG episode, along with gait kinematics measured with external sensors. To delineate pathological changes, we further investigated the modulation of subthalamic activity over a gait cycle and during internally generated voluntary stops as a control condition.

We recorded subthalamic activity in 12 PD patients while performing different tasks such as sitting, standing, walking and walking with voluntary stops. To help trigger FoG episodes, the patients were off medication and completed the gait experiments in a corridor, which was additionally narrowed by two obstacles.
The collected data were then pre-processed, synchronized in time and checked for artefacts. FoG was identified based on video and kinematic data and the LFP signal subsequently divided into different epochs according to the different tasks. Time frequency domains and time-frequency analyses were calculated for Walking, FoG and Stops as well as for the transition periods preceding them. Non-parametric permutation testing was used to identify significant clusters during different conditions.

We found that the subthalamic nucleus (STN) shows a significant attenuation in alpha and beta band power during Walking compared to Standing. Furthermore, the STN displays gait-cycle related modulation of alpha and beta band power.
FoG showed a numerical increase of activity in the lower beta band and a significant decrease in the high beta band. In the time frequency analyses, FoG

was characterised by fluctuating power increases in the beta band. The alpha and beta attenuation, as it could be observed during walking, was no longer present. Moreover, our time-frequency analyses showed that numerical increase and fluctuations in alpha and low beta activity during the gait cycle could already be observed in the transition period before FoG occurs.
In contrast, Stop was characterized by a significant decrease of alpha activity. In the time-frequency analyses alpha and beta activity decreased shortly after the beginning of a Stop. Beta activity returned to normal around 380ms after Stop onset in sense of a rebound. During Pre-Stop, there was a significant attenuation in the alpha band range and the observed suppression of both the lower and upper beta bands was largely preserved from Walking.

We were able to demonstrate, that FoG differs completely in its STN activation patterns from those of normal walking and voluntary stops. The increased alpha and low beta activity in the STN could be a potential cause and indicator of disturbed movement flow and interruption of the STN's oscillatory dynamics required for physiological gait. We were able to show that these changes can be measured using LFPs in freely moving patients and are already visible in the transition phase before the actual occurrence of FoG. They displace the normal gait modulation and indicate the evolution of motor network failure. Those findings highlight the role of the STN in encoding effective forward walking and its diagnostic and potentially therapeutic utility in FoG. Beyond the pathophysiological insights into FoG, our findings provide potential to establish biomarkers that precede the worsening of the patient’s clinical state. This is a key step leading to closed loop stimulation and optimizing current DBS therapy.

6 Zusammenfassung

Freezing of Gait (FoG) ist ein beeinträchtigendes, pathophysiologisch unzureichend verstandenes und damit bislang eingeschränkt therapierbares Symptom der Parkinsonkrankheit. Es ist gekennzeichnet durch eine plötzlich gestörte Vorwärtsprogression des Gehens, führt zu erheblicher Einschränkung der Mobilität und Lebensqualität der Patienten, sowie zu Stürzen mit Hospitalisierung, Morbidität und Mortalität.

Die Tiefe Hirnstimulation bietet mit neuartigen Stimulationsgeräten nun eine Möglichkeit, neuronale Signale aus dem Nucleus subthalamicus (STN) in Echtzeit bei Patienten zu analysieren, während diese laufen und Freezing erleben. So konnten wir mithilfe von THS-Elektroden die subthalamische Aktivität in Form von lokalen Feldpotenzialen (LFPs) während und vor FoG untersuchen. Das LFP-Signal stellt hierbei die summierte elektrische Aktivität von Neuronen in der Nähe der Elektrode dar und wird anhand seiner Frequenzmuster analysiert. Parallel erfolgten Ganganalysen mittels externer Sensoren. Um Veränderungen spezifischer auf FoG zurückführen zu können, untersuchten wir die subthalamische Aktivität während eines normalen Gangzyklus und während vom Patienten willkürlich gewählten Stops als Kontrollbedingung.

In die Studie wurden 12 Morbus-Parkinson-Patienten eingeschlossen und die Aktivität des STN bei der Ausführung verschiedener Aufgaben wie Sitzen, Stehen, Gehen und Gehen mit wiederholten willkürlichen Stops untersucht. Um die Auftretenswahrscheinlichkeit von FoG-Episoden zu erhöhen, pausierten die Patienten Levodopa und führten die Gang-Experimente in einem Korridor durch, der zusätzlich durch zwei Hindernisse verengt wurde.
Die gesammelten Daten wurden anschließend präprozessiert, zeitlich synchronisiert und auf Artefakte überprüft. FoG wurde mittels Videoaufnahmen und anhand der kinematischen Daten identifiziert und das LFP-Signal anschließend entsprechend der verschiedenen Aufgaben in verschiedene Epochen unterteilt. Es wurden Frequenzdomänen und Zeit-Frequenz-Analysen für Gehen, FoG und Stops berechnet sowie für die Transitionsphasen vor FoG

und Stop. Um signifikante Cluster unter den verschiedenen Bedingungen zu identifizieren wurde ein nicht-parametrischer Permutationstest verwendet.
Wir fanden heraus, dass der STN eine signifikante Abschwächung der Alpha- und Beta-Band-Aktivität beim Gehen im Vergleich zum Stehen aufweist. Darüber hinaus zeigt der STN eine mit dem Gangzyklus verbundene Modulation der Alpha- und Beta-Band-Aktivität. FoG hingegen zeigte eine numerische Zunahme der Aktivität im unteren Beta-Band und eine signifikante Abnahme im hohen Beta-Band. In den Zeit-Frequenz-Analysen war FoG durch intermittierende Aktivitätszunahme im Alpha und Beta-Band-Bereich gekennzeichnet. Die beim Gehen beobachtbare Modulation der Frequenzbänder und Kopplung der Aktivitätsmodulation an distinkte Gangphasen war aufgehoben. Weiterhin zeigte sich, dass die Zunahme der Alpha- und Low-Beta-Aktivität bereits in der Transitionsphase vor FoG auftrat.
Im Gegensatz dazu war der willkürliche Stop durch eine signifikante Abnahme der Alpha-Aktivität gekennzeichnet. In den Zeit-Frequenz-Analysen nahm die Alpha- und Beta-Aktivität kurz nach Beginn des Stops ab. Die Beta-Aktivität erreichte etwa 380 ms nach Beginn des Stops erneut den Normalwert, im Sinne eines Rebounds. Während der Transitionsphase vor einem Stop konnte eine signifikante Abschwächung im Alpha-Band beobachtet werden. Die beim Gehen beobachtete Unterdrückung sowohl des unteren als auch des oberen Betabandes blieb weitgehend erhalten.

Wir konnten nachweisen, dass sich die Aktivierungsmuster des STN bei FoG völlig von denen des normalen Gehens und des willkürlichen Stops unterscheiden. Die erhöhte Alpha- und Low-Beta-Band-Aktivität im STN stellen ein Korrelat für einen gestörten Bewegungsfluss und eine Unterbrechung der für den physiologischen Gang erforderlichen oszillatorischen Dynamik des STN dar. Wir konnten zeigen, dass diese Veränderungen mittels LFPs bei frei gehenden Patienten messbar und bereits in der Übergangsphase vor dem eigentlichen Auftreten des FoG sichtbar sind. Sie zeigen eine Störung der normalen Gangmodulation an und deuten auf die zunehmende Beeinträchtigung des motorischen Netzwerks vor und während des FoG hin. Hierbei wird die Rolle des

STN bei der Kodierung des effektiven Vorwärtsgehens deutlich und seine potentielle Rolle, um neues Verständnis und Ansätze für die Therapie des FoG zu entwickeln. Weiterhin liefern unsere Ergebnisse wichtige Hinweise zur Identifikation potenzieller oszillatorischer Biomarker, die FoG vorausgehen - ein wichtiger Baustein in der Entwicklung geschlossener Systeme der Tiefen Hirnstimulation und deren Optimierung.

7 References

Anderson, R. W., Wilkins, K. B., Parker, J. E., Petrucci, M. N., Kehnemouyi, Y., Neuville, R. S.,…Bronte-Stewart, H. M. (2021). Lack of progression of beta dynamics after long-term subthalamic neurostimulation. *Annals of Clinical and Translational Neurology*, *8*(11), 2110-2120. https://doi.org/10.1002/acn3.51463

Arlotti, M., Marceglia, S., Foffani, G., Volkmann, J., Lozano, A. M., Moro, E.,…Priori, A. (2018). Eight-hours adaptive deep brain stimulation in patients with Parkinson disease. *Neurology*, *90*(11), e971-e976. https://doi.org/10.1212/wnl.0000000000005121

Arlotti, M., Rosa, M., Marceglia, S., Barbieri, S., & Priori, A. (2016). The adaptive deep brain stimulation challenge. *Parkinsonism Relat Disord*, *28*, 12-17. https://doi.org/10.1016/j.parkreldis.2016.03.020

Armstrong, M. J., & Okun, M. S. (2020). Diagnosis and Treatment of Parkinson Disease: A Review. *Jama*, *323*(6), 548-560. https://doi.org/10.1001/jama.2019.22360

Ascherio, A., & Schwarzschild, M. A. (2016). The epidemiology of Parkinson's disease: risk factors and prevention. *Lancet Neurol*, *15*(12), 1257-1272. https://doi.org/10.1016/s1474-4422(16)30230-7

Ashkan, K., Rogers, P., Bergman, H., & Ughratdar, I. (2017). Insights into the mechanisms of deep brain stimulation. *Nature Reviews Neurology*, *13*(9), 548-554. https://doi.org/10.1038/nrneurol.2017.105

Balestrino, R., & Martinez-Martin, P. (2017). Neuropsychiatric symptoms, behavioural disorders, and quality of life in Parkinson's disease. *J Neurol Sci*, *373*, 173-178. https://doi.org/10.1016/j.jns.2016.12.060

Balestrino, R., & Schapira, A. H. V. (2020). Parkinson disease. *Eur J Neurol*, *27*(1), 27-42. https://doi.org/10.1111/ene.14108

Barbe, M. T., Amarell, M., Snijders, A. H., Florin, E., Quatuor, E.-L., Schönau, E.,…Timmermann, L. (2014). Gait and upper limb variability in Parkinson's disease patients with and without freezing of gait. *Journal of Neurology*, *261*(2), 330-342. https://doi.org/10.1007/s00415-013-7199-1

Barone, J., & Rossiter, H. E. (2021). Understanding the Role of Sensorimotor Beta Oscillations [Mini Review]. *Frontiers in Systems Neuroscience*, *15*. https://doi.org/10.3389/fnsys.2021.655886

Berger, H. (1929). Über das Elektrenkephalogramm des Menschen. *Archiv für Psychiatrie und Nervenkrankheiten*, *87*(1), 527-570. https://doi.org/10.1007/BF01797193

Beudel, M., Little, S., Pogosyan, A., Ashkan, K., Foltynie, T., Limousin, P.,…Brown, P. (2015). Tremor Reduction by Deep Brain Stimulation Is Associated With Gamma Power Suppression in Parkinson's Disease. *Neuromodulation*, *18*(5), 349-354. https://doi.org/10.1111/ner.12297

Bloem, B. R., Hausdorff, J. M., Visser, J. E., & Giladi, N. (2004). Falls and freezing of gait in Parkinson's disease: A review of two interconnected, episodic phenomena. *Movement Disorders*, *19*(8), 871-884. https://doi.org/10.1002/mds.20115

Bocci, T., Prenassi, M., Arlotti, M., Cogiamanian, F. M., Borellini, L., Moro, E.,…Marceglia, S. (2021). Eight-hours conventional versus adaptive deep brain stimulation of the subthalamic nucleus in Parkinson's disease. *NPJ Parkinsons Dis*, *7*(1), 88. https://doi.org/10.1038/s41531-021-00229-z

Brittain, J. S., & Brown, P. (2014). Oscillations and the basal ganglia: motor control and beyond. *Neuroimage*, *85 Pt 2*(Pt 2), 637-647. https://doi.org/10.1016/j.neuroimage.2013.05.084

Bronte-Stewart, H., Beudel, M., Ostrem, J. L., Fasano, A., Almeida, L., Hassell, T.,…Herrington, T. M. (2023). Adaptive DBS Algorithm for Personalized Therapy in Parkinson's Disease: ADAPT-PD clinical trial methodology and early data (P1-11.002). *Neurology*, *100*(17_supplement_2), 3204. https://doi.org/doi:10.1212/WNL.0000000000203099

Bronte-Stewart, H. M., Petrucci, M. N., O'Day, J. J., Afzal, M. F., Parker, J. E., Kehnemouyi, Y. M.,…Hoffman, S. L. (2020). Perspective: Evolution of Control Variables and Policies for Closed-Loop Deep Brain Stimulation for Parkinson's Disease Using Bidirectional Deep-Brain-Computer Interfaces. *Front Hum Neurosci*, *14*, 353. https://doi.org/10.3389/fnhum.2020.00353

Brown, P. (2003). Oscillatory nature of human basal ganglia activity: Relationship to the pathophysiology of Parkinson's disease. *Movement Disorders*, *18*(4), 357-363. https://doi.org/10.1002/mds.10358

Brown, P., Oliviero, A., Mazzone, P., Insola, A., Tonali, P., & Di Lazzaro, V. (2001). Dopamine dependency of oscillations between subthalamic nucleus and pallidum in Parkinson's disease. *Journal of Neuroscience*, *21*(3), 1033-1038. DOI: 10.1523/JNEUROSCI.21-03-01033.2001

Calabresi, P., Di Filippo, M., Ghiglieri, V., Tambasco, N., & Picconi, B. (2010). Levodopa-induced dyskinesias in patients with Parkinson's disease: filling the bench-to-bedside gap. *Lancet Neurol*, *9*(11), 1106-1117. https://doi.org/10.1016/s1474-4422(10)70218-0

Canessa, A., Palmisano, C., Isaias, I. U., & Mazzoni, A. (2020). Gait-related frequency modulation of beta oscillatory activity in the subthalamic nucleus of parkinsonian patients. *Brain Stimul*, *13*(6), 1743-1752. https://doi.org/10.1016/j.brs.2020.09.006

Canning, C. G., Paul, S. S., & Nieuwboer, A. (2014). Prevention of falls in Parkinson's disease: a review of fall risk factors and the role of physical interventions. *Neurodegener Dis Manag*, *4*(3), 203-221. https://doi.org/10.2217/nmt.14.22

Chen, C.-C., Yeh, C.-H., Chan, H.-L., Chang, Y.-J., Tu, P.-H., Yeh, C.-H.,…Brown, P. (2019). Subthalamic nucleus oscillations correlate with vulnerability to freezing of gait in patients with Parkinson's disease.

Neurobiology of Disease, *132*, 104605. https://doi.org/10.1016/j.nbd.2019.104605

Chen, C. C., Pogosyan, A., Zrinzo, L. U., Tisch, S., Limousin, P., Ashkan, K.,…Brown, P. (2006). Intra-operative recordings of local field potentials can help localize the subthalamic nucleus in Parkinson's disease surgery. *Experimental Neurology*, *198*(1), 214-221. https://doi.org/10.1016/j.expneurol.2005.11.019

Cockx, H., Nonnekes, J., Bloem, B. R., van Wezel, R., Cameron, I., & Wang, Y. (2023). Correction: Dealing with the heterogeneous presentations of freezing of gait: how reliable are the freezing index and heart rate for freezing detection? *Journal of NeuroEngineering and Rehabilitation*, *20*(1), 74. https://doi.org/10.1186/s12984-023-01201-z

Connolly, B. S., & Lang, A. E. (2014). Pharmacological Treatment of Parkinson Disease: A Review. *Jama*, *311*(16), 1670-1683. https://doi.org/10.1001/jama.2014.3654

Cross, K. A., Malekmohammadi, M., Woo Choi, J., & Pouratian, N. (2021). Movement-related changes in pallidocortical synchrony differentiate action execution and observation in humans. *Clin Neurophysiol*, *132*(8), 1990-2001. https://doi.org/10.1016/j.clinph.2021.03.037

Deuschl, G., Paschen, S., & Witt, K. (2013). Chapter 10 - Clinical outcome of deep brain stimulation for Parkinson’s disease. In A. M. Lozano & M. Hallett (Eds.), *Handbook of Clinical Neurology* (Vol. 116, pp. 107-128). Elsevier. https://doi.org/10.1016/B978-0-444-53497-2.00010-3

Deuschl, G., Schade-Brittinger, C., Krack, P., Volkmann, J., Schäfer, H., Bötzel, K.,…Voges, J. (2006). A randomized trial of deep-brain stimulation for Parkinson's disease. *N Engl J Med*, *355*(9), 896-908. https://doi.org/10.1056/NEJMoa060281

Duncan, G. W., Khoo, T. K., Yarnall, A. J., O'Brien, J. T., Coleman, S. Y., Brooks, D. J.,…Burn, D. J. (2014). Health-related quality of life in early Parkinson's disease: the impact of nonmotor symptoms. *Mov Disord*, *29*(2), 195-202. https://doi.org/10.1002/mds.25664

Einevoll, G. T., Kayser, C., Logothetis, N. K., & Panzeri, S. (2013). Modelling and analysis of local field potentials for studying the function of cortical circuits. *Nat Rev Neurosci*, *14*(11), 770-785. https://doi.org/10.1038/nrn3599

Engel, A. K., & Fries, P. (2010). Beta-band oscillations—signalling the status quo? *Current Opinion in Neurobiology*, *20*(2), 156-165. https://doi.org/10.1016/j.conb.2010.02.015

Eusebio, A., Thevathasan, W., Gaynor, L. D., Pogosyan, A., Bye, E., Foltynie, T.,…Brown, P. (2011). Deep brain stimulation can suppress pathological synchronisation in parkinsonian patients. *Journal of Neurology, Neurosurgery & Psychiatry*, *82*(5), 569. https://doi.org/10.1136/jnnp.2010.217489

Falla, M., Cossu, G., & Di Fonzo, A. (2022). Freezing of gait: overview on etiology, treatment, and future directions. *Neurological Sciences*, *43*(3), 1627-1639. https://doi.org/10.1007/s10072-021-05796-w

Fasano, A., Laganiere, S. E., Lam, S., & Fox, M. D. (2017). Lesions causing freezing of gait localize to a cerebellar functional network. *Ann Neurol*, *81*(1), 129-141. https://doi.org/10.1002/ana.24845

Fasano, A., Mure, H., Oyama, G., Murase, N., Witt, T., Higuchi, Y.,…Morelli, N. (2024). Subthalamic nucleus local field potential stability in patients with Parkinson's disease. *Neurobiology of Disease*, *199*, 106589. https://doi.org/10.1016/j.nbd.2024.106589

Feldmann, L. K., Neumann, W. J., Krause, P., Lofredi, R., Schneider, G. H., & Kühn, A. A. (2021). Subthalamic beta band suppression reflects effective neuromodulation in chronic recordings. *European Journal of Neurology*, *28*(7), 2372-2377. DOI: 10.1111/ene.14801

Fereshtehnejad, S. M., Romenets, S. R., Anang, J. B., Latreille, V., Gagnon, J. F., & Postuma, R. B. (2015). New Clinical Subtypes of Parkinson Disease and Their Longitudinal Progression: A Prospective Cohort Comparison With Other Phenotypes. *JAMA Neurol*, *72*(8), 863-873. https://doi.org/10.1001/jamaneurol.2015.0703

Fischer, P., Chen, C. C., Chang, Y. J., Yeh, C. H., Pogosyan, A., Herz, D. M.,…Tan, H. (2018). Alternating Modulation of Subthalamic Nucleus Beta Oscillations during Stepping. *J Neurosci*, *38*(22), 5111-5121. https://doi.org/10.1523/jneurosci.3596-17.2018

Florin, E., Dafsari, H. S., Reck, C., Barbe, M. T., Pauls, K. A., Maarouf, M.,…Timmermann, L. (2013). Modulation of local field potential power of the subthalamic nucleus during isometric force generation in patients with Parkinson's disease. *Neuroscience*, *240*, 106-116. https://doi.org/10.1016/j.neuroscience.2013.02.043

Frank, M. J. (2006). Hold your horses: a dynamic computational role for the subthalamic nucleus in decision making. *Neural Netw*, *19*(8), 1120-1136. https://doi.org/10.1016/j.neunet.2006.03.006

Gao, C., Liu, J., Tan, Y., & Chen, S. (2020). Freezing of gait in Parkinson's disease: pathophysiology, risk factors and treatments. *Transl Neurodegener*, *9*, 12. https://doi.org/10.1186/s40035-020-00191-5

Gatev, P., Darbin, O., & Wichmann, T. (2006). Oscillations in the basal ganglia under normal conditions and in movement disorders. *Movement Disorders*, *21*(10), 1566-1577. https://doi.org/10.1002/mds.21033

Gatev, P., Darbin, O., & Wichmann, T. (2006). Oscillations in the basal ganglia under normal conditions and in movement disorders. *Mov Disord*, *21*(10), 1566-1577. https://doi.org/10.1002/mds.21033

Geng, X., Zhang, J., Jiang, Y., Ashkan, K., Foltynie, T., Limousin, P.,…Wang, S. (2017). Comparison of oscillatory activity in subthalamic nucleus in

Parkinson's disease and dystonia. *Neurobiology of Disease*, *98*, 100-107. https://doi.org/10.1016/j.nbd.2016.12.006

Georgiades, M. J., Shine, J. M., Gilat, M., McMaster, J., Owler, B., Mahant, N., & Lewis, S. J. G. (2019). Hitting the brakes: pathological subthalamic nucleus activity in Parkinson's disease gait freezing. *Brain*, *142*(12), 3906-3916. https://doi.org/10.1093/brain/awz325

Giladi, N., & Hausdorff, J. M. (2006). The role of mental function in the pathogenesis of freezing of gait in Parkinson's disease. *Journal of the Neurological Sciences*, *248*(1), 173-176. https://doi.org/10.1016/j.jns.2006.05.015

Giladi, N., & Nieuwboer, A. (2008). Understanding and treating freezing of gait in parkinsonism, proposed working definition, and setting the stage. *Movement Disorders*, *23*(S2), S423-S425. https://doi.org/10.1002/mds.21927

Goetz, C. G., Poewe, W., Rascol, O., & Sampaio, C. (2005). Evidence-based medical review update: pharmacological and surgical treatments of Parkinson's disease: 2001 to 2004. *Mov Disord*, *20*(5), 523-539. https://doi.org/10.1002/mds.20464

Gwin, J. T., Gramann, K., Makeig, S., & Ferris, D. P. (2011). Electrocortical activity is coupled to gait cycle phase during treadmill walking. *Neuroimage*, *54*(2), 1289-1296. https://doi.org/10.1016/j.neuroimage.2010.08.066

Habets, J. G. V., Heijmans, M., Kuijf, M. L., Janssen, M. L. F., Temel, Y., & Kubben, P. L. (2018). An update on adaptive deep brain stimulation in Parkinson's disease. *Mov Disord*, *33*(12), 1834-1843. https://doi.org/10.1002/mds.115

Halje, P., Brys, I., Mariman, J. J., da Cunha, C., Fuentes, R., & Petersson, P. (2019). Oscillations in cortico-basal ganglia circuits: implications for Parkinson's disease and other neurologic and psychiatric conditions. *J Neurophysiol*, *122*(1), 203-231. https://doi.org/10.1152/jn.00590.2018

Hallett, M. (2008). The intrinsic and extrinsic aspects of freezing of gait. *Mov Disord*, *23 Suppl 2*(0 2), S439-443. https://doi.org/10.1002/mds.21836

Hammond, C., Bergman, H., & Brown, P. (2007). Pathological synchronization in Parkinson's disease: networks, models and treatments. *Trends Neurosci*, *30*(7), 357-364. https://doi.org/10.1016/j.tins.2007.05.004

Hausdorff, J. M., Schaafsma, J. D., Balash, Y., Bartels, A. L., Gurevich, T., & Giladi, N. (2003). Impaired regulation of stride variability in Parkinson's disease subjects with freezing of gait. *Exp Brain Res*, *149*(2), 187-194. https://doi.org/10.1007/s00221-002-1354-8

Haynes, W. I., & Haber, S. N. (2013). The organization of prefrontal-subthalamic inputs in primates provides an anatomical substrate for both functional specificity and integration: implications for Basal Ganglia models and deep brain stimulation. *J Neurosci*, *33*(11), 4804-4814. https://doi.org/10.1523/jneurosci.4674-12.2013

Hell, F., Plate, A., Mehrkens, J. H., & Bötzel, K. (2018). Subthalamic oscillatory activity and connectivity during gait in Parkinson's disease. *Neuroimage Clin*, *19*, 396-405. https://doi.org/10.1016/j.nicl.2018.05.001

Herreras, O. (2016). Local Field Potentials: Myths and Misunderstandings. *Front Neural Circuits*, *10*, 101. https://doi.org/10.3389/fncir.2016.00101

Herrington, T. M., Cheng, J. J., & Eskandar, E. N. (2016). Mechanisms of deep brain stimulation. *Journal of Neurophysiology*, *115*(1), 19-38. https://doi.org/10.1152/jn.00281.2015

Hirtz, D., Thurman, D. J., Gwinn-Hardy, K., Mohamed, M., Chaudhuri, A. R., & Zalutsky, R. (2007). How common are the "common" neurologic disorders? *Neurology*, *68*(5), 326-337. https://doi.org/10.1212/01.wnl.0000252807.38124.a3

Hughes, A. J., Daniel, S. E., Kilford, L., & Lees, A. J. (1992). Accuracy of clinical diagnosis of idiopathic Parkinson's disease: a clinico-pathological study of 100 cases. *J Neurol Neurosurg Psychiatry*, *55*(3), 181-184. https://doi.org/10.1136/jnnp.55.3.181

Jacobs, J. V., Nutt, J. G., Carlson-Kuhta, P., Stephens, M., & Horak, F. B. (2009). Knee trembling during freezing of gait represents multiple anticipatory postural adjustments. *Exp Neurol*, *215*(2), 334-341. https://doi.org/10.1016/j.expneurol.2008.10.019

Jacobsen, N. S. J., Blum, S., Witt, K., & Debener, S. (2021). A walk in the park? Characterizing gait-related artifacts in mobile EEG recordings. *Eur J Neurosci*, *54*(12), 8421-8440. https://doi.org/10.1111/ejn.14965

Jankovic, J., McDermott, M., Carter, J., Gauthier, S., Goetz, C., Golbe, L.,…et al. (1990). Variable expression of Parkinson's disease: a base-line analysis of the DATATOP cohort. The Parkinson Study Group. *Neurology*, *40*(10), 1529-1534. https://doi.org/10.1212/wnl.40.10.1529

Jasper, H., & Penfield, W. (1949). Electrocorticograms in man: Effect of voluntary movement upon the electrical activity of the precentral gyrus. *Archiv für Psychiatrie und Nervenkrankheiten*, *183*(1), 163-174. https://doi.org/10.1007/BF01062488

Jasper, H. H., & Andrews, H. L. (1936). Human Brain Rhythms: I. Recording Techniques and Preliminary Results. *The Journal of General Psychology*, *14*(1), 98-126. https://doi.org/10.1080/00221309.1936.9713141

Jimenez-Shahed, J. (2021). Device profile of the percept PC deep brain stimulation system for the treatment of Parkinson’s disease and related disorders. *Expert Review of Medical Devices*, *18*(4), 319-332. https://doi.org/10.1080/17434440.2021.1909471

Khawaldeh, S., Tinkhauser, G., Torrecillos, F., He, S., Foltynie, T., Limousin, P.,…Brown, P. (2022). Balance between competing spectral states in subthalamic nucleus is linked to motor impairment in Parkinson's disease. *Brain*, *145*(1), 237-250. https://doi.org/10.1093/brain/awab264

Kilavik, B. E., Zaepffel, M., Brovelli, A., MacKay, W. A., & Riehle, A. (2013). The ups and downs of β oscillations in sensorimotor cortex. *Exp Neurol*, *245*, 15-26. https://doi.org/10.1016/j.expneurol.2012.09.014

Kim, C., & Lee, S.-J. (2008). Controlling the mass action of α-synuclein in Parkinson's disease. *Journal of Neurochemistry*, *107*(2), 303-316. https://doi.org/10.1111/j.1471-4159.2008.05612.x

Kim, H. J., Mason, S., Foltynie, T., Winder-Rhodes, S., Barker, R. A., & Williams-Gray, C. H. (2020). Motor complications in Parkinson's disease: 13-year follow-up of the CamPaIGN cohort. *Mov Disord*, *35*(1), 185-190. https://doi.org/10.1002/mds.27882

Klimesch, W. (2012). α-band oscillations, attention, and controlled access to stored information. *Trends Cogn Sci*, *16*(12), 606-617. https://doi.org/10.1016/j.tics.2012.10.007

Kline, J. E., Huang, H. J., Snyder, K. L., & Ferris, D. P. (2015). Isolating gait-related movement artifacts in electroencephalography during human walking. *J Neural Eng*, *12*(4), 046022. https://doi.org/10.1088/1741-2560/12/4/046022

Klocke, P., Loeffler, M. A., Muessler, H., Breu, M.-S., Gharabaghi, A., & Weiss, D. (2024). Supraspinal contributions to defective antagonistic inhibition and freezing of gait in Parkinson's disease. *Brain*, *147*(12), 4056-4071. https://doi.org/10.1093/brain/awae223

Kolb, R., Abosch, A., Felsen, G., & Thompson, J. A. (2017). Use of intraoperative local field potential spectral analysis to differentiate basal ganglia structures in Parkinson's disease patients. *Physiol Rep*, *5*(12). https://doi.org/10.14814/phy2.13322

Kulcsarova, K., Skorvanek, M., Postuma, R. B., & Berg, D. (2024). Defining Parkinson's Disease: Past and Future. *J Parkinsons Dis*, *14*(s2), S257-s271. https://doi.org/10.3233/jpd-230411

Kwok, J. Y. Y., Smith, R., Chan, L. M. L., Lam, L. C. C., Fong, D. Y. T., Choi, E. P. H.,…Bloem, B. R. (2022). Managing freezing of gait in Parkinson's disease: a systematic review and network meta-analysis. *Journal of Neurology*, *269*(6), 3310-3324. https://doi.org/10.1007/s00415-022-11031-z

Kühn, A. A., Kempf, F., Brücke, C., Gaynor Doyle, L., Martinez-Torres, I., Pogosyan, A.,…Brown, P. (2008). High-Frequency Stimulation of the Subthalamic Nucleus Suppresses Oscillatory β Activity in Patients with Parkinson's Disease in Parallel with Improvement in Motor Performance. *The Journal of Neuroscience*, *28*(24), 6165. https://doi.org/10.1523/JNEUROSCI.0282-08.2008

Kühn, A. A., Kupsch, A., Schneider, G.-H., & Brown, P. (2006). Reduction in subthalamic 8–35 Hz oscillatory activity correlates with clinical improvement in Parkinson's disease. *European Journal of Neuroscience*, *23*(7), 1956-1960. https://doi.org/https://doi.org/10.1111/j.1460-9568.2006.04717.x

Kühn, A. A., Trottenberg, T., Kivi, A., Kupsch, A., Schneider, G.-H., & Brown, P. (2005). The relationship between local field potential and neuronal discharge in the subthalamic nucleus of patients with Parkinson's disease. *Experimental Neurology*, *194*(1), 212-220. https://doi.org/10.1016/j.expneurol.2005.02.010

Kühn, A. A., Tsui, A., Aziz, T., Ray, N., Brücke, C., Kupsch, A.,…Brown, P. (2009). Pathological synchronisation in the subthalamic nucleus of patients with Parkinson's disease relates to both bradykinesia and rigidity. *Exp Neurol*, *215*(2), 380-387. https://doi.org/10.1016/j.expneurol.2008.11.008

Kühn, A. A., & Volkmann, J. (2017). Innovations in deep brain stimulation methodology *Movement Disorders*, *32*(1), 11-19. https://doi.org/https://doi.org/10.1002/mds.26703

Lee, A., & Gilbert, R. M. (2016). Epidemiology of Parkinson Disease. *Neurologic Clinics*, *34*(4), 955-965. https://doi.org/10.1016/j.ncl.2016.06.012

Lewis, S. J., & Barker, R. A. (2009). A pathophysiological model of freezing of gait in Parkinson's disease. *Parkinsonism Relat Disord*, *15*(5), 333-338. https://doi.org/10.1016/j.parkreldis.2008.08.006

Lewis, S. J., & Shine, J. M. (2016). The Next Step: A Common Neural Mechanism for Freezing of Gait. *Neuroscientist*, *22*(1), 72-82. https://doi.org/10.1177/1073858414559101

Limousin, P., & Foltynie, T. (2019). Long-term outcomes of deep brain stimulation in Parkinson disease. *Nat Rev Neurol*, *15*(4), 234-242. https://doi.org/10.1038/s41582-019-0145-9

Little, S., Beudel, M., Zrinzo, L., Foltynie, T., Limousin, P., Hariz, M.,…Brown, P. (2016). Bilateral adaptive deep brain stimulation is effective in Parkinson's disease. *J Neurol Neurosurg Psychiatry*, *87*(7), 717-721. https://doi.org/10.1136/jnnp-2015-310972

Little, S., & Brown, P. (2014). The functional role of beta oscillations in Parkinson's disease. *Parkinsonism Relat Disord*, *20 Suppl 1*, S44-48. https://doi.org/10.1016/s1353-8020(13)70013-0

Little, S., & Brown, P. (2020). Debugging Adaptive Deep Brain Stimulation for Parkinson's Disease. *Movement Disorders*, *35*(4), 555-561. https://doi.org/10.1002/mds.27996

Little, S., Pogosyan, A., Neal, S., Zavala, B., Zrinzo, L., Hariz, M.,…Brown, P. (2013). Adaptive deep brain stimulation in advanced Parkinson disease. *Ann Neurol*, *74*(3), 449-457. https://doi.org/10.1002/ana.23951

Little, S., Tripoliti, E., Beudel, M., Pogosyan, A., Cagnan, H., Herz, D.,…Brown, P. (2016). Adaptive deep brain stimulation for Parkinson's disease demonstrates reduced speech side effects compared to conventional stimulation in the acute setting. *Journal of Neurology, Neurosurgery & Psychiatry*, *87*(12), 1388-1389. https://doi.org/10.1136/jnnp-2016-313518

Litvak, V., Florin, E., Tamás, G., Groppa, S., & Muthuraman, M. (2021). EEG and MEG primers for tracking DBS network effects. *Neuroimage*, *224*, 117447. https://doi.org/10.1016/j.neuroimage.2020.117447

Liu, D. F., Zhao, B. T., Zhu, G. Y., Liu, Y. Y., Bai, Y. T., Liu, H. G.,…Zhang, J. G. (2022). Synchronized Intracranial Electrical Activity and Gait Recording in Parkinson's Disease Patients With Freezing of Gait. *Front Neurosci*, *16*, 795417. https://doi.org/10.3389/fnins.2022.795417

Louie, K. H., Gilron, R., Yaroshinsky, M. S., Morrison, M. A., Choi, J., de Hemptinne, C.,…Wang, D. D. (2022). Cortico-Subthalamic Field Potentials Support Classification of the Natural Gait Cycle in Parkinson's Disease and Reveal Individualized Spectral Signatures. *eNeuro*, *9*(6). https://doi.org/10.1523/eneuro.0325-22.2022

Lozano, A. M., Lipsman, N., Bergman, H., Brown, P., Chabardes, S., Chang, J. W.,…Krauss, J. K. (2019). Deep brain stimulation: current challenges and future directions. *Nat Rev Neurol*, *15*(3), 148-160. https://doi.org/10.1038/s41582-018-0128-2

Mahlknecht, P., Foltynie, T., Limousin, P., & Poewe, W. (2022). How Does Deep Brain Stimulation Change the Course of Parkinson's Disease? *Mov Disord*. https://doi.org/10.1002/mds.29052

Mancini, M., Smulders, K., Cohen, R. G., Horak, F. B., Giladi, N., & Nutt, J. G. (2017). The clinical significance of freezing while turning in Parkinson's disease. *Neuroscience*, *343*, 222-228. https://doi.org/10.1016/j.neuroscience.2016.11.045

Mann, J. M., Foote, K. D., Garvan, C. W., Fernandez, H. H., Jacobson, C. E. t., Rodriguez, R. L.,…Okun, M. S. (2009). Brain penetration effects of microelectrodes and DBS leads in STN or GPi. *J Neurol Neurosurg Psychiatry*, *80*(7), 794-797. https://doi.org/10.1136/jnnp.2008.159558

Maris, E., & Oostenveld, R. (2007). Nonparametric statistical testing of EEG- and MEG-data. *Journal of Neuroscience Methods*, *164*(1), 177-190. https://doi.org/10.1016/j.jneumeth.2007.03.024

Marsden, C. D. (1990). Parkinson's disease. *Lancet*, *335*(8695), 948-952. https://doi.org/10.1016/0140-6736(90)91006-v

Mathiopoulou, V., Lofredi, R., Feldmann, L. K., Habets, J., Darcy, N., Neumann, W. J.,…Kühn, A. A. (2024). Modulation of subthalamic beta oscillations by movement, dopamine, and deep brain stimulation in Parkinson's disease. *NPJ Parkinsons Dis*, *10*(1), 77. https://doi.org/10.1038/s41531-024-00693-3

Melki, R. (2015). Role of Different Alpha-Synuclein Strains in Synucleinopathies, Similarities with other Neurodegenerative Diseases. *J Parkinsons Dis*, *5*(2), 217-227. https://doi.org/10.3233/jpd-150543

Milosevic, L., Scherer, M., Cebi, I., Guggenberger, R., Machetanz, K., Naros, G.,…Gharabaghi, A. (2020). Online Mapping With the Deep Brain

Stimulation Lead: A Novel Targeting Tool in Parkinson's Disease. *Mov Disord*, *35*(9), 1574-1586. https://doi.org/10.1002/mds.28093

Moore, O., Peretz, C., & Giladi, N. (2007). Freezing of gait affects quality of life of peoples with Parkinson's disease beyond its relationships with mobility and gait. *Mov Disord*, *22*(15), 2192-2195. https://doi.org/10.1002/mds.21659

Moore, S. T., MacDougall, H. G., & Ondo, W. G. (2008). Ambulatory monitoring of freezing of gait in Parkinson's disease. *J Neurosci Methods*, *167*(2), 340-348. https://doi.org/10.1016/j.jneumeth.2007.08.023

Nachev, P., Kennard, C., & Husain, M. (2008). Functional role of the supplementary and pre-supplementary motor areas. *Nat Rev Neurosci*, *9*(11), 856-869. https://doi.org/10.1038/nrn2478

Neumann, W.-J., Degen, K., Schneider, G.-H., Brücke, C., Huebl, J., Brown, P., & Kühn, A. A. (2016). Subthalamic synchronized oscillatory activity correlates with motor impairment in patients with Parkinson's disease. *Movement Disorders*, *31*(11), 1748-1751. https://doi.org/10.1002/mds.26759

Neumann, W. J., Memarian Sorkhabi, M., Benjaber, M., Feldmann, L. K., Saryyeva, A., Krauss, J. K.,…Denison, T. (2021). The sensitivity of ECG contamination to surgical implantation site in brain computer interfaces. *Brain Stimul*, *14*(5), 1301-1306. https://doi.org/10.1016/j.brs.2021.08.016

Neumann, W. J., Staub-Bartelt, F., Horn, A., Schanda, J., Schneider, G. H., Brown, P., & Kühn, A. A. (2017). Long term correlation of subthalamic beta band activity with motor impairment in patients with Parkinson's disease. *Clin Neurophysiol*, *128*(11), 2286-2291. https://doi.org/10.1016/j.clinph.2017.08.028

Nieuwboer, A., & Giladi, N. (2013). Characterizing freezing of gait in Parkinson's disease: models of an episodic phenomenon. *Mov Disord*, *28*(11), 1509-1519. https://doi.org/10.1002/mds.25683

Nonnekes, J., Giladi, N., Guha, A., Fietzek, U. M., Bloem, B. R., & Růžička, E. (2019). Gait festination in parkinsonism: introduction of two phenotypes. *Journal of Neurology*, *266*(2), 426-430. https://doi.org/10.1007/s00415-018-9146-7

Nonnekes, J., Ružicka, E., Nieuwboer, A., Hallett, M., Fasano, A., & Bloem, B. R. (2019). Compensation Strategies for Gait Impairments in Parkinson Disease: A Review. *JAMA Neurol*, *76*(6), 718-725. https://doi.org/10.1001/jamaneurol.2019.0033

Nordin, A. D., Hairston, W. D., & Ferris, D. P. (2018). Dual-electrode motion artifact cancellation for mobile electroencephalography. *J Neural Eng*, *15*(5), 056024. https://doi.org/10.1088/1741-2552/aad7d7

Nutt, J. G., Bloem, B. R., Giladi, N., Hallett, M., Horak, F. B., & Nieuwboer, A. (2011). Freezing of gait: moving forward on a mysterious clinical

phenomenon. *Lancet Neurol*, *10*(8), 734-744. https://doi.org/10.1016/s1474-4422(11)70143-0

Okuma, Y., Silva de Lima, A. L., Fukae, J., Bloem, B. R., & Snijders, A. H. (2018). A prospective study of falls in relation to freezing of gait and response fluctuations in Parkinson's disease. *Parkinsonism Relat Disord*, *46*, 30-35. https://doi.org/10.1016/j.parkreldis.2017.10.013

Okun, M. S., Gallo, B. V., Mandybur, G., Jagid, J., Foote, K. D., Revilla, F. J.,…Tagliati, M. (2012). Subthalamic deep brain stimulation with a constant-current device in Parkinson's disease: an open-label randomised controlled trial. *The Lancet Neurology*, *11*(2), 140-149. https://doi.org/https://doi.org/10.1016/S1474-4422(11)70308-8

Oswal, A., Yeh, C.-H., Neumann, W.-J., Gratwicke, J., Akram, H., Horn, A.,…Litvak, V. (2020). Neural signatures of pathological hyperdirect pathway activity in Parkinson's disease. *bioRxiv*, 2020.2006.2011.146886. https://doi.org/10.1101/2020.06.11.146886

Ozturk, M., Abosch, A., Francis, D., Wu, J., Jimenez-Shahed, J., & Ince, N. F. (2020). Distinct subthalamic coupling in the ON state describes motor performance in Parkinson's disease. *Movement Disorders*, *35*(1), 91-100.

Pfurtscheller, G., & Lopes da Silva, F. H. (1999). Event-related EEG/MEG synchronization and desynchronization: basic principles. *Clin Neurophysiol*, *110*(11), 1842-1857. https://doi.org/10.1016/s1388-2457(99)00141-8

Pfurtscheller, G., Neuper, C., Brunner, C., & da Silva, F. L. (2005). Beta rebound after different types of motor imagery in man. *Neuroscience Letters*, *378*(3), 156-159. /https://doi.org/10.1016/j.neulet.2004.12.034

Pfurtscheller, G., Neuper, C., & Kalcher, J. (1993). 40-Hz oscillations during motor behavior in man. *Neurosci Lett*, *164*(1-2), 179-182. https://doi.org/10.1016/0304-3940(93)90886-p

Plotnik, M., Giladi, N., & Hausdorff, J. M. (2012). Is freezing of gait in Parkinson's disease a result of multiple gait impairments? Implications for treatment. *Parkinsons Dis*, *2012*, 459321. https://doi.org/10.1155/2012/459321

Poewe, W., Seppi, K., Tanner, C. M., Halliday, G. M., Brundin, P., Volkmann, J.,…Lang, A. E. (2017). Parkinson disease. *Nat Rev Dis Primers*, *3*, 17013. https://doi.org/10.1038/nrdp.2017.13

Priori, A., Foffani, G., Pesenti, A., Tamma, F., Bianchi, A. M., Pellegrini, M.,…Villani, R. M. (2004). Rhythm-specific pharmacological modulation of subthalamic activity in Parkinson's disease. *Experimental Neurology*, *189*(2), 369-379. https://doi.org/10.1016/j.expneurol.2004.06.001

Quinn, E. J., Blumenfeld, Z., Velisar, A., Koop, M. M., Shreve, L. A., Trager, M. H.,…Brontë-Stewart, H. (2015). Beta oscillations in freely moving Parkinson's subjects are attenuated during deep brain stimulation. *Movement Disorders*, *30*(13), 1750-1758. https://doi.org/10.1002/mds.26376

Redgrave, P., Rodriguez, M., Smith, Y., Rodriguez-Oroz, M. C., Lehericy, S., Bergman, H.,…Obeso, J. A. (2010). Goal-directed and habitual control in the basal ganglia: implications for Parkinson's disease. *Nat Rev Neurosci*, *11*(11), 760-772. https://doi.org/10.1038/nrn2915

Salmelin, R., Hámáaláinen, M., Kajola, M., & Hari, R. (1995). Functional Segregation of Movement-Related Rhythmic Activity in the Human Brain. *NeuroImage*, *2*(4), 237-243. https://doi.org/10.1006/nimg.1995.1031

Salomon, A., Gazit, E., Ginis, P., Urazalinov, B., Takoi, H., Yamaguchi, T.,…Hausdorff, J. M. (2024). A machine learning contest enhances automated freezing of gait detection and reveals time-of-day effects. *Nature Communications*, *15*(1), 4853. https://doi.org/10.1038/s41467-024-49027-0

Savitt, J. M., Dawson, V. L., & Dawson, T. M. (2006). Diagnosis and treatment of Parkinson disease: molecules to medicine. *J Clin Invest*, *116*(7), 1744-1754. https://doi.org/10.1172/jci29178

Schaafsma, J. D., Balash, Y., Gurevich, T., Bartels, A. L., Hausdorff, J. M., & Giladi, N. (2003). Characterization of freezing of gait subtypes and the response of each to levodopa in Parkinson's disease. *Eur J Neurol*, *10*(4), 391-398. https://doi.org/10.1046/j.1468-1331.2003.00611.x

Schapira, A. H. V., Chaudhuri, K. R., & Jenner, P. (2017). Non-motor features of Parkinson disease. *Nat Rev Neurosci*, *18*(7), 435-450. https://doi.org/10.1038/nrn.2017.62

Scholten, M., Klemt, J., Heilbronn, M., Plewnia, C., Bloem, B. R., Bunjes, F.,…Weiss, D. (2017). Effects of Subthalamic and Nigral Stimulation on Gait Kinematics in Parkinson's Disease. *Front Neurol*, *8*, 543. https://doi.org/10.3389/fneur.2017.00543

Scholten, M., Schoellmann, A., Ramos-Murguialday, A., López-Larraz, E., Gharabaghi, A., & Weiss, D. (2020). Transitions between repetitive tapping and upper limb freezing show impaired movement-related beta band modulation. *Clinical Neurophysiology*, *131*(10), 2499-2507. https://doi.org/10.1016/j.clinph.2020.05.037

Schuepbach, W. M. M., Rau, J., Knudsen, K., Volkmann, J., Krack, P., Timmermann, L.,…Deuschl, G. (2013). Neurostimulation for Parkinson's Disease with Early Motor Complications. *New England Journal of Medicine*, *368*(7), 610-622. https://doi.org/10.1056/NEJMoa1205158

Seeber, M., Scherer, R., & Müller-Putz, G. R. (2016). EEG Oscillations Are Modulated in Different Behavior-Related Networks during Rhythmic Finger Movements. *J Neurosci*, *36*(46), 11671-11681. https://doi.org/10.1523/jneurosci.1739-16.2016

Shackleford, M. R., Mishra, V., & Mari, Z. (2022). Levodopa-Carbidopa Intestinal Gel May Improve Treatment-Resistant Freezing of Gait in Parkinson's Disease. *Clinical Parkinsonism & Related Disorders*, 100148.

Shine, J. M., Moustafa, A. A., Matar, E., Frank, M. J., & Lewis, S. J. (2013). The role of frontostriatal impairment in freezing of gait in Parkinson's disease. *Front Syst Neurosci*, *7*, 61. https://doi.org/10.3389/fnsys.2013.00061

Singh, A., Kammermeier, S., Plate, A., Mehrkens, J. H., Ilmberger, J., & Bötzel, K. (2011). Pattern of local field potential activity in the globus pallidus internum of dystonic patients during walking on a treadmill. *Exp Neurol*, *232*(2), 162-167. https://doi.org/10.1016/j.expneurol.2011.08.019

Singh, A., Plate, A., Kammermeier, S., Mehrkens, J. H., Ilmberger, J., & Bötzel, K. (2013). Freezing of gait-related oscillatory activity in the human subthalamic nucleus. *Basal Ganglia*, *3*(1), 25-32. https://doi.org/10.1016/j.baga.2012.10.002

Snijders, A. H., Haaxma, C. A., Hagen, Y. J., Munneke, M., & Bloem, B. R. (2012). Freezer or non-freezer: clinical assessment of freezing of gait. *Parkinsonism Relat Disord*, *18*(2), 149-154. https://doi.org/10.1016/j.parkreldis.2011.09.006

Stam, M. J., van Wijk, B. C. M., Sharma, P., Beudel, M., Piña-Fuentes, D. A., de Bie, R. M. A.,…Buijink, A. W. G. (2023). A comparison of methods to suppress electrocardiographic artifacts in local field potential recordings. *Clin Neurophysiol*, *146*, 147-161. https://doi.org/10.1016/j.clinph.2022.11.011

Stein, E., & Bar-Gad, I. (2013). Beta oscillations in the cortico-basal ganglia loop during parkinsonism. *Experimental Neurology*, *245*, 52-59. https://doi.org/10.1016/j.expneurol.2012.07.023

Stolk, A., Brinkman, L., Vansteensel, M. J., Aarnoutse, E., Leijten, F. S., Dijkerman, C. H.,…Toni, I. (2019). Electrocorticographic dissociation of alpha and beta rhythmic activity in the human sensorimotor system. *Elife*, *8*. https://doi.org/10.7554/eLife.48065

Storzer, L., Butz, M., Hirschmann, J., Abbasi, O., Gratkowski, M., Saupe, D.,…Schnitzler, A. (2017). Bicycling suppresses abnormal beta synchrony in the Parkinsonian basal ganglia. *Ann Neurol*, *82*(4), 592-601. https://doi.org/10.1002/ana.25047

Syrkin-Nikolau, J., Koop, M. M., Prieto, T., Anidi, C., Afzal, M. F., Velisar, A.,…Bronte-Stewart, H. (2017). Subthalamic neural entropy is a feature of freezing of gait in freely moving people with Parkinson's disease. *Neurobiol Dis*, *108*, 288-297. https://doi.org/10.1016/j.nbd.2017.09.002

Takakusaki, K. (2017). Functional Neuroanatomy for Posture and Gait Control. *J Mov Disord*, *10*(1), 1-17. https://doi.org/10.14802/jmd.16062

Tamir, I., Wang, D., Chen, W., Ostrem, J. L., Starr, P. A., & de Hemptinne, C. (2020). Eight cylindrical contact lead recordings in the subthalamic region localize beta oscillations source to the dorsal STN. *Neurobiology of Disease*, *146*, 105090. https://doi.org/10.1016/j.nbd.2020.105090

Tan, D. M., McGinley, J. L., Danoudis, M. E., Iansek, R., & Morris, M. E. (2011). Freezing of Gait and Activity Limitations in People With Parkinson's

Disease. *Archives of Physical Medicine and Rehabilitation*, *92*(7), 1159-1165. https://doi.org/10.1016/j.apmr.2011.02.003

Tan, H., Fischer, P., Shah, S. A., Vidaurre, D., Woolrich, M. W., & Brown, P. (2018). Decoding Movement States in Stepping Cycles Based on Subthalamic LFPs in Parkinsonian Patients. *Annu Int Conf IEEE Eng Med Biol Soc*, *2018*, 1384-1387. https://doi.org/10.1109/embc.2018.8512545

Tan, H., Pogosyan, A., Ashkan, K., Green, A. L., Aziz, T., Foltynie, T.,…Brown, P. (2016). Decoding gripping force based on local field potentials recorded from subthalamic nucleus in humans. *Elife*, *5*. https://doi.org/10.7554/eLife.19089

Thenaisie, Y., Lee, K., Moerman, C., Scafa, S., Gálvez, A., Pirondini, E.,…Moraud, E. M. (2022). Principles of gait encoding in the subthalamic nucleus of people with Parkinson's disease. *Sci Transl Med*, *14*(661), eabo1800. https://doi.org/10.1126/scitranslmed.abo1800

Thenaisie, Y., Palmisano, C., Canessa, A., Keulen, B. J., Capetian, P., Jiménez, M. C.,…Contarino, M. F. (2021). Towards adaptive deep brain stimulation: clinical and technical notes on a novel commercial device for chronic brain sensing. *J Neural Eng*, *18*(4). https://doi.org/10.1088/1741-2552/ac1d5b

Tolosa, E., Garrido, A., Scholz, S. W., & Poewe, W. (2021). Challenges in the diagnosis of Parkinson's disease. *Lancet Neurol*, *20*(5), 385-397. https://doi.org/10.1016/s1474-4422(21)00030-2

Tosserams, A., Weerdesteyn, V., Bal, T., Bloem, B. R., Solis-Escalante, T., & Nonnekes, J. (2022). Cortical Correlates of Gait Compensation Strategies in Parkinson Disease. *Ann Neurol*, *91*(3), 329-341. https://doi.org/10.1002/ana.26306

Tripoliti, E., Zrinzo, L., Martinez-Torres, I., Frost, E., Pinto, S., Foltynie, T.,…Limousin, P. (2011). Effects of subthalamic stimulation on speech of consecutive patients with Parkinson disease. *Neurology*, *76*(1), 80-86. https://doi.org/10.1212/WNL.0b013e318203e7d0

Trottenberg, T., Kupsch, A., Schneider, G.-H., Brown, P., & Kühn, A. A. (2007). Frequency-dependent distribution of local field potential activity within the subthalamic nucleus in Parkinson's disease. *Experimental Neurology*, *205*(1), 287-291. https://doi.org/10.1016/j.expneurol.2007.01.028

Tykocki, T., Nauman, P., Koziara, H., & Mandat, T. (2013). Microlesion effect as a predictor of the effectiveness of subthalamic deep brain stimulation for Parkinson's disease. *Stereotact Funct Neurosurg*, *91*(1), 12-17. https://doi.org/10.1159/000342161

Uhlhaas, P. J., & Singer, W. (2006). Neural synchrony in brain disorders: relevance for cognitive dysfunctions and pathophysiology. *Neuron*, *52*(1), 155-168. https://doi.org/10.1016/j.neuron.2006.09.020

van Burik, M., & Pfurtscheller, G. (1999). Functional Imaging of Postmovement Beta Event-Related Synchronization. *Journal of Clinical Neurophysiology*, *16*(4).

Vandenbossche, J., Deroost, N., Soetens, E., Coomans, D., Spildooren, J., Vercruysse, S.,…Kerckhofs, E. (2012). Freezing of gait in Parkinson's disease: disturbances in automaticity and control. *Front Hum Neurosci*, *6*, 356. https://doi.org/10.3389/fnhum.2012.00356

Vercruysse, S., Gilat, M., Shine, J. M., Heremans, E., Lewis, S., & Nieuwboer, A. (2014). Freezing beyond gait in Parkinson's disease: A review of current neurobehavioral evidence. *Neuroscience & Biobehavioral Reviews*, *43*, 213-227. https://doi.org/10.1016/j.neubiorev.2014.04.010

Vitek, J. L., Jain, R., Chen, L., Tröster, A. I., Schrock, L. E., House, P. A.,…Starr, P. A. (2020). Subthalamic nucleus deep brain stimulation with a multiple independent constant current-controlled device in Parkinson's disease (INTREPID): a multicentre, double-blind, randomised, sham-controlled study. *Lancet Neurol*, *19*(6), 491-501. https://doi.org/10.1016/s1474-4422(20)30108-3

Wang, D. D., & Choi, J. T. (2020). Brain Network Oscillations During Gait in Parkinson's Disease [Mini Review]. *Frontiers in Human Neuroscience*, *14*. https://doi.org/10.3389/fnhum.2020.568703

Weaver, F. M., Follett, K., Stern, M., Hur, K., Harris, C., Marks, W. J., Jr.,…Huang, G. D. (2009). Bilateral deep brain stimulation vs best medical therapy for patients with advanced Parkinson disease: a randomized controlled trial. *Jama*, *301*(1), 63-73. https://doi.org/10.1001/jama.2008.929

Weinberger, M., Hutchison, W. D., Lozano, A. M., Hodaie, M., & Dostrovsky, J. O. (2009). Increased gamma oscillatory activity in the subthalamic nucleus during tremor in Parkinson's disease patients. *J Neurophysiol*, *101*(2), 789-802. https://doi.org/10.1152/jn.90837.2008

Weinberger, M., Mahant, N., Hutchison, W. D., Lozano, A. M., Moro, E., Hodaie, M.,…Dostrovsky, J. O. (2006). Beta Oscillatory Activity in the Subthalamic Nucleus and Its Relation to Dopaminergic Response in Parkinson's Disease. *Journal of Neurophysiology*, *96*(6), 3248-3256. https://doi.org/10.1152/jn.00697.2006

Weintraub, D., & Mamikonyan, E. (2019). The Neuropsychiatry of Parkinson Disease: A Perfect Storm. *Am J Geriatr Psychiatry*, *27*(9), 998-1018. https://doi.org/10.1016/j.jagp.2019.03.002

Weiss, D., Klotz, R., Govindan, R. B., Scholten, M., Naros, G., Ramos-Murguialday, A.,…Gharabaghi, A. (2015). Subthalamic stimulation modulates cortical motor network activity and synchronization in Parkinson's disease. *Brain*, *138*(Pt 3), 679-693. https://doi.org/10.1093/brain/awu380

Weiss, D., Schoellmann, A., Fox, M. D., Bohnen, N. I., Factor, S. A., Nieuwboer, A.,…Lewis, S. J. G. (2020). Freezing of gait: understanding the complexity of an enigmatic phenomenon. *Brain*, *143*(1), 14-30. https://doi.org/10.1093/brain/awz314

Weiss, D., Volkmann, J., Fasano, A., Kühn, A., Krack, P., & Deuschl, G. (2021). Changing Gears – DBS For Dopaminergic Desensitization in Parkinson's

Disease? *Annals of Neurology*, *90*(5), 699-710. https://doi.org/https://doi.org/10.1002/ana.26164

Weiss, D., Walach, M., Meisner, C., Fritz, M., Scholten, M., Breit, S.,…Krüger, R. (2013). Nigral stimulation for resistant axial motor impairment in Parkinson's disease? A randomized controlled trial. *Brain*, *136*(Pt 7), 2098-2108. https://doi.org/10.1093/brain/awt122

Williams, A., Gill, S., Varma, T., Jenkinson, C., Quinn, N., Mitchell, R.,…Wheatley, K. (2010). Deep brain stimulation plus best medical therapy versus best medical therapy alone for advanced Parkinson's disease (PD SURG trial): a randomised, open-label trial. *Lancet Neurol*, *9*(6), 581-591. https://doi.org/10.1016/s1474-4422(10)70093-4

Yin, Z., Zhu, G., Zhao, B., Bai, Y., Jiang, Y., Neumann, W.-J.,…Zhang, J. (2021). Local field potentials in Parkinson's disease: A frequency-based review. *Neurobiology of Disease*, *155*, 105372. https://doi.org/10.1016/j.nbd.2021.105372

Yoshida, F., Martinez-Torres, I., Pogosyan, A., Holl, E., Petersen, E., Chen, C. C.,…Brown, P. (2010). Value of subthalamic nucleus local field potentials recordings in predicting stimulation parameters for deep brain stimulation in Parkinson's disease. *J Neurol Neurosurg Psychiatry*, *81*(8), 885-889. https://doi.org/10.1136/jnnp.2009.190918

Zaidel, A., Spivak, A., Grieb, B., Bergman, H., & Israel, Z. (2010). Subthalamic span of β oscillations predicts deep brain stimulation efficacy for patients with Parkinson’s disease. *Brain*, *133*(7), 2007-2021. https://doi.org/10.1093/brain/awq144

8 Declaration of own contribution

The work was conducted at the Centre for Neurology, Department of Neurodegenerative Diseases, University of Tübingen, under the supervision of Prof. Dr. Daniel Weiß.

The study was designed by Prof. Dr. Daniel Weiß in collaboration with Dr. Maria-Sophie Breu, who was an assistant physician and member of the research group at the time.

All experiments were carried out and documented by me, following initial training by Dr. Maria-Sophie Breu, and in collaboration with Dr. Philipp Klocke (resident physician, member of the research group) or Dr. Moritz Loeffler (resident physician, member of the research group).

The data preprocessing, as well as the statistical analysis and interpretation, were conducted independently by me, with support from Dr. Philipp Klocke and Prof. Dr. Daniel Weiß for complex issues.

The necessary MATLAB scripts were written by Dr. Philipp Klocke and myself.

The literature review was conducted exclusively by me.

I hereby declare that I have written the manuscript independently and have used no sources other than those cited.

Tübingen, 21.02.2026

Hannah Müßler

9 Publications

Some of this work has been published in

Philipp Klocke, Moritz A Loeffler, Hannah Muessler, Maria-Sophie Breu, Alireza Gharabaghi, Daniel Weiss, Supraspinal contributions to defective antagonistic inhibition and freezing of gait in Parkinson's disease, *Brain*, Volume 147, Issue 12, December 2024, Pages 4056–4071, https://doi.org/10.1093/brain/awae223

10 Funding

This project was funded by the IZKF (Interdisziplinäres Zentrum für Klinische Forschung).

11 Acknowledgements

This dissertation would not have been possible without the support and cooperation of many people, to whom I would like to express my sincere gratitude below.

First and foremost, I would like to thank my supervisor Prof. Dr. Daniel Weiß for giving me the opportunity to pursue my doctoral thesis in the exciting field of Deep brain stimulation and FoG, and for his continuous guidance, valuable advice, and ongoing support throughout the project. He has greatly contributed to both my personal and scientific development.

I would like to sincerely thank my second supervisor Dr. Philipp Klocke, who supported me in every way, answered all my questions with patience, and became not only a wonderful office neighbour but also a valued friend.

Another heartfelt thank you goes to Dr. Moritz Löffler, with whom every recording session was a pleasure. He continuously nurtured my interest in neurology — even beyond the scope of this dissertation — and supported me with advice and friendship far beyond his professional responsibilities.

I gratefully acknowledge the support of Dr. Maria-Sophie Breu for introducing me to the subject and for getting me excited about it from the very beginning.

I would like to warmly thank my family, especially my parents, for their support in every aspect of my life. They have always done their utmost to make everything possible for me.

Finally, I would also like to thank the team at the IZKF for their great efforts in providing additional scientific training for the funded doctoral students, organizing excellent lectures, offering valuable advice for the dissertation, and significantly contributing to the success of this project.